# The effects of acid aspiration on tissue-resident macrophages in extra-pulmonary organs

Inaugural Dissertation submitted to the
Faculty of Medicine, Justus Liebig University Giessen
in partial fulfillment of the requirements for the
Doctor Medicinae (Dr. med.)

by Langelage, Martin

Gießen 2024

From the Faculty of Medicine of the Justus Liebig University Giessen

Department of Internal Medicine V

Supervisor: PD Dr. med. univ. Ulrich Matt, PhD

Supervisor: Prof. Dr. Soni Savai Pullamsetti, PhD

Date of doctoral defense: 06.02.2024

# Table of contents

# 1 Introduction

## 1.1 Acid aspiration pneumonitis

### 1.1.1 Definition

Aspiration is defined as the inhalation of foreign or endogenous materials into the airways, which can comprise food particles, foreign bodies, oropharyngeal material, or gastric contents. Acid aspiration, in particular, represents the inhalation of larger amounts of acidic gastric contents (Son et al., 2017). Aspiration pneumonitis is an inflammation of the lungs following an event of sterile acid aspiration and was first described in 1946 by Mendelson and colleagues (Mendelson, 1946). Although often used as synonyms by clinicians, it is important to differentiate aspiration pneumonia from aspiration pneumonitis, since the first is bacterial pneumonia following the aspiration of colonized oropharyngeal material, while the latter is an initially sterile inflammation in response to the chemical damage (Marik, 2001).

### 1.1.2 Epidemiology & Risk factors

Impaired consciousness, resulting in reduced protective reflexes, is the main risk factor for aspiration. Causes for reduced consciousness are manifold and include alcohol abuse, drug overdose, trauma, or seizure (Marik, 2001). Adnet and Baud were able to show a correlation between the impairment of consciousness, measured by Glasgow Coma Scale scores, and the risk of aspiration (Adnet and Baud, 1996). Aspiration happens in approximately 1:4000 elective surgeries, 1:3000 general anesthesias, up to 20% of emergency intubations (Roshan et al., 2021), with a strong correlation between aspiration events and patients' general state of health (Warner et al., 1993), and in around 10% of patients with drug overdose (Aldrich et al., 1980). Furthermore, aspiration commonly occurs in healthy individuals during sleep (Huxley et al., 1978). Hence, aspiration of gastric contents is a frequent event in a multitude of settings.

### 1.1.3 Pathophysiology

The initial phase of aspiration pneumonitis is characterized by chemical damage to the epithelium and the activation of capsaicin-sensitive afferent neurons (Kennedy Thomas P. MU et al., 1989). Minutes after the apical damage, the alveolar epithelial cells release $H_2O_2$ which depolarizes endothelial mitochondria, leading to a loss of the endothelial barrier function and thereby resulting in pulmonary edema (Hough et al., 2019).

Concurrently, pulmonary blood flow is redistributed towards the damaged areas (Richter et al., 2013) and pulmonary hypertension emerges (Pawlik et al., 2009), which leads to impaired gas exchange (Richter et al., 2013) and combined respiratory and metabolic acidosis in the case of a large aspiration volume (Pawlik et al., 2009). Within two hours after the aspiration event, pulmonary blood flow is redirected to non-injured areas of the lung by counterregulatory mechanisms (Richter et al., 2015). The arterial partial pressure ($PaO_2$) of oxygen declines after the aspiration took place (Richter et al., 2013). When the aspirated volume was sizeable, the $PaO_2$ remains severely diminished for approximately one day (Setzer et al., 2018). Additionally, a disturbance in the alveolar surfactant layer (Davidson et al., 2005), as well as inflammatory processes that occur following the aspiration contribute to impaired gas exchange.

As a result of the chemical damage, danger-associated molecular patterns (DAMPs), such as oxidized phospholipids (Imai et al., 2008) and mitochondrial desoxyribonucleic acid (DNA) (Davidson et al., 2013) accumulate in the lungs. Those DAMPs are recognized by alveolar macrophages (AMs) which produce - among other proinflammatory cytokines - tumor necrosis factor-alpha (TNF-α) (Beck-Schimmer et al., 2005), peaking a few hours after aspiration (Davidson et al., 1999). Secretion of chemokines by epithelial cells and AMs attracts neutrophils into the alveolar space within a few hours after the aspiration. The neutrophilic influx is not limited to the areas of the lungs affected by the aspirate but also involves initially undamaged areas due to a TNF-α-mediated upregulation of endothelial ICAM-1 (intercellular adhesion molecule-1) (Nagase et al., 1996) as well as an increased expression of CD-18 on neutrophils (Goldman et al., 1990; Goldman et al., 1995). Once migrated into the lung parenchyma, the neutrophils further enhance the inflammatory process via the release of reactive oxygen species (ROS), elastases (Goldman. et al., 1992), the formation of neutrophil extracellular traps (Li et al., 2018) and secretion of large amounts of defensins (Bdeir et al., 2010). However, neutrophil-derived ROS are not exclusively deleterious. Davidson and colleagues unveiled that the nicotinamide adenine dinucleotide phosphate (NADPH) oxidase of neutrophils, which constitutes their main source of ROS, also appears to limit the inflammation (Davidson et al., 2013). Depending on the experimental model used, neutrophil numbers peak 12 hours (Matt et al., 2009) to one day (Setzer et al., 2018) after aspiration. At this time point, they constitute the largest fraction of leukocytes in the lung (Patel et al., 2012). As a result of the inflammatory process, coagulative necrosis and serofibrinous exsudation develop, peaking around one day after the aspiration (Amigoni et al., 2008). Additionally, lung

edema and impairment in alveolar fluid clearance are most distinct at this time (Patel et al., 2012).

Subsequently, the immune response shifts from an inflammatory process to the resolution of inflammation, including efferocytosis of epithelial cells and neutrophils. AM numbers also recuperate after dropping early after acid aspiration (Better et al., 2023). Blood gases recover and return to baseline level which may take up to two weeks depending on the magnitude of the initial aspiration (Amigoni et al., 2008). However, there is still histologic evidence for chronic inflammation with fibrotic tendencies in the parts of the lungs damaged by the aspirate weeks after the aspiration took place according to some authors (Amigoni et al., 2008).

### 1.1.4 Symptoms & diagnosis

Acid aspiration and the following pneumonitis cause a spectrum of clinical appearances, ranging from the absence of any symptoms in around two-thirds of patients to the development of acute respiratory distress syndrome (ARDS) (Warner et al., 1993). The most common symptoms are dyspnea, tachypnea, cough, and shortness of breath immediately after the aspiration event (Marik, 2001). If the pneumonitis is severe (e.g., large volume, low pH), hypotension and acid-base disturbances may emerge, thus requiring intensive care treatment and mechanical ventilation. A direct correlation between the volume and the pH of the aspirate to the severity of the lung damage was shown (Exarhos et al., 1965). However, the pH appears to be more influential (James et al., 1984). Some authors also refer to a pH of less than 2,5 (Mendelson, 1946; Marik, 2011) or a volume of the aspirate greater than 0,3ml per kilogram body weight (Marik, 2001) as a threshold for the development of a severe lung injury.

When the aspiration event is witnessed, the diagnosis is easily made. But due to the variety of clinical appearances and often unwitnessed aspirations for example in patients delivered by emergency medical services or microaspirations in intubated patients, aspiration-related pathologies are often misdiagnosed. An indicator of recent aspiration is the presence of foreign material in the upper airways or the oropharynx during patient examination or bronchoscopy. Pepsin and lipid-laden macrophages in bronchioalveolar lavage were proposed as biomarkers for aspiration (Hu et al., 2015). However, these parameters require the performance of bronchoalveolar lavage, which itself is an invasive procedure afflicted with a plethora of risks and lipid-laden macrophages lack specificity for pulmonary aspiration (Knauer-Fischer and Ratjen, 1999).

In chest imaging, aspiration pneumonitis has rather unspecific manifestations like pulmonary infiltrates, airway thickening, and pulmonary edema. Yet there are predilection sites, namely the posterior segments of the upper lobes in recumbent patients and basal segments of especially the right lung when patients are sitting or standing during the aspiration (Johnson and Hirsch, 2003). However, the aspirate may be diffusely distributed by coughing. Therefore many potential differential diagnoses like community-acquired pneumonia, cardiogenic or noncardiogenic pulmonary edema, and pulmonary hemorrhage have to be considered (Prather et al., 2014).

Since clinical and laboratory findings are rather unspecific, e.g. elevation of C-reactive protein (CRP) or leukocytosis, sampling of respiratory material for microbiological testing should be performed to ascertain bacterial infection. El-Solh showed that procalcitonin has a poor prognostic value to distinguish acid pneumonitis from bacterial aspiration pneumonia (El-Solh et al., 2011). Fever or clinical deterioration might signify a bacterial infection, and justify antibiotic therapy, particularly if microbiological samples detected compatible bacteria (Raghavendran et al., 2011; Mandell and Niederman, 2019).

## 1.1.5 Complications

Two main complications may occur after acid aspiration: the development of ARDS and bacterial superinfection. Metheny and colleagues were able to delineate gastric aspiration as the strongest independent risk factor for bacterial pneumonia in the intensive care (Metheny et al., 2006). Moreover, gastric aspiration constitutes one of the leading causes for the development of ARDS (Eworuke et al., 2018), which - despite all advances in modern medicine - has a mortality rate of up to 40% with no causative treatment available (Matthay et al., 2019).

The mechanism that accounts for the increased susceptibility to bacterial superinfections is largely undefined. Experimental models showed that bacterial infection after acid aspiration results in an enormous uncontrolled bacterial outgrowth (Rotta et al., 2004; Matt et al., 2009). Mitsushima et al. demonstrated that the early epithelial damage facilitates bacterial adhesion of *Pseudomonas aeruginosa (P. aeruginosa)* (Mitsushima et al., 2002). Importantly, the ability of alveolar macrophage (AMs) to clear bacteria is diminished during the resolution of acid aspiration, resulting in uncontrolled bacterial outgrowth and impaired survival during a superinfection with *P. aeruginosa* in a murine model (Matt et al., 2009; Better et al., 2023)

### 1.1.6 Treatment

The treatment of aspiration pneumonitis is mainly supportive. Commonly used measures include primarily the suctioning of the upper airways after a witnessed aspiration event, the prevention of further aspiration, fluid management, and continuous clinical surveillance (Marik, 2001).

The prophylactic administration of antibiotics is not recommended since the ongoing inflammation is sterile and clinical studies could not present a benefit for prophylactic antimicrobial therapy in terms of the number of patients transferred to intensive care units or overall mortality (Dragan et al., 2018). Moreover, antibiotic prophylaxis was significantly associated with fewer antibiotic-free days and a more frequent escalation of antimicrobial therapy (Dragan et al., 2018). In case of clinical deterioration after 48 hours, antibiotics may be considered (Mandell and Niederman, 2019).

Administration of corticosteroids did not show any beneficial effects (Gates et al., 1983; Bernard Gordon R. et al., 1987), but a higher rate of complications in terms of gram-negative secondary infections (Wolfe et al., 1977).

If invasive ventilation is required, a lung-protective strategy with low tidal volumes and a high positive end-expiratory pressure (PEEP) seems to be advantageous due to reduced ventilator-associated lung injury (Haase et al., 2019) and nephroprotective effects (Imai et al., 2003). The inspiratory oxygen fraction should be preferably low since exposure to high oxygen concentrations after acid aspiration increases pulmonary damage (Nader-Djalal et al., 1998) and may, therefore, pioneer the development of ARDS (Knight et al., 2000).

## 1.2 Systemic response

### 1.2.1 Inter-organ crosstalk after acute lung injury

Severe lung injuries affect extra-pulmonary organs. Darmon and colleagues were able to show in a multicenter study that acute lung injury (ALI) is an independent risk factor for the occurrence of acute kidney injury (AKI) (Darmon et al., 2014). Additionally, ALI caused by influenza virus infection is significantly associated with an increased risk of cardiovascular events (Smeeth Liam et al., 2004). Animal experiments, as well as autopsy studies in humans, revealed - among others - myocarditis, ischemic heart disease, encephalitis, tubular necrosis in the kidneys, hepatitis, or myopathy after influenza

pneumonia (Sellers et al., 2017). In general, alveolar hypoxia was shown to cause rapid systemic inflammation (Chen et al., 2016).

Interestingly, recent research demonstrated the importance of the liver during lung diseases. Acute or chronic liver diseases increase the risk of developing ALI or ARDS and negatively impact the outcome (Zhai et al., 2009; Gacouin et al., 2016; Yang et al., 2019). Although this phenomenon is not entirely understood, elevated bilirubin levels were shown to damage mitochondria (Ostrow et al., 2004), induce apoptosis (Fernandes et al., 2006), and cause hemolysis (Brito et al., 2000). Additionally, impaired liver function leads to impaired clearance of senescent platelets and thus increases pulmonary microvascular thrombosis (Herrero et al., 2020). Moreover, the occurrence of ALI following the intravenous application of endotoxins requires interactions with the liver. Siore and colleagues established a porcine model in which they either perfused the lungs only or the liver and the lungs in physiological order with lipopolysaccharide (LPS) enriched blood. In this model, ALI only developed after lung and liver perfusion (Siore et al., 2005). On the other hand, Hillard et al. were able to demonstrate that an intact hepatic acute-phase response (APR) is mandatory for the resolution of bacterial pneumonia and introduced the term "lung-liver axis" (Hilliard et al., 2015). Thus, crosstalk of the two organs is important during systemic and pulmonary inflammations. However, the mechanisms responsible for the involvement of extra-pulmonary organs after ALI remain largely unknown. Domenech and colleagues hypothesized hypercapnia, hypoxia, and released cytokines to be the main contributors (Domenech et al., 2017), while Chao et al. delineated a key role for AMs in initiating a systemic inflammation following alveolar hypoxia (Chao et al., 2009).

### 1.2.2 Systemic inflammatory response to acid aspiration

Acid aspiration mainly affects the lungs by causing the previously described aspiration pneumonitis. However, there is plenty of experimental evidence for the involvement of extra-pulmonary organs after acid-induced ALI. Heuer and colleagues observed a marked inflow of neutrophils and lymphocytes into the kidneys, the liver and the heart several hours after aspiration in a pig model. Moreover, they found tubular necrosis in the kidney, myocardial and hepatic necrosis, alterations in the hippocampus, and edema formation in several organs (Heuer et al., 2012). Intriguingly, these effects could not be explained by circulatory depression or hypoxemia (Heuer et al., 2012). Goldman and colleagues also observed an influx of neutrophils in the heart and the kidneys (Goldman et al., 1993).

Furthermore, this study identified neutrophils as a pivotal contributor to extra-pulmonary organ damage (Goldman et al., 1993). Interestingly, Schertel and colleagues found that myocardial edema formation after acid aspiration was independent of neutrophil influx, suggesting the existence of additional pathomechanisms (Schertel et al., 1996). Manny et al. additionally reported aggregates of platelets in the bloodstream minutes after the aspiration took place as well as vascular congestion in the liver (Manny et al., 1986). Overall, the precise mechanisms and the clinical consequences of extra-pulmonary responses to acid aspiration are unclear.

## 1.3 Tissue-resident macrophages

### 1.3.1 Ontogeny

Until recently tissue-resident macrophages (TRMs) were considered to be an integral part of the mononuclear phagocytic system, as described by van Furth and colleagues (van Furth and Cohn, 1968). However, research over the last decade has revealed that TRMs originate from fetal precursor cells, and can self-maintain locally without the contribution of bone marrow-derived cells (Kierdorf et al., 2015). Development of TRMs proceeds in three waves: the first wave comprises yolk sac-derived macrophages, the second originates from fetal liver monocytes, which by themselves originate from yolk sac-derived cells, and the third arises from bone marrow-derived monocytes (Kierdorf et al., 2015). These precursor cells settle in every organ during organogenesis and evolve through organ-specific environmental stimuli in TRMs with specialization to the demands of each organ. Depending on the tissue, the contribution of these three sites of origin to the whole macrophage pool in the adult varies. Brain TRMs, for example, are exclusively comprised of yolk sac-derived cells (Prinz et al., 2021), lung and liver TRMs originate mostly from fetal liver monocytes, while intestinal macrophages in adult animals are constantly replenished from bone marrow-derived blood monocytes, a phenomenon also referred to as "monocyte waterfall" (Bain et al., 2014). Overall, most TRMs can maintain themselves under steady-state conditions by self-renewal. During inflammations, bone marrow-derived monocytes are recruited to the site of inflammation via various chemokines to assist or to replenish TRMs, a process referred to as "niche replenishment" (Ginhoux and Guilliams, 2016). A common feature of almost all TRMs in mice is the abundant expression of the F4/80 surface antigen, a member of the epidermal growth

factor-seven transmembrane receptor family, which is often used to identify TRMs (Gordon et al., 2011; Gordon and Pluddemann, 2017).

**1.3.2 Function**

TRMs fulfill a multitude of immune and non-immune-related functions. Initially, macrophages were assumed to be only first-line phagocytic cells to combat invading pathogens. Research of the last decades, however, revealed an abundance of additional functions equally important to tissue homeostasis. One of their earliest tasks is a regulatory role during organogenesis in the embryo, becoming evident by the occurrence of severe developmental abnormalities in their absence (Wynn et al., 2013).

The expression of a vast array of pathogen recognition receptors (PRRs) for the detection of DAMPs, and PAMPs (pathogen-associated molecular patterns), such as Toll-like receptors (TLRs) or nucleotide-binding oligomerization domain-like (NOD-like) receptors enables them to serve as tissue-sentinels. Ligation of the receptors initiates an inflammatory response and recruits other immune cells via the secretion of various chemokines. PRRs trigger signaling events supporting antibacterial properties (Li and Wu, 2021) like phagocytosis or the release of antibacterial molecules such as ROS (West et al., 2011). In addition, scavenger receptors like MARCO or CD36 are PRRs that are most likely directly involved in bacterial uptake (van der Laan et al., 1999; Sharif et al., 2013). Once a pathogen is phagocytosed, it is confined to a newly formed organelle called phagosome (Flannagan et al., 2015). During the maturation of the phagosome, its interior becomes acidic. Additionally, a multitude of antibacterial peptides and enzymes is secreted (Flannagan et al., 2009). Alongside these proteins, large amounts of ROS are secreted in the phagosome lumen to eradicate pathogens (Herb and Schramm, 2021).

During an inflammatory process, TRM numbers might significantly drop, such as during viral infections (Schulte-Schrepping et al., 2020) (Ghoneim et al., 2013), or acid aspiration (Better et al., 2023), which leads to niche replenishment by monocyte-derived macrophages (MDMs) (Davies et al., 2013), which were shown to exhibit a different functional polarization (Zigmond et al., 2014)

Importantly, TRMs also have major roles in the resolution of inflammation by regulating tissue repair and clearance of apoptotic cells (Dalli and Serhan, 2017; Better et al., 2023) .The latter is referred to as efferocytosis and is also crucial for maintaining tissue homeostasis in a steady-state (Wynn and Vannella, 2016; Roberts et al., 2017).

Besides sentinel functions shared by all TRMs, requirements by the organs of residence shape tissue-specific effector functions. Liver TRMs, for example, promote a certain level of immunotolerance against gut-derived PAMPs and DAMPs (Tacke and Zimmermann, 2014; Nobs and Kopf, 2021). Cardiac TRMs fulfill a pivotal role in the controlling of electrical conduction between cardiomyocytes (Maarten Hulsmans et al.) while splenic red pulp TRMs can promote extramedullary hematopoiesis and clear senescent erythrocytes from the bloodstream (Borges da Silva et al., 2015).

Importantly, Kupffer cells and splenic macrophages, as well as kidney TRMs were shown to clear bacteria from the blood stream (Wong et al., 2013; Borges da Silva et al., 2015; Stamatiades et al., 2016; Nobs and Kopf, 2021).

Recently, liver TRMs were shown to have crucial roles in the emergence of acute liver injury (Tsutsui and Nishiguchi, 2014) as well as in the development of liver fibrosis (Koyama and Brenner, 2017). Similar findings were made with kidney TRMs in the genesis as well as the resolution of AKI and chronic kidney disease (CKD) (Cao et al., 2015). Thus, TRMs constitute a promising target to alter inflammatory processes. Yet to date, only a few macrophage-specific interventions have reached advanced stages of testing like phase III or IV trials (Kazankov et al., 2019).

Stimulation with LPS/IFN-y or IL-4 of bone marrow-derived macrophages (BMDMs) *in vitro* results in two distinct phenotypes referred to as "M1" and "M2" respectively. While M1-macrophages exhibit pro-inflammatory features, M2-macrophages display anti-inflammatory and wound-healing abilities (Orecchioni et al., 2019). While this classification was useful to explore macrophage functions induced by defined stimulations *in vitro*, it does not reflect the complexity of inflammations *in vivo*. Thus, it is more adequate to consider macrophage activation states as a spectrum, with M1 and M2 phenotypes representing artificial extremes of the polarization spectrum. During inflammations *in vivo,* a plethora of signals shapes effector functions of TRMs to adapt to organ requirements (Lavin et al., 2014), with the ultimate goal to restore homeostasis. Yet, to date, we have limited knowledge of the effector functions of TRMs during different inflammations within and beyond the site of residence.

### 1.3.3 Immunometabolism

Immunometabolism has become a field of intensive research over the last decade with a special focus on macrophages. Different stimuli applied to macrophages lead to divergent

metabolic responses impacting immunologic functions. Induction of the previously described M1 phenotype in BMDMs causes a marked increase in glycolytic activity and a distinct downregulation of oxidative phosphorylation (OXPHOS), mostly through inhibition of the tricarboxylic acid cycle (TCA cycle) at its key regulator enzymes isocitrate dehydrogenase-1 (IDH-1) and succinate dehydrogenase (SDH) (Mills and O'Neill, 2016). This phenomenon is referred to as the "broken TCA cycle".

The inhibition of IDH-1 and SDH leads to the accumulation of upstream metabolites, first and foremost citrate and succinate (O'Neill and Pearce, 2016). Accumulating citrate is used for different purposes: the induction of ROS as well as NO generation, synthesis of fatty acids and prostaglandins, and metabolization to itaconic acid via immune responsive gene-1 (IRG-1, also known as aconitate decarboxylase-1, ACOD-1) (Lampropoulou et al., 2016). Itaconic acid has direct antimicrobial properties by inhibiting the glyoxylate shunt, a TCA cycle variation found in bacteria, fungi, and protists (McFadden and Purohit, 1977). Furthermore, itaconic acid can inhibit SDH. Succinate, on the other hand, has proinflammatory properties via increased interleukin-1ß (IL-1ß) production due to hypoxia-inducible factor 1 alpha (HIF-1α) stabilization. It also acts as an agonist to succinate receptor-1 (SUCNR-1), which likewise mediates increased IL-1ß and TNF-α production (Mills and O'Neill, 2016).

On the other hand, the induction of an M2 phenotype in BMDMs causes a marked increase in OXPHOS (Saha et al., 2017). It is, however, important to remember that those observations were made in BMDMs. The distinct metabolic signatures found in BMDMs are not transferrable to TRMs. AMs, for example, were shown to primarily rely on OXPHOS upon LPS stimulation while inhibition of glucose metabolism did not diminish the secretion of pro-inflammatory cytokines (Woods et al., 2019) contrasting the "M1-like" metabolic signature. Moreover, peritoneal TRMs were shown to be perfectly adapted to the unique composition of metabolites found in the peritoneal cavity. Peritoneal macrophages (PMs) can substantially increase mitochondrial metabolism as well as the respiratory burst upon zymosan stimulation when cultured in a glutamate-enriched medium, a metabolite that is abundantly present in the peritoneum. Moreover, the mitochondrial metabolism of PMs depends less on glycolysis-derived fuels when compared to BMDMs  (Davies et al., 2017).

## 1.4 Aims

TRMs fulfill an abundance of organ-specific functions in health and disease, which are indispensable for tissue homeostasis and effective immune responses. Acid aspiration was shown to affect various organs. Thus, we hypothesize that TRMs are involved or might even trigger extrapulmonary inflammatory responses to acid pneumonitis. Against this background my doctoral thesis pursues the following aims:

- establishing a method to isolate kidney, liver, peritoneal and splenic TRMs

- analysis of major cytokines and metabolic enzymes of isolated TRMs after acid aspiration at a transcriptional level

- assessment of immune effector functions of TRMs after acid aspiration *ex vivo*

# 2 Material & methods

## 2.1 Materials

### 2.1.1 Machines & devices

| Device | Manufacturers designation | Company |
|---|---|---|
| Anesthesia machine | MiniHub V2.1 gas anesthesia workstation for small animals | TemSega (France) |
| Benchtop centrifuge | Heraeus Fresco 21 Micro Centrifuge | Thermo Fisher (United States) |
| Cell Counter | NucleoCounter NC-250 | ChemoMetec (Denmark) |
| Centrifuge | Heraeus Multifuge 3 S-R Refrigerated Centrifuge | Thermo Fisher (United States) |
| Flow cytometer | BD LSRFortessa | Becton Dickinson (United States) |
| Incubator | Heracell VIOS 160i CO2 incubator single chamber | Thermo Fisher (United States) |
| Microscopes | BX41 light microscope | Olympus (Germany) |
| | EVOS M700 | Thermo Fisher (United States) |
| Multiplex reader | Bio-Plex MAGPIX Multiplex Reader | BIO-RAD (United States) |
| NanoDrop | NanoDrop One Microvolume UV-Vis Spectrophotometer with WiFi | Thermo Fisher (United States) |
| pH meter | FiveEasy Plus pH meter FP20-Std-Kit | Mettler Toledo (United States) |
| Pipettes | Eppendorf Reference® 2, 0,5 – 10 µL pipette | Eppendorf (Germany) |
| | Eppendorf Reference® 2, 10 – 100 µL pipette | |

| | Eppendorf Reference® 2, 100 – 1,000 μL pipette | |
| --- | --- | --- |
| | Eppendorf Reference® 2, 2 – 20 μL pipette | |
| | Eppendorf Reference® 2, 20 – 200 μL pipette | |
| qPCR machines | QuantStudio™ 3 Real-Time PCR System, 96-well, 0.1 mL | Thermo Fisher (United States) |
| | StepOne™ Real-Time PCR System, laptop | |
| Seahorse | Seahorse XFe96 Analyzer | Agilent (United States) |
| Serological pipet | Pipetboy | Integra (Germany) |
| Sterile workbench | Heraeus MSC-Advantage Class II Biological Safety Cabinets | Thermo Fisher (United States) |
| Thermocycler | Veriti Thermal Cycler | |
| Tissue dissociator | gentleMACS Dissociator | Miltenyi Biotech (Germany) |
| Tissue ruptor | Tissue Ruptor II | Qiagen (Germany) |
| Tube rotator | MACSmix Tube Rotator | Miltenyi Biotech (Germany) |
| Vortex | Vortex Genie 2 | Thermo Fisher (United States) |

## 2.1.2 Reagents and consumables

| Designation | Catalog number | Company |
|---|---|---|
| 100µm cell strainer, yellow | 83.3945.100 | Sarstedt (Germany) |
| 10ml serological pipettes | 607 180 | Greiner Bio-One (Germany) |
| 12ml cell culture tube | 164160 | |
| 15ml conical bottom tube | 188 271 | |
| 25ml serological pipettes | 760 180 | |
| 48 Well Cell Culture Plate F-bottom | 677 102 | |
| 50ml conical bottom tubes | 227 261 | |
| 50ml serological pipettes | 768 180 | |
| 5x first strand buffer | P/NY02321 | Life Technologies (United States) |
| 96 Well Cell Culture Plate F-bottom | 655 180 | Greiner Bio-One (Germany) |
| 96 Well Cell Culture Plate U-bottom | 650 180 | |
| Agilent Seahorse XF96 cell culture Microplate | 101085-004 | Agilent (United States) |
| Agilent Seahorse XFe96 FluxPaks | 102416-100 | |
| Anti-F4/80 MicroBeads | 130-110-443 | Miltenyi Biotech (Germany) |
| Antimycin A from Streptomyces sp. | A8674-100MG | Sigma Aldrich (United States) |
| Aprotinin | 10236624001 | Merck (Germany) |
| BD Eclipse Needle 23G | 305892 | Becton Dickinson (United States) |
| BD Eclipse Needle 27G | 305770 | |
| BD Vasculon Plus 26G | 393300 | |
| Bio-Plex Pro Mouse Cytokine 23-plex Assay | #M60009RDPD | BIO-RAD (United States) |
| Bovine Serum Albumin (BSA) | A7030-50G | Sigma Aldrich (United States) |

| | | |
|---|---|---|
| Butterfly needle 21G | 4056520-01 | Braun (Germany) |
| C Tubes | 130-093-237 | Miltenyi Biotech (Germany) |
| CD19 MicroBeads | 130-121-301 | |
| Collagenase D | 11088866 | Merck (Germany) |
| Columbia Agar with Sheep blood Plus | PB5039A | Oxoid (Germany) |
| Dispase II | 4942078001 | Roche (Switzerland) |
| DMEM (dulbeco´s modified eagles' medium) | 11960085 | Life Technologies, Gibco (United States) |
| DMSO (dimethylsulfoxide) | D2650-5X5ML | Sigma-Aldrich (United States) |
| DNAse | 1853502 | Serva (Germany) |
| dNTP (deoxynucleotide triphosphate) Mix 10µM each | 18427013 | Thermo Fisher (United States) |
| DTT (dithiothreitol) | O/NY00147 | Life Technologies (United States) |
| EDTA (ethylenediaminetetraacetic acid) | 108418 | Merck (Germany) |
| FACS Clean solution | 340345 | Becton Dickinson (United States) |
| FACS Rinse solution | 340346 | |
| Falcon 5ml Round Bottom Polystyrene Test Tube, with Cell Strainer Snap Cap | 352235 | Corning (United States) |
| FBS (Fetal Bovine Serum) | 10270-106 | Life Technologies, Gibco (United States) |
| FCCP (carbonyl cyanide-p-trifluoromethoxyphenylhydrazone) | Ab141229 | Abcam (United Kingdom) |
| Fixation/Permeabilization Solution Kit with BD GolgiPlug | 555028 | Becton Dickinson (United States) |
| Gamunex 10% | | Grifols (Spain) |
| HBSS (hanks buffered saline solution) | 14175-053 | Life Technologies, Gibco (United States) |

| | | |
|---|---|---|
| HCl_hydrochloric acid solution 0,1M 50ml | 2104 | Sigma-Aldrich (United States) |
| HEPES buffer (4-(2-hydroxyethyl)-1-piperazineethanesulfonic acid) | 15630080 | Life Technologies, Gibco (United States) |
| Injekt Solo 2-piece single-use syringe 20ml | 4606205V | Braun (Germany) |
| Insulin syringe for U-100 Insulin (1ml / 100 I.U.) | 9161708V | |
| Isoflurane 250ml | | Baxter (United States) |
| Ketaset 100mg/ml injection solution | | Zoetis (United States) |
| *Klebsiella Pneumoniae* | 700721 | American Type Culture Collection (United States) |
| LB medium | X968.1 | Carl Roth (Germany) |
| LD columns | 130-042-901 | Miltenyi Biotech (Germany) |
| Leupeptin | L2884-1MG | Merck (Germany) |
| Lysing buffer 10x for RBC | 555899 | Becton Dickinson (United States) |
| MACS multi stand | 130-042-303 | Miltenyi Biotech (Germany) |
| Magnesium chloride | 208337-1KG | Sigma-Aldrich (United States) |
| Micro tube 0.5ml | 72.698 | Sarstedt (Germany) |
| Micro tube 1.3ml K3E | 411504005 | |
| Micro tube 1.5ml | 72.690.001 | |
| MicroAmp™ Clear Adhesive Film | 4306311 | Applied Biosystems (United States) |
| MicroAmp™ Fast Optical 96-Well Reaction Plate, 0.1 mL | 4346907 | |
| Microscope slides 3x1 inch. Ground edges | 03-0013/45 | R. Langenbrinck GmbH (Germany) |

| | | |
|---|---|---|
| MiDi MACS | 130-042-301 | Miltenyi Biotech (Germany) |
| M-MLV Reverse Transcriptase Buffer | 18057018 | Thermo Fisher (United States) |
| Mouse Intubation Pack | 000A3747 | Hallowell EMC (United States) |
| MS columns | 130-042-201 | Miltenyi Biotech (Germany) |
| NaCl | 3957.1 | Carl Roth (Germany) |
| NaCl 0,9% 100ml injection solution | | Braun (Germany) |
| NC-slide A8 | 942-0003 | ChemoMetec (Denmark) |
| Nuclease-free water | | Merck (Germany) |
| Octo MACS | 130-042-108 | Miltenyi Biotech (Germany) |
| Oligomycin A | Ab143423 | Abcam (United Kingdom) |
| PBS (phosphate-buffered saline) | D1408-500ML | Merck (Germany) |
| PCR 8er-CapStrips, colorless, domed | 711040 | Biozym (Germany) |
| PCR 8er-SoftStrips, 0.1 ml, colorless | 711150 | |
| Penicillin-Streptomycin 5000 U/ml | P0781-100ML | Sigma-Aldrich (United States) |
| Pepstatin A | 10253286001 | Merck (Germany) |
| pipette tips 1000µl, blue | 70.762.010 | Sarstedt (Germany) |
| pipette tips 10µl, white | P866.1 | Carl Roth (Germany) |
| pipette tips 200µl, yellow | 70.760.012 | Sarstedt (Germany) |
| *Pseudomonas Aeruginosa* cryo stock (PA103) | | own breading |
| RNaseOUT™ Recombinant Ribonuclease Inhibitor | 10777019 | Life Technologies (United States) |

| RNeasy MicroKit | 74004 | Qiagen (Germany) |
|---|---|---|
| RNeasy Mini Kit | 74104 | |
| Rotenone | R8875-1G | Sigma-Aldrich (United States) |
| RPMI 1640 Medium, no glutamine | 31870-074 | Life Technologies, Gibco (United States) |
| RPMI medium | 31870-074 | |
| Seahorse XF base medium 500 ml | 103334-100 | Agilent (United States) |
| Seahorse XF Calibrant Solution 500 mL | 100840-000 | |
| Solution 12 DAPI (4′,6-diamidino-2-phenylindole) | 910-3012 | ChemoMetec (Denmark) |
| SYBR Green | 172-5124 | BIO-RAD (United States) |
| Tris | 4855.2 | Carl Roth (Germany) |
| Xylariem 20mg injection solution | | Ecuphar GmbH (Germany) |

## 2.1.3 Buffers and media

Digestion buffer for liver and spleen (Stamatiades et al., 2016):

| Reagent | Concentration |
|---|---|
| HBSS | |
| Collagenase D | 1 mg/ml |
| Dispase II | 2,4 U/ml |
| DNAse | 100 U/ml |
| FBS | 3% |

Digestion buffer for kidneys:

| Reagent | Concentration |
|---|---|
| HBSS | |
| Collagenase D | 3 mg/ml |
| Dispase II | 2,4 U/ml |

| Reagent | Concentration |
|---|---|
| DNAse | 1000 U/ml |
| FBS | 3% |
| CaCl$_2$ | 5 mM |

Greenberger lysis buffer (Ramakers et al., 2007):

| Reagent | Concentration |
|---|---|
| distilled water | |
| NaCl | 300 mmol/l |
| Tris | 15 mmol/l |
| MgCl$_2$ | 2 mmol/l |
| Triton X 100 | 2 mmol/l |
| Pepstatin A | 20 ng/ml |
| Leupeptin | 20 ng/ml |
| Aprotinin | 20 ng/ml |

Culture medium for macrophages:

| Reagent | Concentration |
|---|---|
| RPMI 1640 medium | |
| FBS | 2,5% |
| Penicillin/Streptomycin | 1% |
| HEPES buffer | 2,5% |

Assay medium for bacterial killing:

| Reagent | Concentration |
|---|---|
| RPMI 1640 medium | |
| FBS | 2,5% |
| HEPES buffer | 2,5% |

FACS (fluorescence-activated cell sorting) buffer:

| Reagent | Concentration |
|---|---|
| PBS | |
| FBS | 10% |
| NaN$_3$ | 0,1% |

MACS (magnetic cell separation) buffer:

| Reagent | Concentration |
|---------|---------------|
| HBSS | |
| EDTA | 2 mM |
| BSA | 0,5% |

## 2.1.4 FACS dyes & antibodies

| Target | Fluorochrome / dye | Clone | Isotype | Host species | Company | Catalog number |
|--------|--------------------|-------|---------|--------------|---------|----------------|
| CD11b | FITC | M1/70 | IgG$_{2b}$, κ | rat | BioLegend | 101206 |
| CD11c | PE | HL3 | IgG$_1$, λ2 | armenian hamster | Becton Dickinson | 557401 |
| CD45 | PE | 30-F11 | IgG$_{2b}$, κ | rat | | 553081 |
| CD45 | APC Cy7 | 30-F11 | IgG$_{2b}$, κ | | BioLegend | 103116 |
| F4/80 | FITC | BM8 | IgG$_{2a}$, κ | | | 123108 |
| F4/80 | BV 605 | T45-2342 | IgG$_{2a}$, κ | | Becton Dickinson | 743281 |
| IL-1ß | APC | NJTEN3 | IgG$_1$, κ | | Thermo Fisher | 17-7114-80 |
| IL-6 | APC | MP5-20F3 | IgG$_1$ | | Becton Dickinson | 561367 |
| Ly6C | PE Cy7 | HK1.4 | IgG$_{2c}$, κ | | BioLegend | 128018 |
| Ly6G | APC | 1A8 | IgG$_{2a}$, κ | | | 127614 |
| Mitochon-drial ROS | MitoSOX Red | | | | Thermo Fisher | M36008 |
| Nucleic acid | Sytox - Pacific Blue | | | | BioLegend | 425305 |
| TNF-α | APC | MP6-XT22 | IgG$_1$ | rat | Becton Dickinson | 561062 |

## 2.1.5 Primers

All primers were designed with NCBI Primer Blast to span an exon-exon junction and purchased from MetaBion (Germany).

| Gene | Forward sequence 5´ - 3´ | Reverse sequence 5´ - 3´ |
|---|---|---|
| ACOD-1 / IRG-1 | AGT TTT CTG GCC TCG ACC TG | CGG GAA GCT CTT AAA GGC CA |
| ß-Actin | ACC CTA AGG CCA ACC GTG A | CAG AGG CAT ACA GGG ACA GCA |
| Enolase-1 | AGG AAG ACA GAG TGG GAG GC | GGC GGA TTT CTG GCA GTA GG |
| HK-2 (Hexokinase-2) | TCG GTT TCT CTA TTT GGC CCC | GAG ATA CTG GTC AAC CTT CTG C |
| IL-10 | GGC AGA GAA GCA TGG CCC AGA A | AAT CGA TGA CAG CGC CTC AGC C |
| IL-1β | CCT TGT GCA AGT GTC TGA AGC | GTC ATC ACT GTC AAA AGG TTG C |
| IL-6 | GTC TGC AAG AGA CTT CCA TCC | GTC TGT GAA GTC TCC TCT CCG |
| IDH-1 | CAG TCG CCC AAG GTT ATG GC | TGG TAC ATG CGG TAG TGA CG |
| KC (keratinocyte-derived chemokine) | GAC GAG ACC AGG AGA AAC AGG GTT | AAC GGA GAA AGA AGA CAG ACT GCT |
| Pfkfb 3 (Phosphofructo-kinase / fructose-2,6-bisphosphatase 3) | GAC GAC CCT ACT GTT GTG GC | GGG TCA AGA GGC TGG TAG C |
| TNF-α | GCC TCT TCT CAT TCC TGC TT | TGG GAA CTT CTC ATC CCT TTG |

## 2.2 Methods

### 2.2.1 Mice & animal experiments

### 2.2.1.1 Mice

Female C57BL/6N mice, aged 10-12 weeks, were purchased from Charles River Laboratories. Mice were housed under a standard day/night rhythm under specific pathogen-free conditions. Standard rodent chow and water were available ad libitum. All animal experiments were performed in compliance with the guidelines required by law from the Regierungspräsidium Gießen (G42/2018).

### 2.2.1.2 HCl application

Mice were anesthetized with isoflurane and intubated. The catheter was placed proximal to the carina to affect both lungs. For induction of acid pneumonitis 50µl of 0,1M HCl were administered. Respectively, 50µl of 0,9% NaCl were administered for sham treatment.

### 2.2.1.3 Harvest of solid organs

Mice were euthanized with an intraperitoneal injection of ketamine/xylazine (dosage see below), followed by neck dissection. The mice were then placed in a supine position, the limbs were fixated, and the abdomen and thorax were disinfected with 70% ethanol. Subsequently, the abdomen was opened, and blood was sampled via the inferior caval vein (see chapter 2.2.1.4). When blood sampling was omitted, the inferior caval vein was cut to exsanguinate the mice. Afterward, the diaphragm was carefully punctured with scissors. Subsequently, the thorax was opened in the cranial direction beginning at the xiphoidal processus. Then, the left ventricle was punctured with a butterfly needle, connected to a syringe prefilled with 25ml cooled HBSS, and the systemic circulation was flushed with a flow rate of 1ml per second. Flushing was considered successful when the liver was completely bleached. Subsequently, the organs were extracted, the gall bladder was removed from the liver and adipose tissue was removed from the kidneys. The liver was placed in a 15ml conical bottom tube filled with 3ml HBSS, and the kidneys and the spleen were placed in 1,5ml micro tubes filled with 1ml HBSS. All organs were stored on ice until the organ harvesting was completed. Both kidneys from one mouse were harvested, and cells were pooled and analyzed as one sample.

The following anesthesia was used with a dose of 160µl per 20g bodyweight:

- NaCl 0,9%          75%

- Ketamine        12,5%

- Xylazine        12,5%

**2.2.1.4 Blood sampling**

A 1,3ml ETDA tube was prefilled with 200µl NaCl 0,9%, closed, and shaken a few times to bring the ETDA into solution. Afterward, a 23G needle was placed on a one ml syringe and the ETDA-NaCl was aspirated into the syringe. Then the animals were euthanized and processed as described in 2.2.1.3. When blood sampling was required, the exposed inferior caval vein was not cut but punctured with the previously prepared 23G needle connected to a syringe containing the EDTA-NaCl solution. Blood was slowly aspirated. When a volume of one ml was reached or no more blood could be aspirated, blood sampling was stopped, the syringe disconnected from the needle, and the EDTA blood was immediately transferred to the respective 1,3ml EDTA tube, and stored in a fridge (4°C) until further processing. To obtain the plasma, blood samples were centrifuged at 2.500rpm (rounds per minute) for 10 minutes at 4°C. Supernatants were transferred in 1,5ml micro tubes and immediately frozen at -80°C.

**2.2.1.5 Peritoneal lavage**

After the mice were euthanized, they were placed in a supine position, and their limbs were fixated. The abdomen was disinfected with 70% ethanol afterward, and the abdominal fur and skin were carefully removed to visualize the peritoneum. Then the peritoneum was punctured with a 26G needle connected to a syringe prefilled with 8ml cooled HBSS which was carefully injected into the peritoneal cavity. The fixation of the lower extremities was loosened afterward, the mice were grasped at the proximal end of the tail and gently shaken 20 times. Then the mice were placed in the right lateral position and the extremities were fixated again. The peritoneum was punctured with a 23G needle connected to a new syringe. The needle was gently pulled in a ventral direction and the lavage fluid was carefully aspirated, transferred in a 50ml conical bottom tube, and stored on ice.

**2.2.1.6 Whole organ homogenates**

A 12ml cell culture tube was filled with 500µl PBS and thereafter the respective organ was added. Then the organ was dissociated with a Tissue Ruptor for approximately 10 seconds with maximal strength. 30 µl from the generated homogenate were pipetted in a 1,5ml micro Tube prefilled with 350µl RLT buffer. The micro tube was closed and

vortexed with maximal strength for 30 seconds immediately afterward and then frozen at -80°C. Another 100µl of the homogenate were pipetted in a 1,5ml micro tube filled with 900µl Greenberger lysis buffer (Ramakers et al., 2007). After incubating for one hour on ice, the tube was centrifuged at 3.000g for 7 minutes and directly afterward at 14.000rpm for 10 minutes. The supernatant was transferred to another 1,5ml micro tube and stored at -80°C.

### 2.2.2 Macrophage isolation

### 2.2.2.1 Cell counting

19µl of the respective cell suspension were mixed with 1µl DAPI solution in a 0,5ml micro tube. Now, 10µl of the mixture were transferred in a respective counting slide chamber and analyzed with an NC-250 NucleoCounter and NucleoView software.

### 2.2.2.2 Isolation of liver macrophages

After extraction, the liver was placed in a petri dish and cut into smaller pieces which were then transferred into a gentleMACS C Tube. After adding 5ml of digestion buffer, the C tube was incubated for 5 minutes at 37°C and 5% $CO_2$. Now the organ fragments were dissociated on a gentleMACS Dissociator. Afterward, the C tube was placed in a MACSmix Tube Rotator, which was set to maximum speed, and placed in an incubator for 25 minutes at 37°C and 5% $CO_2$. Then, the content of the C tube was rinsed through a 100µm filter placed on a 50ml conical bottom tube to remove undigested tissue residues. The C tube was filled with 7,5ml RPMI medium and gently shaken a few times. Also, the medium was rinsed through the filter. The processing of the created single-cell suspension was in principle performed as described by Li and colleagues (Li et al., 2014). In brief, the cell suspension was centrifuged at 300g for 5 minutes at 10°C, the supernatant removed and the pellet resuspended in 10ml RPMI medium. This was performed twice. Then the cell suspension was centrifuged at 50g for three minutes at 10°C to enrich non-parenchymatous cells, which stayed in the supernatant while the bigger hepatocytes pelletized. The supernatant was transferred to a new 50ml conical bottom tube and the cell number was determined.

Macrophages were isolated by using anti-F4/80 MicroBeads according to manufacturers' instructions. In brief, the previously generated single-cell suspensions were centrifuged and resuspended in MACS buffer and MicroBeads, both adjusted to the cell number. After 15 minutes of incubation in a fridge, cell suspensions were washed with MACS buffer

and then rinsed through magnetic MS columns in which MicroBead-labeled cells were retained.

### 2.2.2.3 Isolation of kidney macrophages

After harvesting both kidneys, the organs were placed in a petri dish and cut into smaller pieces. Then, 5ml of prewarmed kidney digestion buffer were added to the petri dish and the organ fragments were minced in pieces <1mm with the plunger of a syringe. The content of the petri dish was transferred in a gentleMACS C tube and dissociated on a gentleMACS Dissociator. Afterward, it was placed in a MACSmix Tube Rotator, set to maximum speed, and incubated at 37°C and 5% $CO_2$ for 30 minutes. Now the content of the C tube was rinsed through a 100µm filter placed on a 50ml conical bottom tube. The C tube was then filled with 7,5ml RPMI medium, shaken gently a few times, and the medium was also rinsed through the filter. The suspension was centrifuged at 50g for three minutes at 10°C. This centrifugation step resulted in single cells remaining in the supernatant while undigested tissue fragments were pelletized (Li et al., 2014). The supernatant was transferred in a 15ml conical bottom tube and the cell number was determined. Subsequently, macrophages were isolated via positive selection using anti-F4/80 MicroBeads as described.

### 2.2.2.4 Isolation of peritoneal macrophages

For qPCR: after performing a peritoneal lavage, the cell number was determined. First B-lymphocytes were depleted by using CD19-MicroBeads and LD columns according to manufacturers' instructions. Afterwards, cell numbers were determined in the flow-through, now depleted from B-lymphocytes. Macrophages were isolated in a positive selection using anti-F4/80 MicroBeads and MS columns according to manufacturers´ instructions. In brief, the B cell-depleted cell suspension was centrifuged and resuspended in F4/80 MicroBead solution. After the incubation time, the cell solution was washed and rinsed through MS columns. F4/80 labeled cells were retained in the column and washed out in the final step. This method achieved a very high purity of cells (98-99%) but low numbers (~ $1*10^5$ per animal). Therefore, a different approach was used for functional *ex vivo* assays.

For *ex vivo* assays: the cell number in the peritoneal lavage was determined and afterward, the lavage fluid was centrifuged at 500g for 10 minutes at 10°C. Now cells were resuspended in a volume of culture medium which resulted in a cell concentration of

$4*10^5$ cells per 100µl. Then cells were seeded with $4*10^5$ cells per well in a 96-well plate. After three hours of incubation, cells were washed with NaCl 0,9% to remove all non-adherent cells.

## 2.2.2.5 Isolation of splenic macrophages

For qPCR: after organ harvest, the spleen was cut into smaller pieces in a petri dish. The fragments were transferred into a 1,5ml micro tube and one ml of digestion buffer was added. The micro tube was incubated at 37°C and 5% $CO_2$ for 30 minutes. Then the content from the micro tube was transferred to a gentleMACS C tube and 4ml RPMI medium were added. The organ was dissociated with a gentleMACS Dissociator two times in a row. The content of the C tube was rinsed through a 100µm filter placed on a 50ml conical bottom tube.

Subsequently, an LD column was rinsed with two milliliters of MACS buffer. Afterward the single-cell suspension, without being labeled with MicroBeads before, was rinsed through the columns, thereby retaining all intrinsically magnetic cells, including red pulp macrophages due to their ferromagnetic properties (Franken et al., 2015) and mainly erythrocytes due to a markedly low flow rate. Then the LD column was rinsed with two ml MACS buffer and afterward retained material was eluted with 4ml MACS buffer in a 15ml conical bottom tube. The cell number was determined, and macrophages were isolated by positive selection using anti-F4/80 MicroBeads and MS columns according to manufacturers' instructions as described above. Due to the higher flow rate, non-labeled cells were lost. Macrophages were eluted from the MS column in a 15ml conical bottom tube and their number was determined. This method achieved a high purity of cells (~ 93%) but generated low numbers of cells (~$2*10^5$ per animal) and was therefore not used for *ex vivo* assays.

For *ex vivo* assays: To obtain spleen macrophages for *ex vivo* assays, we made use of the strong adherence of macrophages. Spleen homogenates were generated as described above. Now the homogenates were centrifuged at 500g for 10 minutes at 10°C and resuspended in two ml of red blood cell (RBC) lysis buffer. After two minutes of incubating at room temperature, 10ml of culture medium were added to stop the lysis reaction. Then cell numbers were determined and homogenates were washed once with NaCl 0,9%. Afterward, homogenates were centrifuged at 500g for 10 minutes at 10°C and resuspended in a volume of culture medium which resulted in a cell concentration of $5*10^5$ cells per 100µl. Finally, cells were seeded in 96-well plates and incubated for two

hours (37°C, 5% $CO_2$), and subsequently washed with NaCl to remove non-adherent cells.

**2.2.2.6 FACS analysis of MicroBead-isolated cells**

After eluting the cells from the MS columns, the cell number was determined. The cell suspension was transferred into a 1,5ml micro tube and centrifuged at 500g for 10 minutes. The supernatant was discarded and the pellet was resuspended in 50µl antibody mix. After 30 minutes of incubation in a fridge protected from light, the cell suspension was centrifuged again at 500g for 10 minutes. The supernatant containing the unbound antibodies was discarded and the pellet was resuspended in 500µl FACS buffer and transferred in polystyrene round-bottom tubes. Sytox was added immediately before analysis.

The antibody mix comprised:

- FACS buffer

- CD45,           PE,           1:100

- F4/80,          FITC,         1:50

- Sandoglobulin,               1:10

- Sytox,          Pacific Blue,  1:1000

The analysis was done with a BD LSRFortessa using FACS DIVA software. Data were analyzed with FlowJo Version 10.6.2

**2.2.3 Transcriptional profile analysis**

**2.2.3.1 Cell lysis for RNA extraction**

After eluting the cells from the MS columns, which were used for the final F4/80 positive selection, in a 15ml falcon tube, their number was determined. Afterward, cells were centrifuged at 500g for 10 minutes at 10°C, the supernatant discarded and the pellet resuspended in 350µl RLT buffer. The RLT buffer containing the cells was transferred in a 1,5ml micro tube, vortexed with maximal strength for 30 seconds, and immediately afterward stored at -80°C. This was performed similarly for all types of macrophages.

## 2.2.3.2 RNA isolation

The ribonucleic acid (RNA) was isolated from macrophages with the RNeasy Micro kit according to the manufactures´ instructions. The only deviation was the use of 20µl RNase-free water to elute the RNA from the Spin-columns in the final step instead of the recommended amount of 14µl. The obtained RNA was immediately used for complementary DNA (cDNA) synthesis.

## 2.2.3.3 cDNA synthesis

**Step 1:**

To synthesize cDNA, the concentration of RNA was determined. Subsequently, the following reaction mix was pipetted for each well of a PCR (polymerase chain reaction) 8-Well SoftStrip:

| Reagent | Concentration / amount | Volume |
|---|---|---|
| RNA | 250ng | calculated from concentration |
| Random Hexamers | 10µM | 1,5µl |
| dNTPs | 10mM each | 1µl |
| Nuclease-free water | | 10µl minus the volume of added RNA eluate |

The volume of RNA eluate to be added was calculated as follows:

$$c = \frac{m}{V} \qquad \text{rearranged to: } V = \frac{m}{c}$$

c = concentration; m = mass (here 250ng); V = volume

If the RNA concentration was 25ng/µl or lower, 10µl of RNA eluate and no nuclease-free water were used.

Afterward, the following program was used:

| 65°C | 5 min |
|---|---|
| 4°C | ∞ |

**Step 2:**

The following reaction mix was added to each well:

| Reagent | Concentration | Volume |
|---|---|---|
| 5x first strand buffer | 5x | 4µl |
| DTT | 0,1 M | 2µl |
| RNase inhibitor | 10 mM | 1µl |
| RT M-MLV | 200 U/µl | 1µl |

Afterward, the following program was used:

| 25°C | 10 min |
|---|---|
| 37°C | 50 min |
| 70°C | 15 min |
| 4°C | ∞ |

The cDNA was stored at -20°C.

**2.2.3.4 qPCR**

The following reaction mix was used for each well in a 96-well qPCR (quantitative PCR) plate:

| Sybr Green 2x | 5µl |
|---|---|
| forward Primer | 0,2µl |
| reverse Primer | 0,2µl |
| nuclease-free water | 3,6µl |
| cDNA | 1µl |

A master mix comprising Sybr Green, forward and reverse primer as well as nuclease-free water was created for each primer pair and pipetted in the respective wells of a 96-well qPCR reaction plate. One µl of cDNA was added afterward, the plate was then sealed and centrifuged at 1.000g for one minute. Each target gene in a sample was analyzed in three technical replicates. The housekeeping gene was ß-actin. The following program was used for the PCR reaction:

| 95°C | 10 min |
|------|--------|
| 95°C | 15 sec |
| 60°C | 1 min |
| 95°C | 15 sec |
| 60°C | 1 min |
| 95°C | 15 sec |

40x

qPCR data were analyzed with the ΔΔCt method and the results are shown as fold changes to sham treatment (Livak and Schmittgen, 2001).

### 2.2.4 Follow-up analysis

### 2.2.4.1 Multiplex cytokine analysis

Protein concentrations of selected cytokines and chemokines were measured via Bio-Plex Multiplex Immunoassay System, using a Bio-Plex MAGPIX Multiplex Reader (BIO-RAD) and a 23-plex assay kit according to manufacturers' instructions. Data were analyzed with Bio-Plex Data Pro software.

### 2.2.4.2 Seahorse extracellular flux analysis

One day before the actual extracellular flux (XF) analysis was performed, a calibration plate was prepared by adding 200µl of XF calibrant solution to each well and placed in a $CO_2$-free incubator (37°C) overnight.

Preparation of the media and injections: the pH of media was adjusted to 7,4. Injections were prepared in assay medium as a stock solution with the following concentrations before being added to the respective chambers:

- oligomycin:               8µM

- FCCP:                     36µM

- rotenone & antimycin:     10µM each

Assay procedure:

Liver TRMs were isolated as described in 2.2.2.2 and seeded at $1*10^5$ live cells per well in a Seahorse XF96 cell culture microplate with culture medium. After three hours of incubation (37°C, 5% $CO_2$) cells were washed three times with Seahorse XF base medium, and subsequently, 175µl assay medium (minimal DMEM without glucose, pH

7,4) were added. Now, cells were incubated (37°C) in the absence of $CO_2$ for 30 minutes. In the meantime, the previously prepared calibration plate was run on the Seahorse XFe96 Analyzer. For the mitochondrial stress test the following injections were used for each well:

| Number of the injection | Reagent | Volume | Final concentration in each well |
|---|---|---|---|
| 1 | oligomycin | 25µl | 1µM |
| 2 | FCCP | 25µl | 4µM |
| 3 | rotenone & antimycin | 25µl | 1µM each |

Data were analyzed with Wave Desktop Software version 2.6.1 and are shown with GraphPad Prism 7.

### 2.2.4.3 Bacterial killing assay

*P. aeruginosa* bacterial solution:

A cryo-stock of *P. aeruginosa* was thawed and one plastic bead was added in 50ml of Luria Broth (LB) medium. After 16 hours of incubation (37°C, 5% $CO_2$) while constantly shaking, one ml of the bacterial solution was added to 100ml of LB medium. After another 6 hours of incubation (37°C, 5% $CO_2$) while constantly shaking, optic density (OD) was measured. When an OD of two was reached, the bacterial solution was transferred in two 50ml falcon tubes, centrifuged at 4000rpm for 10 minutes at 10°C. The supernatant was discarded and the pellet was resuspended in 50ml NaCl. This was repeated for a total amount of three spinning cycles. After the third centrifugation, the pellets were resuspended in 5ml NaCl 0,9% each and pooled. The bacterial solution was now diluted at 1:2000 to reach a final concentration of $1*10^7$ colony forming units (CFU) per ml.
To verify the inoculum, a dilution series of the previously generated bacterial solution was created with a dilution factor of 10. The diluting medium was NaCl 0,9%. From each dilution step, 10µl were pipetted on blood agar plates in duplicates and incubated overnight (37°C, 5% $CO_2$).

*Klebsiella pneumoniae (K. pneumoniae)* bacterial solution:

A cryosolution was thawed at room temperature to inoculate a blood agar plate, which was then incubated (37°C, 5% $CO_2$) overnight. Multiple single colonies were then picked and transferred in two ml of LB medium and incubated (37°C, 5% $CO_2$) overnight while shaking at 180rpm. On the following day, 8ml of new LB medium was added. Now the bacterial solution was again incubated (37°C, 5% $CO_2$) while shaking for 90 minutes, resulting in an OD of approximately 1,8 to 1,9. Then the bacterial solution was centrifuged at 4.500g for 10 minutes. The pellet was resuspended in 10ml NaCl 0,9% and subsequently, diluted with NaCl 0,9% until an OD of 1 was reached. to obtain a final concentration of $5,5*10^8$ CFU/ml.

To verify the inoculum, a dilution series of the previously generated bacterial solution was created with a dilution factor of 10 in NaCl 0,9%. From each dilution step, 10µl were pipetted on blood agar plates in duplicates and incubated overnight (37°C, 5% $CO_2$).

Assay procedure:

Macrophages were isolated as previously described and seeded in two 96-well U-bottom plates (labeled T0 and T1) with $1*10^5$ live cells per well in culture medium with three wells per condition on each plate. After three hours of incubation (37°C, 5% $CO_2$), cells on both plates were washed 4 times with 200µl NaCl 0,9% to remove the antibiotics from the culture medium. Now, 190µl of killing-assay medium were added to each well. Afterward, 10µl of *P. aeruginosa* bacterial solution were added to create a multiplicity of infection (MOI) of one. For splenic or peritoneal macrophages volumes were respectively altered to generate a MOI of 5. After 90 minutes of incubation (37°C, 5% $CO_2$), cells on both plates were washed 4 times with 200µl NaCl 0,9% to remove all extracellular bacteria. In each well from plate T1 200µl of assay medium were added and the plate was incubated for another hour (37°C, 5% $CO_2$). Cells on plate T0 were lysed immediately after the washing steps by adding 200µl of distilled water to each well followed by thorough up and down pipetting for 5 minutes. Four times 10µl of undiluted and 1:10 diluted lysate fluid from each well were applied on blood agar plates, which were incubated (37°C, 5% $CO_2$) overnight. After an additional hour of incubation, cells on plate T1 were lysed as described for T0. The next morning, the CFU count was determined. The intracellular bacterial load at T0 represents the amount of phagocytosed

bacteria while the difference between T0 and T1 illustrates the amount of eradicated bacteria.

The assay was performed identically with *K. pneumoniae* except for the use of a MOI of 10 and respectively altered volumes of medium and bacterial solution.

### 2.2.4.4 Assessment of mitochondrial ROS

Liver TRMs were isolated as described in 2.2.2.2 and seeded with $1,5*10^5$ cells per well in a 48-well plate in 300µl of culture medium with 6 wells per condition and one negative control. After two hours of incubation (37°C, 5% $CO_2$), each well was washed once with PBS, and afterward, heat-killed *P. aeruginosa* was added to the culture medium with a MOI of 100 in three wells of each condition. The remaining wells received new culture medium without bacteria. Following an incubation period of 7 hours, each well was washed with PBS twice, and afterward, 480µl DMSO containing 3,5µM MitoSOX RED was added. After another 20 minutes of incubation, cells were washed twice, scraped off the plate, transferred to FACS tubes, and immediately stored on ice. The analysis was done with a BD LSRFortessa using FACS DIVA software. Data were analyzed with FlowJo Version 10.6.2.

### 2.2.4.5 FACS analysis of peritoneal lavage cells

Peritoneal lavage cells were obtained as described in chapter 2.2.1.5 and transferred in 15ml conical bottom tubes. Then, the lavage fluid was centrifuged at 1.400rpm for 10 minutes at 10°C and the supernatant was discarded. Afterward, the pellet was resuspended in 75µl of antibody mix, transferred in a 1,5ml Micro Tube, and incubated at 4°C for 30 minutes protected from light. The cell suspensions were then centrifuged at 1.400rpm for 10 minutes at 10°C and resuspended in 500µl of FACS buffer and stored in a fridge until analysis. Immediately before the FACS measurements, the cell suspensions were transferred in a 5ml round-bottom polystyrene tube and Sytox was added.

The antibody mix comprised:

- FACS buffer

- CD45,          APC Cy7,      1:100

- Ly6G,          APC,          1:50

- Ly6C,          PE Cy7,       1:50

- F4/80,            BV 605,            1:50

- CD11c,           FITC,              1:50

- CD11b,           PE,                1:50

- Sandoglobulin,                      1:10

- Sytox,           Pacific Blue,      1:1000

The analysis was done with a BD LSRFortessa using FACS DIVA software. Data were analyzed with FlowJo Version 10.6.2.

## 2.2.4.6 FACS analysis of kidney single-cell suspensions

Kidneys were harvested as described in 2.2.1.3 and single-cell suspensions were generated as described in 2.2.2.3. Subsequently, single-cell suspensions were centrifuged with 500g for 10 minutes at 10°C and the supernatant was discarded. Pellets were resuspended in 1ml of 1x RBC lysing buffer and incubated for three minutes while gently shaking. Afterward, 10ml of RPMI medium containing 2% FBS was added to stop the lysis. Cell suspensions were centrifuged at 500g for 10 minutes at 10°C and pellets were resuspended in 10ml of RPMI medium containing 2% FBS. Cell suspensions were again centrifuged with 500g for 10 minutes at 10°C and pellets were resuspended in 100µl of antibody mix. The antibody mix was similar to the one for peritoneal lavage cells as described in 2.2.4.5. After incubating for 30 minutes at 4°C protected from light, the cell suspensions were centrifuged with 1.400rpm for 10 minutes at 10°C, pellets were resuspended in 500µl of FACS buffer and afterward transferred in 5ml round-bottom polystyrene tubes. Sytox was added immediately before the analysis of a sample. The analysis was done with a BD LSRFortessa using FACS DIVA software. Data were analyzed with FlowJo Version 10.6.2

## 2.2.4.7 Intracellular cytokine staining in kidney macrophages

Kidneys were harvested and processed as described in 2.2.4.6. The staining procedure for surface antigens was performed as described in 2.2.4.6 using the same antibody mix but without APC-conjugated antibodies. After 30 minutes of incubation, each sample was divided into three aliquots of similar volume due to all three anti-cytokine antibodies being conjugated with APC. The cell suspensions were then fixed, permeabilized, and stained for intracellular cytokines with the Fixation/Permeabilization Kit according to manufacturers´ instructions.

The antibody mix for intracellular cytokines comprised:

- 1x BD Perm/Wash buffer

- IL-1b or IL-6 or TNF, APC,   1:50

The analysis was done with a BD LSRFortessa using FACS DIVA software. Data were analyzed with FlowJo Version 10.6.2

**2.2.4.8 FACS analysis of liver single-cell suspensions**

Livers were harvested as described in 2.2.1.3 and single suspensions were generated as described in 2.2.2.2. Then, the cell suspensions were centrifuged with 500g for 10 minutes at 10°C and resuspended in 1000µl of RBC lysis buffer, and incubated at room temperature for two minutes while gently shaking. Afterward, 10ml of culture medium was added to stop the lysis reaction, and cell suspensions were washed with PBS. Subsequently, cell suspensions were resuspended in 1500µl of MACS buffer and split into two aliquots: 1000µl for macrophage staining and 500µl for neutrophil staining. After centrifugation with 500g for 10 minutes at 10°C, cells were resuspended in 100µl of antibody mix and incubated for 30 minutes at 4°C protected from light. Finally, cell suspensions were centrifuged and resuspended in 500µl of FACS buffer.

The antibody mix for macrophage staining comprised:

- FACS buffer

- CD45,          APC Cy7,     1:100

- Ly6C,          PE Cy7,       1:50

- F4/80,         BV 605,       1:50

- MHC II,        FITC,          1:50

- Tim4,          PE,             1:50

- Sandoglobulin,               1:10

- Sytox,         Pacific Blue,  1:1000

The antibody mix for neutrophil staining comprised:

- FACS buffer

- CD45,             APC Cy7,       1:100

- Ly6G,             APC,           1:50

- CD11b,            PE,            1:50

- Sandoglobulin,                   1:10

- Sytox,            Pacific Blue,   1:1000

The analysis was done with a BD LSRFortessa using FACS DIVA software. Data were analyzed with FlowJo Version 10.6.2

## 2.2.5 Histology

After harvesting livers or kidneys, the organs were immediately transferred to 4% paraformaldehyde (PFA) and incubated overnight. The following day, they were embedded in paraffin. The organ, now contained in a paraffin cube, was cooled to 4°C and sliced with a thickness of 3,5µm. The sections were collected in a water bath (37°C) and afterward transferred on glass slides. The slides were dried at 37°C overnight.

Hematoxyline & eosin (HE) staining was done with the following reagents for indicated time points.

| Reagent | Time (minutes) |
|---|---|
| NeoClear | 05:00 |
| NeoClear | 05:00 |
| Ethanol 100% | 00:30 |
| Ethanol 100% | 00:30 |
| Ethanol 96% | 00:30 |
| Ethanol 96% | 00:30 |
| Ethanol 70% | 00:30 |
| Ethanol 70% | 00:30 |
| Hematoxylin | 03:00 |
| HCl 0,1% | 00:02 |
| Flowing faucet water | 03:00 |
| Eosin | 03:00 |
| Flowing faucet water | 00:30 |
| Ethanol 70% | 00:30 |

| Ethanol 96% | 00:30 |
|---|---|
| Ethanol 100% | 00:30 |
| Ethanol 100% | 00:30 |
| Ethanol 100% | 02:00 |
| NeoClear | 05:00 |
| NeoClear | 05:00 |

Kidney and liver slides were analyzed by a veterinary pathologist via light microscopy in a blinded fashion.

## 2.2.6 Measurement of kidney and liver function parameters from plasma

Plasma samples were measured by the central laboratory of the university hospital of Gießen for the determination of aspartate transaminase (AST, glutamic oxaloacetic transaminase, GOT), alanine transaminase (ALT, glutamate-pyruvate transaminase, GPT), creatinine, and urea were measured.

The GOT/AST activity, as well as the GPT/ALT activity, were measured using the Siemens reagent on the ADVIA XPT analyzer from Siemens (ASTP5P method). The creatinine concentration was measured using Siemens enzymatic reagent on the ADVIA XPT analyzer from Siemens. The enzymatic creatinine-2 method was based on the enzymatic reactions described by Fossati, Prencipe, and Berti. The urea concentration was measured using the Siemens reagent on the ADVIA XPT analyzer from Siemens. The analysis was done using the ADVIA Chemistry Urea Nitrogen Concentrate 1.

## 2.2.7 Statistics

Statistical analysis was done with Microsoft Excel version 2019 and GraphPad Prism version 7.00. Descriptive statistics is done by displaying all data as mean with the standard error of the mean (SEM) unless stated otherwise.

Statistical interference was done by an unpaired two-tailed Student´s t-test or a two-way ANOVA analysis. All results with a p-value $\leq$ 0,05 were considered statistically significant. Significance is shown as follows:

* indicating $p \leq 0,05$, ** indicating $p \leq 0,01$, *** indicating $p \leq 0,001$

# 3. Results

## 3.1 Flow cytometric analysis of MicroBead-isolated TRMs

In the first step, we assessed the quality of the MicroBead-based isolation of TRMs. Therefore, microbead-isolated macrophages were analyzed with flow cytometry for the expression of macrophage surface markers. Thereby a uniform cell population expressing high levels of CD45 and F4/80 was detected in preparations from each organ (Fig. 3.1 A-D).
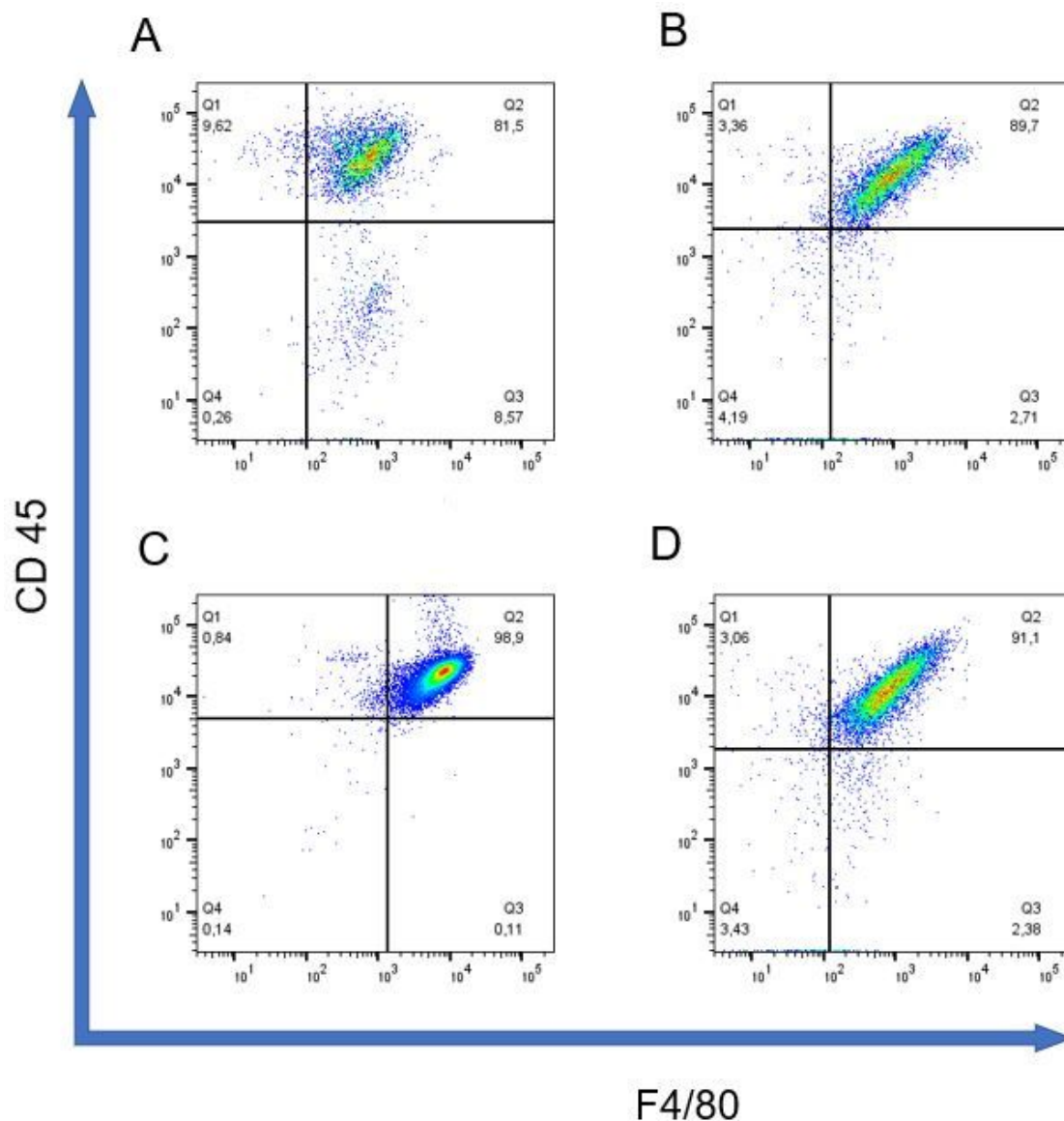


**Figure 3.1 Flow cytometry of MicroBead-isolated cells.** The isolated cells were gated as follows: after the exclusion of debris, doublets, and dead cells (Sytox[pos]), cells were analyzed for CD45 (y-axis) and F4/80-expression (x-axis). Shown are kidney (**A**), liver (**B**), peritoneal (**C**), and splenic (**D**) TRMs.

## 3.2 Kidney

### 3.2.1 Transcriptional profile of kidney macrophages

Kidneys were harvested from mice after sham or acid treatment and renal TRMs were isolated. The expression of key metabolic enzymes, as well as hallmark cytokines, was subsequently analyzed by real-time PCR.

Kidney TRMs did not show altered transcriptional levels of key metabolic enzymes 24h after acid aspiration compared to kidney TRMs of sham-treated animals (Fig. 3.2 A). In contrast, there was a strong upregulation of pro-inflammatory cytokines, namely IL-1ß, IL-6, and TNF-α. The anti-inflammatory cytokine IL-10 was also upregulated without reaching statistical significance (Fig. 3.2 B).
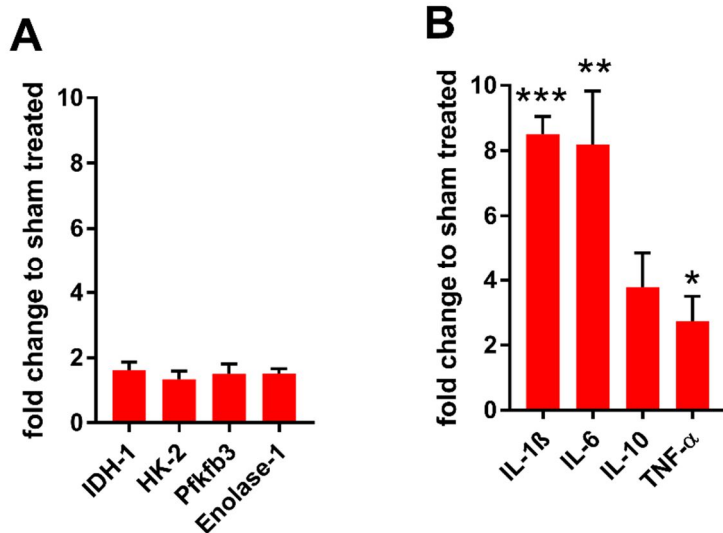


**Figure 3.2 Transcriptional profile of kidney TRMs 24h after acid aspiration**. Transcriptional changes of metabolic enzymes (**A**) and cytokines (**B**) were analyzed via RT-qPCR and are shown as fold changes to kidney TRMs from animals 24h after sham treatment normalized to the housekeeping-gene ß-actin.

Similarly, metabolic enzymes were not transcriptionally altered in kidney TRMs 8d after acid aspiration (Fig. 3.3 A). However, there was a distinct upregulation of IL-10, while the transcription of pro-inflammatory cytokines normalized compared to 24h after acid aspiration (Fig. 3.3 B).
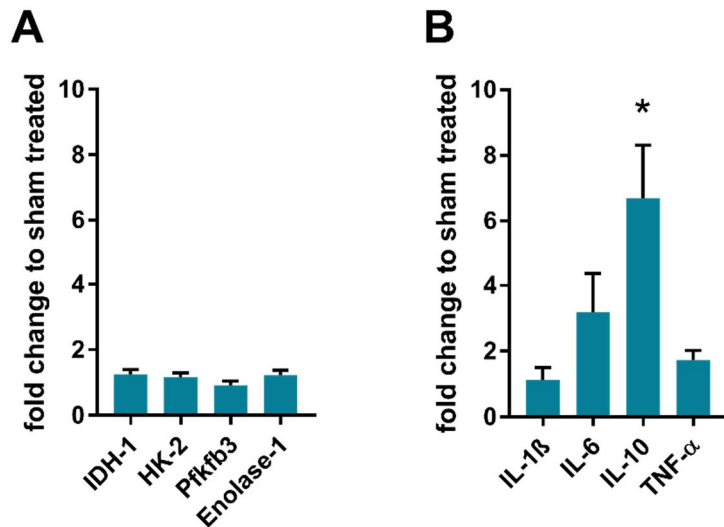
**Figure 3.3 Transcriptional profile of kidney TRMs 8d after acid aspiration**. Transcriptional changes of metabolic enzymes (**A**) and cytokines (**B**) were analyzed via RT-qPCR and are shown as fold changes to kidney TRMs from animals 8d after sham treatment normalized to the housekeeping-gene ß-actin.

### 3.2.2 Flow cytometric analysis of intracellular cytokines

To investigate whether the observed transcriptional upregulation of pro-inflammatory cytokines translates into higher amounts of protein, cytokine levels in kidney TRMs were analyzed via flow cytometry 24h after sham treatment or acid aspiration. Although no alteration met statistical significance, there was an obvious increase in the amount of IL-6 within kidney TRMs (Fig. 3.4 A), as well as TNF-α in inflammatory monocytes (Fig. 3.4 B). On the other hand, a trend towards lower levels of IL-1ß and TNF-α was detected in kidney TRMs (Fig. 3.4 A). Protein levels of IL-1ß and IL-6 in monocytes were below the detection limit of the assay.
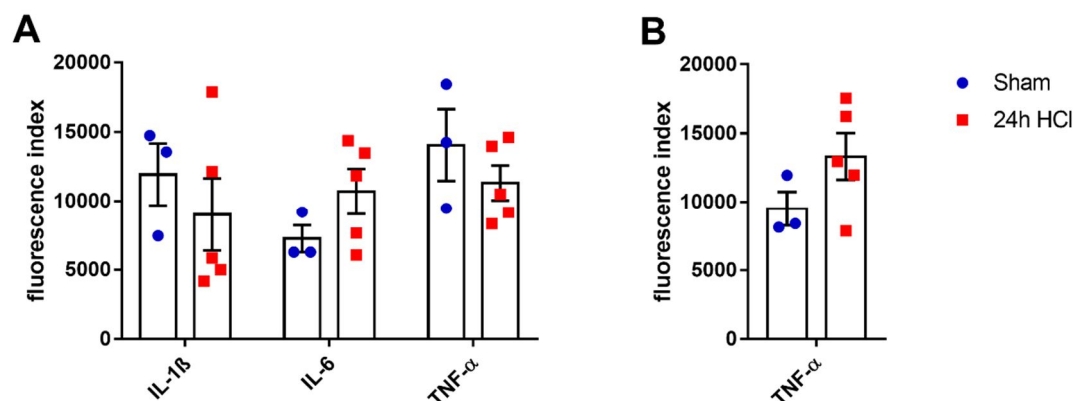


**Figure 3.4 Flow cytometric analysis of intracellular protein levels in kidney TRMs and monocytes.** Gating and calculations were done as follows: debris and doublets were excluded. Cells were fixed. Leukocytes were then gated as CD45-positive cells. Kidney TRMs (**A**) were gated as F4/80$^{pos}$ and Ly6C$^{neg}$ leukocytes. Monocytes (**B**) were gated as Ly6C$^{pos}$ and F4/80$^{neg}$ to F4/80$^{low}$. From here, TRM and monocyte

populations were further subdivided into cytokine[pos] and cytokine[neg]. The fluorescence index was calculated afterward as the product of the mean fluorescence intensity in the cytokine[pos] subpopulation and the percentage of the cytokine[pos] subpopulation from all TRMs or monocytes.

### 3.2.3 *In vitro* stimulation of kidney macrophages with murine plasma

To test if soluble factors in the blood plasma trigger an inflammatory response in kidney TRMs 24h after aspiration, kidney TRMs from untreated mice were isolated and cultured in serum-free medium *in vitro*. Subsequently, kidney TRMs were incubated for 12h with plasma taken from mice 12h after acid aspiration. At this time point the pulmonary inflammation peaks in terms of cytokine release and neutrophil influx (Matt et al., 2009). Protein concentrations in the supernatants were measured with a multiplex immunoassay. Thereby we detected no significant IL-1ß secretion (Fig. 3.5 A). Similarly, IL-6 levels were at the detection limit. However, kidney TRMs incubated with plasma from sham-treated animals secreted higher levels of IL-6 (Fig. 3.5 B). In contrast, TNF-α levels were significantly upregulated when renal TRMs were cultured with plasma from HCl-treated animals, while those that were cultured with plasma from sham-treated mice secreted only very small amounts of TNF-α (Fig. 3.5 C).
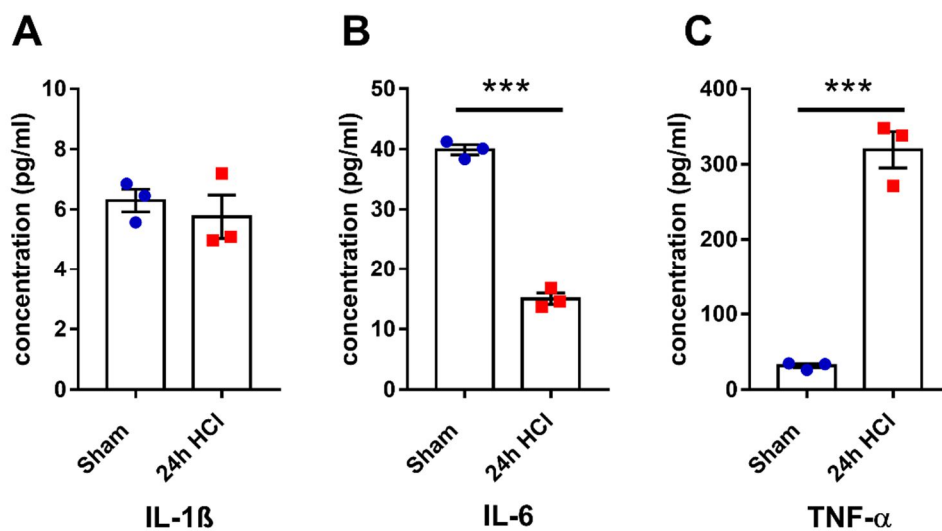


**Figure 3.5 Cytokine secretion of kidney TRMs after *in vitro* coincubation with plasma from mice that underwent sham or acid treatment 12h before.** Kidney TRMs were isolated and 12 hours *in vitro* co-cultured with plasma from animals that underwent sham or acid treatment 12h prior. Cell culture supernatants were measured for IL-1ß (**A**), IL-6 (**B**), and TNF-α (**C**).

### 3.2.4 Renal damage and inflammation

To test if the observed pro-inflammatory transcriptional alterations in macrophages reflect an ongoing inflammation within the kidneys, we analyzed the composition of innate immune cells by flow cytometry 24h after sham or acid treatment.

Overall CD45 positive cells were unchanged (Fig. 3.6 A). In line, similar levels of neutrophils (Fig. 3.6 B), kidney TRMs (Fig. 3.6 C), and monocytes (Fig. 3.6.D) were detected at this time point.
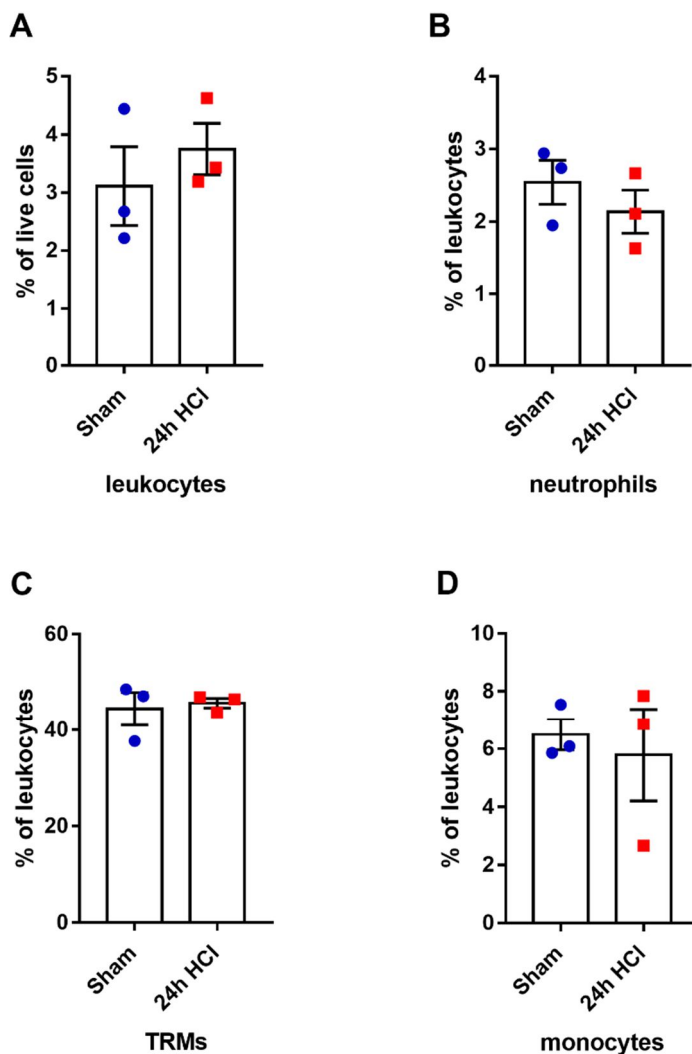


**Figure 3.6 Flow cytometry of kidney homogenates 24h after acid aspiration or sham treatment.** After the exclusion of debris, doublets, and dead cells (Sytox$^{pos}$), leukocytes (**A**) were gated as CD45$^{pos}$ cells. Neutrophils (**B**) were gated as CD11b$^{pos}$ and Ly6G$^{pos}$ leukocytes. TRMs (**C**) were defined as F4/80$^{pos}$ and Ly6C$^{neg}$ leukocytes. Monocytes (**D**) were gated as Ly6C$^{pos}$ and F4/80$^{neg}$ to F4/80$^{low}$.

To test if acid aspiration results in impaired kidney function, we measured retention parameters 24h and 8d after the lung injury. Neither the plasma levels of creatinine nor urea did show any alteration compared to sham treatment one day after the hit. However, 8 days after acid aspiration creatinine, as well as urea levels, were significantly higher compared to control animals.
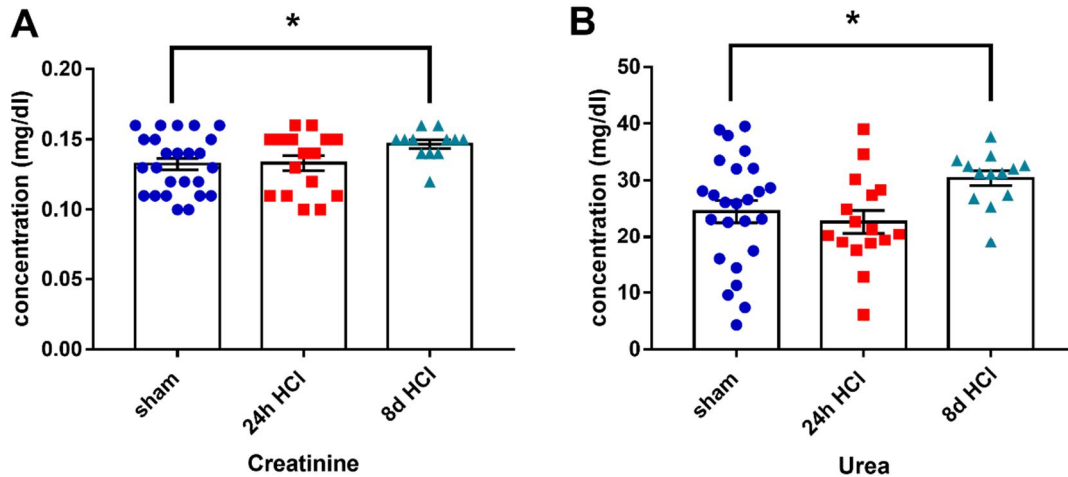
**Figure 3.7 Plasma levels of retention parameters after acid aspiration.** Plasma levels of creatinine (**A**) and urea (**B**) were measured at indicated time points after acid aspiration. Graphs show pooled data from 3 different experiments.

In line with the FACS analysis, a histologic assessment of kidney tissue performed by a veterinary pathologist in a blinded fashion revealed similar levels of interstitial leukocytes. Moreover, the tubular system, as well as the glomeruli displayed no signs of tissue damage or inflammation (Fig. 3.8).
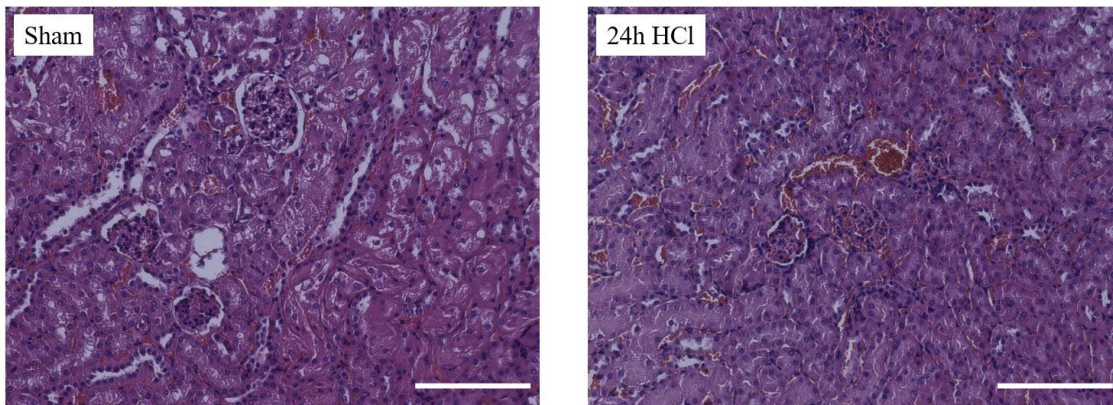


**Figure 3.8 Histology of kidneys 24h after acid aspiration or sham treatment.** Slides were stained with hematoxylin and eosin. Magnification is 20x. The scale bar represents 200µm. Shown are representative sections (n = 3/condition).

## 3.3 Liver

### 3.3.1 Transcriptional profile of liver macrophages

Livers were harvested after sham or acid treatment and liver TRMs were isolated. The expression of key metabolic enzymes, as well as hallmark cytokines, was subsequently analyzed by real-time PCR.

Key metabolic enzymes exhibited significant alterations. The main regulator enzyme of the TCA cycle, IDH-1, was downregulated by more than 90% compared to sham treatment. Similarly, the pacemaker enzyme of glycolysis, Pfkfb3, was downregulated by approximately 80%. Moreover, the glycolysis enzyme enolase-1, as well as ACOD-1, were downregulated in a non-significant manner (Fig. 3.9 A).

In contrast, apart from a trend towards higher levels of IL-6, liver TRMs did not display any notable transcriptional alterations of major cytokines 24h after acid aspiration (Fig. 3.9 B).
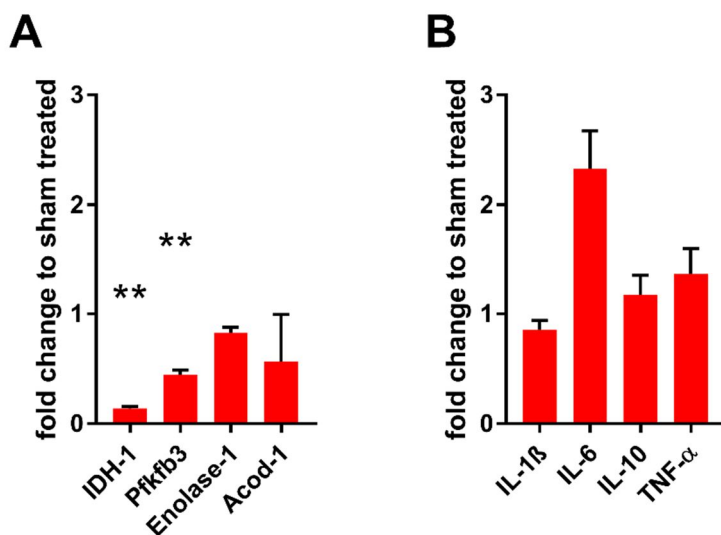


**Figure 3.9 Transcriptional profile of liver TRMs 24h after acid aspiration**. Transcriptional changes of metabolic enzymes (**A**) and cytokines (**B**) were analyzed via RT-qPCR and are shown as fold changes to liver TRMs from animals 24h after sham treatment normalized to the housekeeping-gene ß-actin.

Eight days after acid aspiration the mRNA expression of key metabolic enzymes changed markedly. The expression of IDH-1 and Pfkfb3 transcripts, heavily downregulated 24h after the aspiration event, was back to the level of sham-treated animals 8d after acid treatment while enolase-1 and ACOD-1 were upregulated, yet only enolase-1 met statistical significance (Fig 3.10 A). Cytokines were not significantly altered in liver TRMs compared to sham treatment, albeit a slight increase in IL-1ß and IL-10 was detected (Fig. 3.10 B).
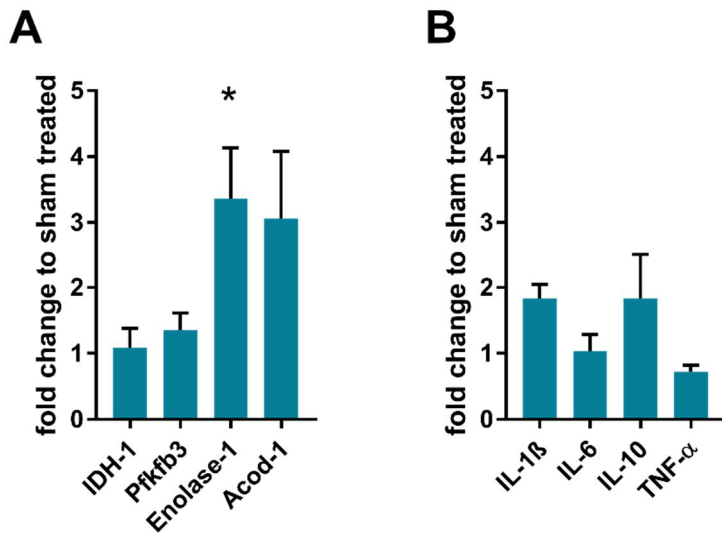
**Figure 3.10 Transcriptional profile of liver TRMs 8d after acid aspiration**. Transcriptional changes of metabolic enzymes (**A**) and cytokines (**B**) were analyzed via RT-qPCR and are shown as fold changes to liver TRMs from animals 8d after sham treatment normalized to the housekeeping-gene ß-actin.

### 3.3.2 Seahorse XF analysis of OCR in liver macrophages

Next, we wanted to assess if the alterations in key metabolic transcripts found in liver TRMs 24h after acid aspiration have a functional relevance. Therefore, we performed an *ex vivo* seahorse XF analysis of isolated liver TRMs, focusing on mitochondrial metabolism.

In line with the transcriptome analysis, hepatic TRMs harvested 24h after acid aspiration displayed a significantly lower OCR rate during the entire time course. Strikingly, macrophages from sham-treated animals increased the OCR distinctly after the addition of an uncoupling agent, while the OCR in liver TRMs from acid-treated animals rose only slightly (Fig. 3.11).

In more detail, liver TRMs 24h after acid aspiration exhibited lower levels of maximal respiration, spare capacity non-mitochondrial oxygen consumption, basal respiration, adenosine triphosphate (ATP) production, and proton leak compared to sham treatment (Fig 3.12).
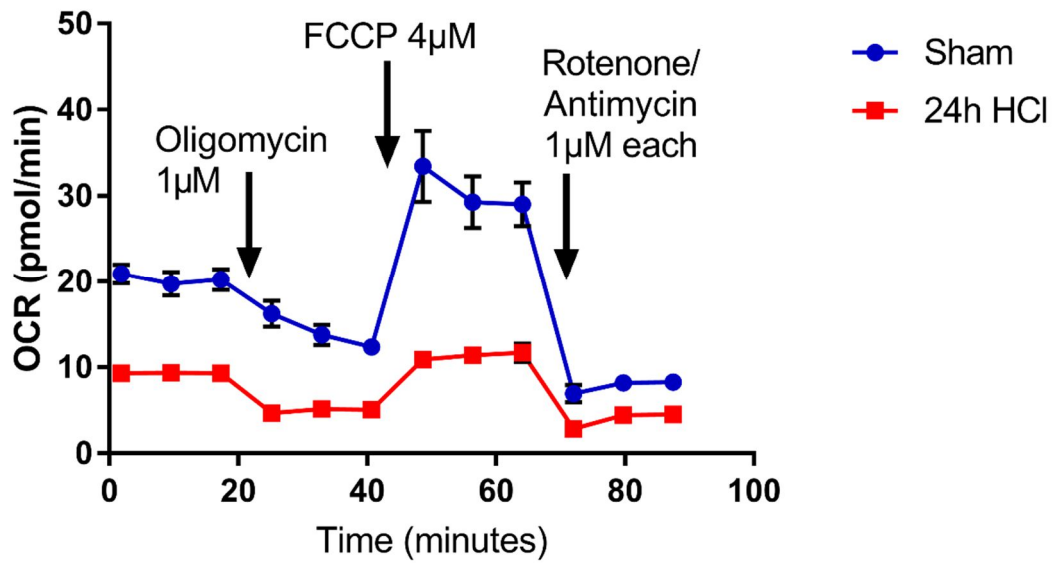
**Figure 3.11 *Ex vivo* OCR measurement in liver TRMs 24h after sham treatment or acid aspiration.**
OCR rate was measured at 12 indicated time points during the assay. Each dot represents a different time
point. Oligomycin, an inhibitor of the ATPase, was added after the third measurement. The uncoupling
agent FCCP was added after the sixth measurement. After the ninth measurement, rotenone and antimycin
were added. Rotenone inhibited complex I of the respiratory chain and antimycin complex III.
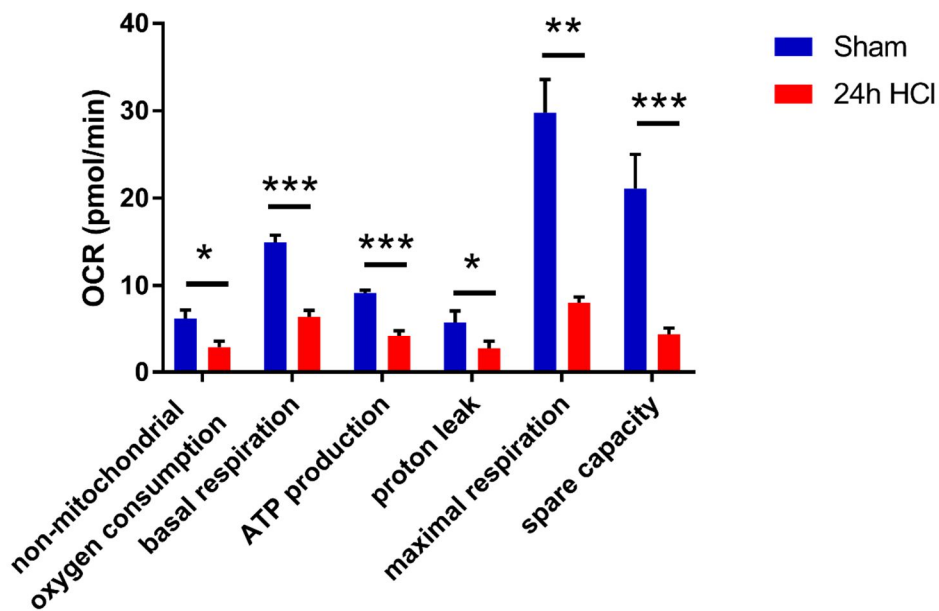


**Figure 3.12 Detailed analysis of OCR data from liver TRMs undergoing a mitochondrial stress test.**
Non-mitochondrial oxygen consumption was defined as the minimum rate after the addition of rotenone &
antimycin. Basal respiration was calculated as the difference between the basal OCR rate at the third

measurement before the first injection and the non-mitochondrial oxygen consumption. ATP production is computed as the difference between the OCR rate at the third measurement and the OCR rate at the sixth measurement. The proton leak is the difference between the OCR rate at the sixth measurement and the OCR rate at the tenth measurement. Maximal respiration is the difference in OCR rates between the seventh measurement and the tenth. The spare capacity is the difference in OCR rates between maximal and basal respiration.

### 3.3.3 Assessment of mitochondrial ROS in liver macrophages

Importantly, liver TRMs were shown to contribute to the clearance of bacterial pathogens from the blood stream (McDonald et al., 2020). Mitochondrial ROS (mROS) are mainly produced along the electron transport chain (ETC) and were shown to contribute to bacterial killing in macrophages (West et al., 2011). Therefore, we tested mROS generation of liver TRMs after acid aspiration in response to bacteria. Liver TRMs were harvested and stimulated *ex vivo* with heat-killed *P. aeruginosa*. Here, liver TRMs harvested from animals that underwent sham treatment were able to significantly increase mROS production when exposed to *P. aeruginosa*, while those from acid-treated animals were unable to mount mROS in response to bacteria (Fig. 3.13).
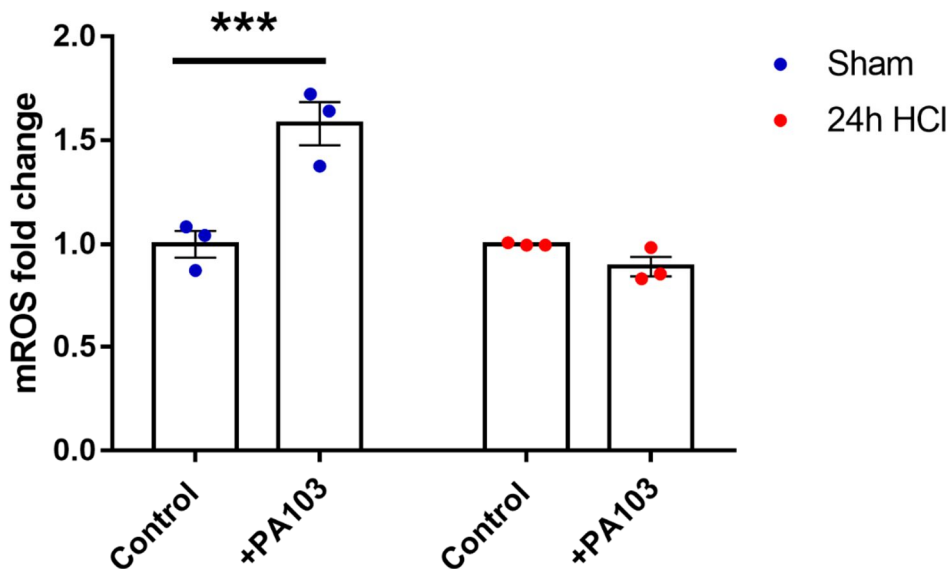


**Figure 3.13 *Ex vivo* production of mROS upon bacterial stimulation in liver TRMs 24h after sham or acid treatment**. Liver TRMs were harvested after acid pneumonitis or sham treatment and stimulated *ex vivo* with heat-killed *P. aeruginosa* (PA). Production of mROS was assessed using MitoSOX via flow cytometry. Gating was as follows: debris was excluded from cells followed by the exclusion of mROS^{neg} cells. The fluorescence index was calculated as the product of the percentage of mROS^{pos} cells and their mean fluorescence intensity. Shown is the fold change to the respective control.

In the same experiment, supernatants were collected to measure concentrations of cytokines and chemokines. Here, liver TRMs from animals that underwent acid treatment secreted reduced amounts of pro-inflammatory mediators like monocyte chemoattractant protein-1 (MCP-1), macrophage inflammatory protein-1 α (MIP-1α), MIP-1β, IL-6, and TNF-α as well as the anti-inflammatory IL-10 (Fig 3.14). Of note, cell viability was similar in both groups (data not shown).
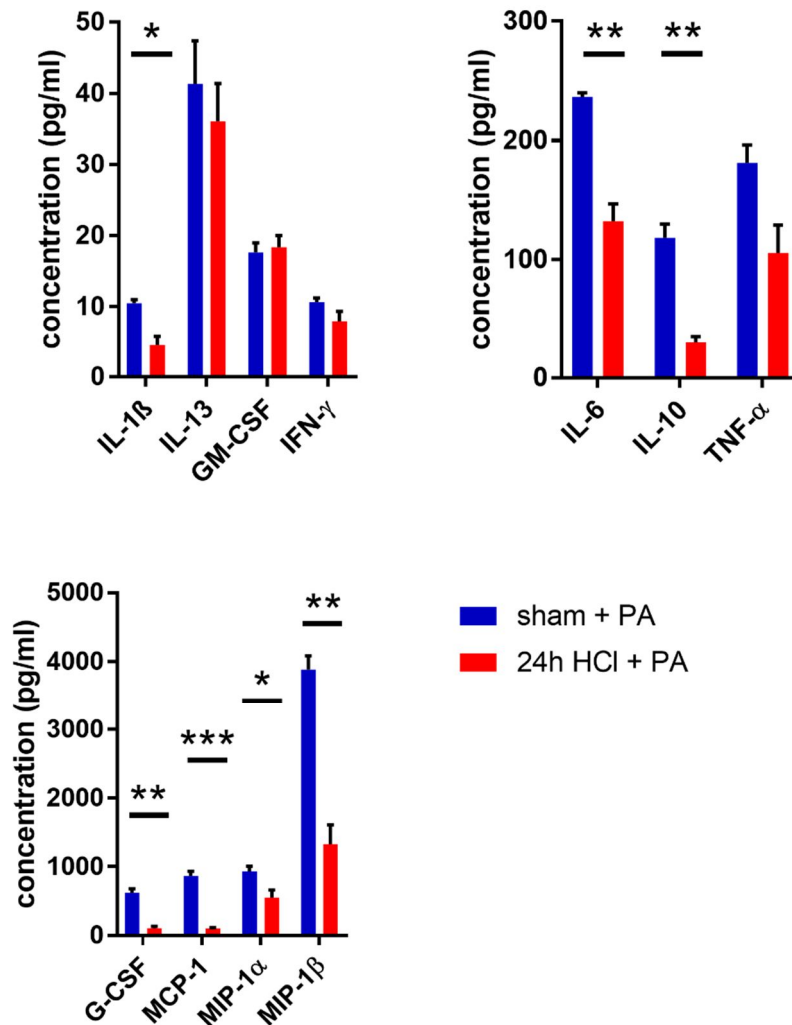


**Figure 3.14 Production of cytokines upon bacterial stimulation of liver TRMs 24h after sham or acid treatment**. Liver TRMs were harvested 24h after sham or acid treatment and *ex vivo* stimulated with heat-killed *P. aeruginosa*. Supernatants were collected and cytokine concentrations were analyzed via multiplex immunoassay.

### 3.3.4 Bactericidal properties of liver macrophages

To investigate whether the observed immunometabolic alterations 24h after acid aspiration in liver TRMs influence their ability to eradicate bacteria, we performed an *ex vivo* killing assay after acid aspiration with *P. aeruginosa*. In brief, liver TRMs were isolated and *ex vivo* co-cultured with living bacteria. At indicated time points, cells were lysed and the intracellular bacterial load was determined. The difference in bacterial load between both time points indicates the bacterial killing capacity of the macrophages, and the first time point the phagocytic capacity.

When exposed to *P. aeruginosa*, liver TRMs from both, acid and sham treatment, exhibited a similar ability to phagocytose bacteria (Fig. 3.15 A), whereas hepatic TRMs from acid-treated animals displayed a pronounced impaired killing capacity (Fig. 3.15 B): liver TRMs harvested after sham treatment were able to eradicate around 70% of intracellular bacteria within one hour, while after acid treatment this ratio declined to roughly 50%.
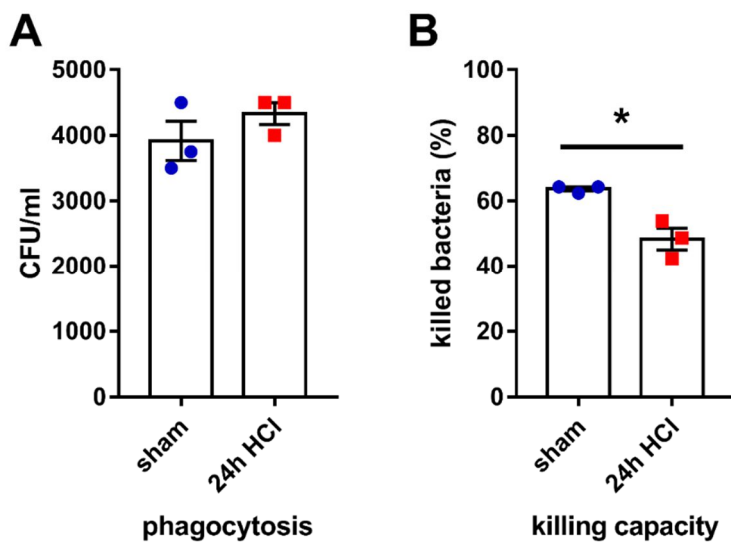


**Figure 3.15 *Ex vivo* bacterial killing capacity of liver TRMs 24h after sham or acid treatment.** Liver TRMs were harvested after sham or acid treatment, allowed to adhere, and co-cultured with living *P. aeruginosa* with a MOI of one. After one hour (T0), cells on the first plate were lysed to determine the intracellular bacterial load, representing the number of bacteria phagocytosed (**A**). After another one and a half hours (T1), cells on the second plate were lysed to determine the remaining intracellular bacterial load. The difference marks the portion of bacteria killed (**B**).

Part A shows the bacterial load in each well after the lysis of the macrophages. Part B shows the killing capacity, which was calculated as 100% minus the percentage of bacteria remaining at T1 compared to T0.

Next, we tested if the observed impaired bactericidal properties are pathogen-specific. Therefore, we performed the same assay with *K. pneumoniae*. Similarly, there was no difference in phagocytosis of extracellular bacteria between both treatments (Fig 3.16 A), while liver TRMs harvested one day after acid aspiration demonstrated an impaired ability to kill intracellular bacteria comparable to *P. aeruginosa* (Fig. 3.16 B).
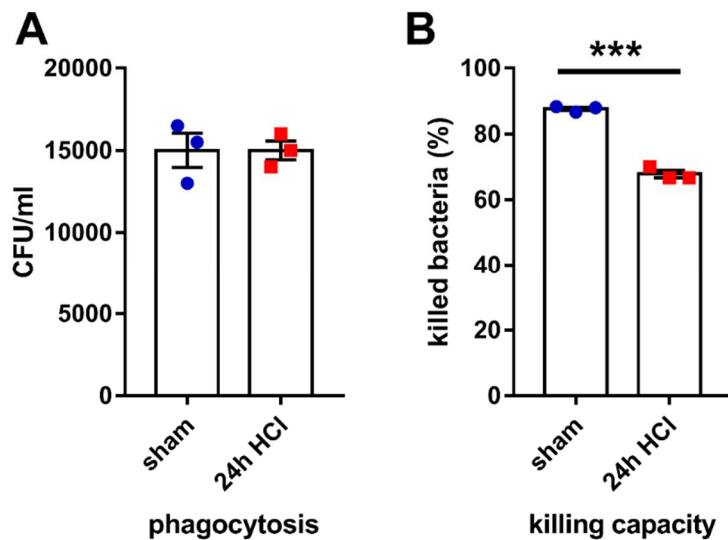


**Figure 3.16.** *Ex vivo* **bacterial killing assay with liver TRMs 24h after sham or acid treatment with *K. pneumoniae*.** Liver TRMs were harvested after sham or acid treatment, allowed to adhere, and co-cultured with living *K. pneumoniae* at a MOI of 10. After one hour (T0), cells on the first plate were lysed to determine the intracellular bacterial load, representing the number of bacteria phagocytosed (**A**). After another one and a half hours (T1), cells on the second plate were lysed to determine the remaining intracellular bacterial load. The difference equals the portion of bacteria killed (**B**).

Part A shows the bacterial load in each well after the lysis of the macrophages. Part B shows the killing capacity, which was calculated as 100% minus the percentage of bacteria remaining at T1 compared to T0.

### 3.3.5 Flow cytometric analysis of liver macrophage composition

To test if the observed phenotype is caused by an alteration in the composition of macrophage subpopulations, we analyzed the composition of liver macrophages and other immune cells by flow cytometry 24h after sham treatment or acid aspiration.

One day after the aspiration event, there was a significant decrease in leukocyte numbers within livers by around one quarter (Fig. 3.17 A). The overall number of macrophages was also reduced in acid-treated animals but failed to reach statistical significance (Fig. 3.17 B). Capsular macrophages only posed a small proportion of all liver macrophages and their numbers were unaltered by acid aspiration (Fig. 3.17 C). Kupffer cells constitute

the largest macrophage subpopulation and their numbers remained unchanged (Fig. 3.17 D). The second-largest macrophage subpopulation are MDMs which were slightly yet significantly decreased one day after acid aspiration (Fig. 3.17 E). We did not detect a neutrophil influx after acid aspiration (Fig 3.17 F).

Liver TRMs were isolated in a positive selection via F4/80. Thus, the isolated cells used for *ex vivo* assays comprised multiple macrophage populations but did not include F4/80[neg] MDMs. Among all F4/80^{pos} cells the percentage of Kupffer cells was similar in both groups (Fig. 3.18).
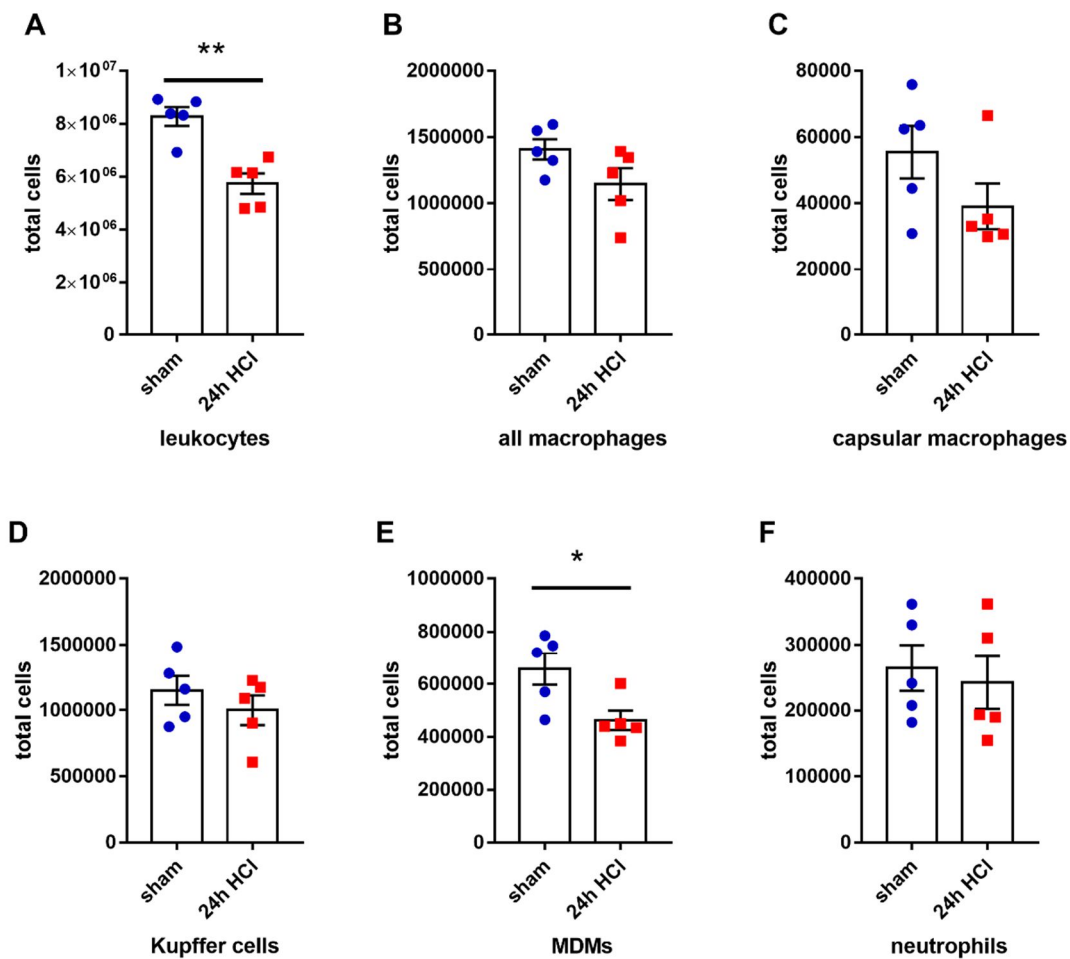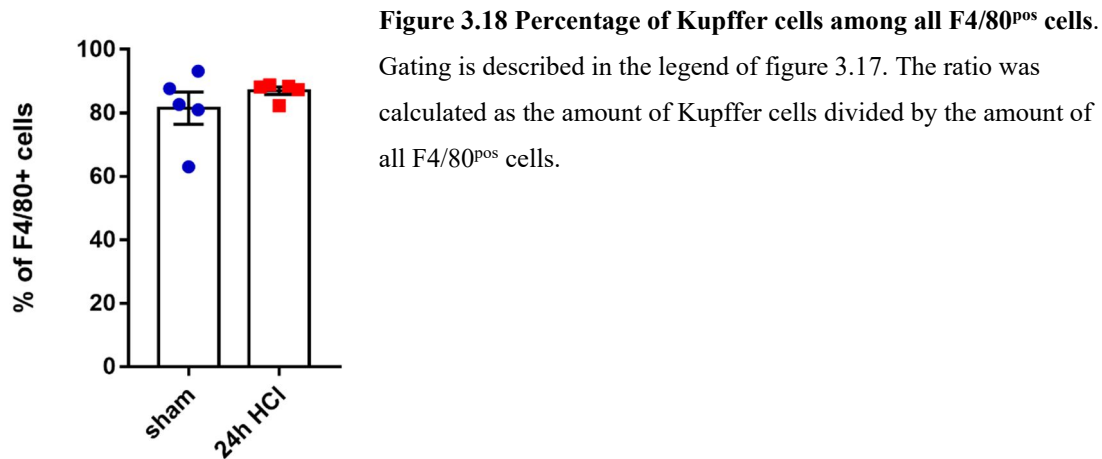


**Figure 3.17 Composition of innate immune cells in liver homogenates 24h after sham or acid treatment**. Gating was as follows: after the exclusion of debris, doublets, and dead cells (Sytox^{pos}), leukocytes (**A**) were then gated as CD45^{pos} cells. The "all macrophages" population (**B**) was gated as F4/80^{pos} leukocytes. Capsular macrophages (**C**) were gated as F4/80^{pos}, MHC-II[pos], and Tim4^{neg} leukocytes while Kupffer cells (**D**) were defined as F4/80^{pos} and Tim4^{pos} leukocytes. MDMs (**E**) were gated as F4/80^{neg} and Ly6C^{pos} leukocytes. Neutrophils (**F**) were defined as CD11b^{pos} and Ly6G^{pos} leukocytes.

**Figure 3.18 Percentage of Kupffer cells among all F4/80$^{pos}$ cells**. Gating is described in the legend of figure 3.17. The ratio was calculated as the amount of Kupffer cells divided by the amount of all F4/80$^{pos}$ cells.

### 3.3.6 Hepatic damage and inflammation

To investigate if acid aspiration induces liver inflammation or damage that might cause the observed dysfunction in hepatic TRMs, plasma levels of liver function parameters, namely ALT and AST, were assessed. There was no difference after 24h or 8d between sham or acid treatment (Fig. 3.19).
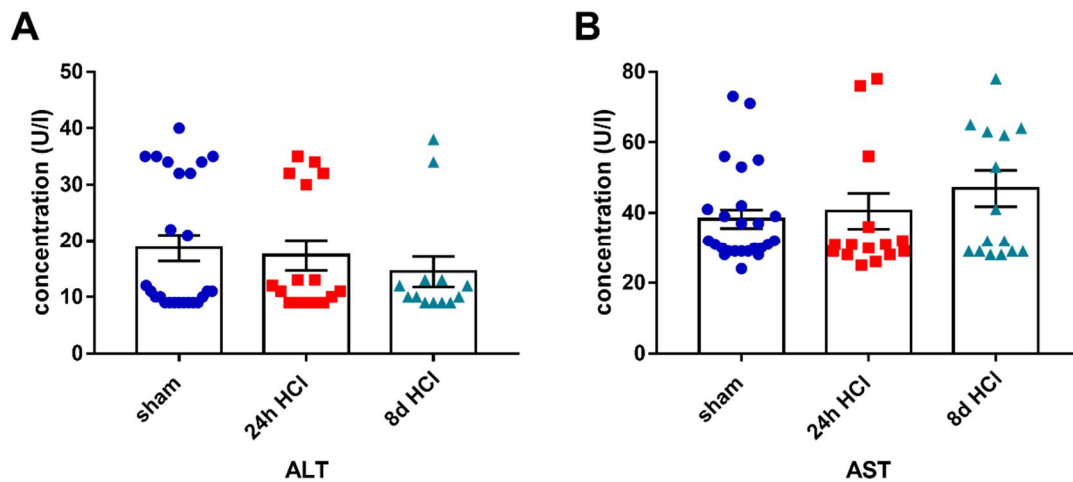


**Figure 3.19 Blood levels of liver function parameters after acid aspiration.** Plasma levels of ALT (**A**) and AST (**B**) were measured at indicated time points after acid aspiration. Graphs show pooled data from 3 different experiments.

Moreover, we did not detect a difference in a variety of pro-and anti-inflammatory cytokines measured in whole organ homogenates of livers 24h after acid or sham treatment (Fig. 3.20).
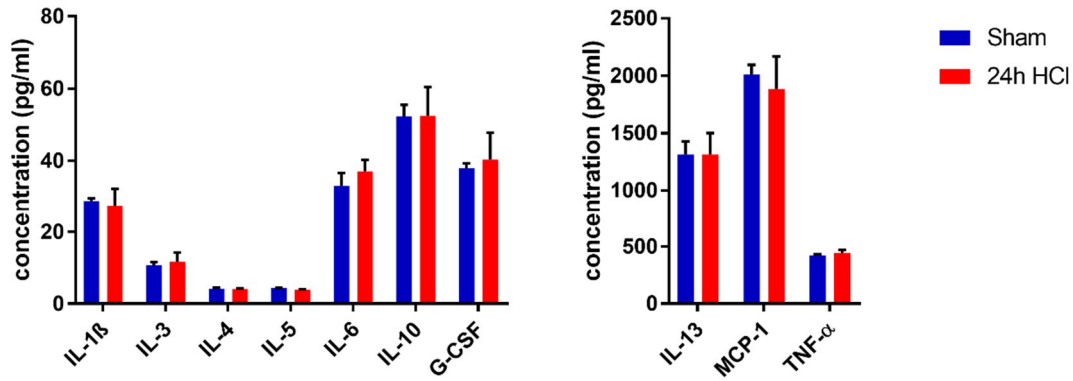
**Figure 3.20 Cytokine concentrations in liver whole organ homogenates after acid aspiration.** Concentrations of different cytokines were measured with a multiplex immunoassay 24h after sham or acid treatment in liver whole organ homogenates.

Finally, livers were harvested 24h after sham or acid treatment for histological assessment of inflammatory or degenerative changes by a veterinary pathologist in a blinded fashion. Here, neither sham nor acid treatment caused any notable damage to the liver parenchyma. Corresponding to the flow cytometry data, we observed no influx of neutrophils or monocytes.
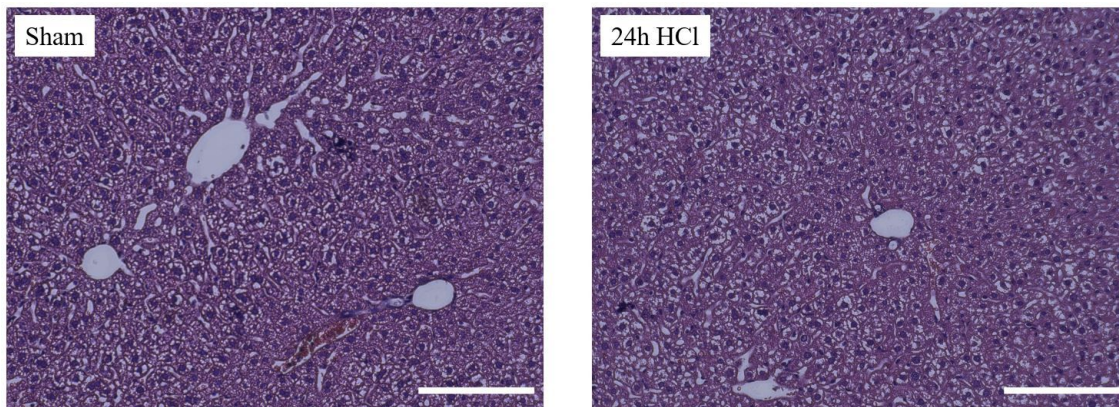


**Figure 3.21 Liver histology 24h after sham or acid treatment.** Representative image of liver tissue 24h after sham or acid treatment. Slides were stained with hematoxylin and eosin. Magnification is 20x. The scale bar represents 200µm (n = 3/condition).

## 3.4 Peritoneum

### 3.4.1 Transcriptional profile of peritoneal macrophages

Peritoneal lavage was performed after sham or acid treatment and peritoneal TRMs were isolated from the lavage fluid. The expression of key metabolic enzymes, as well as important cytokines, were subsequently analyzed by real-time PCR.

One day after the aspiration event peritoneal TRMs displayed a notable reduction in the transcription of metabolic enzymes. IDH-1, as well as various glycolysis enzymes, were downregulated by approximately 40% after acid treatment in comparison to sham treatment (Fig. 3.22 A). However, the transcription of major cytokines was barely affected: IL-6 was slightly lower after acid aspiration, while other pro-inflammatory cytokines such as IL-1ß and TNF-α as well as the anti-inflammatory IL-10 remained unchanged (Fig. 3.22 B).



**Figure 3.22 Transcriptional profile of peritoneal TRMs 24h after acid aspiration**. Transcriptional changes of metabolic enzymes (**A**) and cytokines (**B**) were analyzed via RT-qPCR and are shown as fold changes to peritoneal TRMs from animals 24h after sham treatment normalized to the housekeeping-gene ß-actin.

Eight days after acid aspiration a similar pattern for metabolic enzymes was observed (Fig. 3.23 A). Strikingly, 8d after acid treatment, peritoneal TRMs exhibited a distinct increase in transcription of pro-inflammatory cytokines, specifically IL-1ß, IL-6, and TNF-α. Similarly, the anti-inflammatory cytokine IL-10 was increased 8 days after acid aspiration in PMs (Fig. 3.23 B).
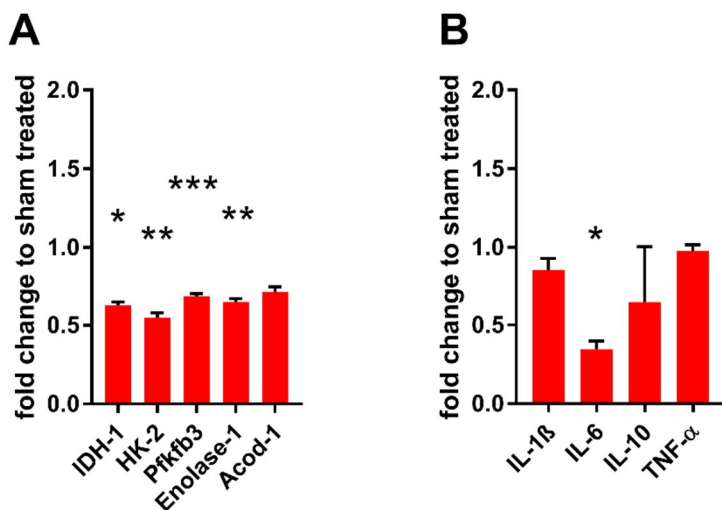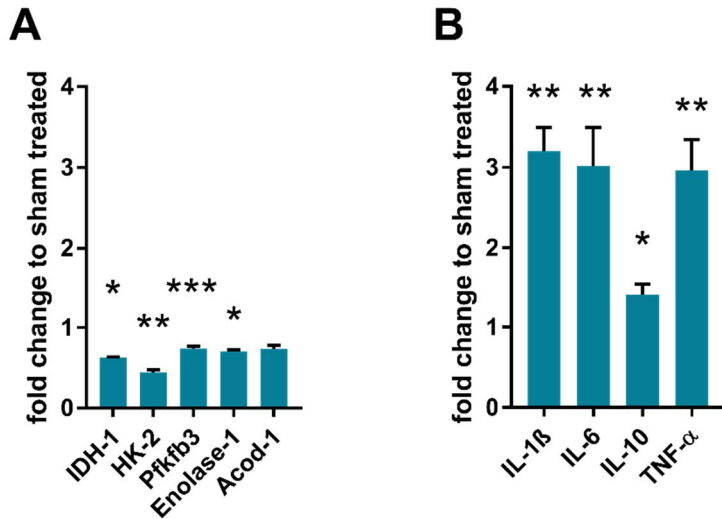
**Figure 3.23 Transcriptional profile of peritoneal TRMs 8d after acid aspiration**. Transcriptional changes of metabolic enzymes (**A**) and cytokines (**B**) were analyzed via RT-qPCR and are shown as fold changes to peritoneal TRMs from animals 8d after sham treatment normalized to the housekeeping-gene ß-actin.

### 3.4.2 Bactericidal properties of peritoneal macrophages

Due to the profound impact of transcriptional changes 24h after acid aspiration in key metabolic enzymes, in particular IDH-1, the ability of peritoneal TRMs to combat *P. aeruginosa* was assessed. However, peritoneal TRMs did not show an altered ability to phagocyte extracellular bacteria (Fig. 3.24 A) nor to eradicate intracellular bacteria 24h after acid aspiration. (Fig 3.24 B).



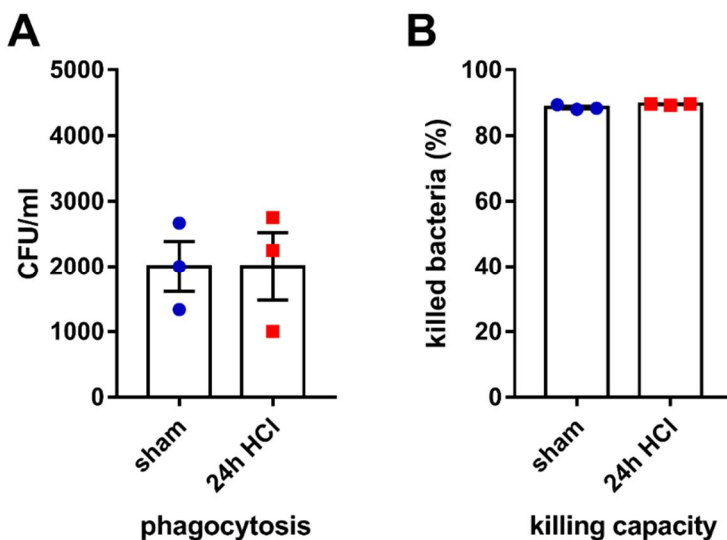**Figure 3.24 *Ex vivo* bactericidial properties of peritoneal macrophages 24h after sham or acid treatment.** Peritoneal TRMs were harvested, and the assay was performed as described for liver macrophages. Part (**A**) shows the bacterial load in each well after the lysis of the macrophages. Part (**B**) shows the killing capacity, which was calculated as 100% minus the percentage of bacteria remaining at T1 compared to T0.

### 3.4.3 Flow cytometric analysis of peritoneal innate immune cells

To test if the transcriptional upregulation of inflammatory cytokines translates into protein secretion, we measured cytokines in the peritoneal lavage fluid (PLF) after acid aspiration. However, the same cytokines that we tested on a transcriptional level were not detectable 8 days after acid aspiration in the PLF (data not shown). In line, the composition of innate immune cells within the peritoneal cavity was unaltered: no influx of neutrophils (Fig. 3.25 A) or monocytes (Fig 3.25 B) was detected. Of note, peritoneal TRM levels displayed an increase of approximately one-quarter 8d after the aspiration event which did not meet statistical significance (Fig. 3.25 C).

Recent research revealed the existence of two subpopulations of peritoneal TRMs: large peritoneal macrophages (LPMs) and small peritoneal macrophages (SPMs). LPMs make up the majority of peritoneal macrophages (PMs) under steady-state conditions while SPMs rapidly increase in numbers and become the dominant population during infection or inflammation (Cassado et al., 2015). Further analysis showed that the numbers of LPMs remained unaffected at 24h and 8d after acid aspiration (Fig. 3.25 D). SPM numbers were unaltered 24h after aspiration but reduced 8d after acid aspiration (Fig. 3.25 E).
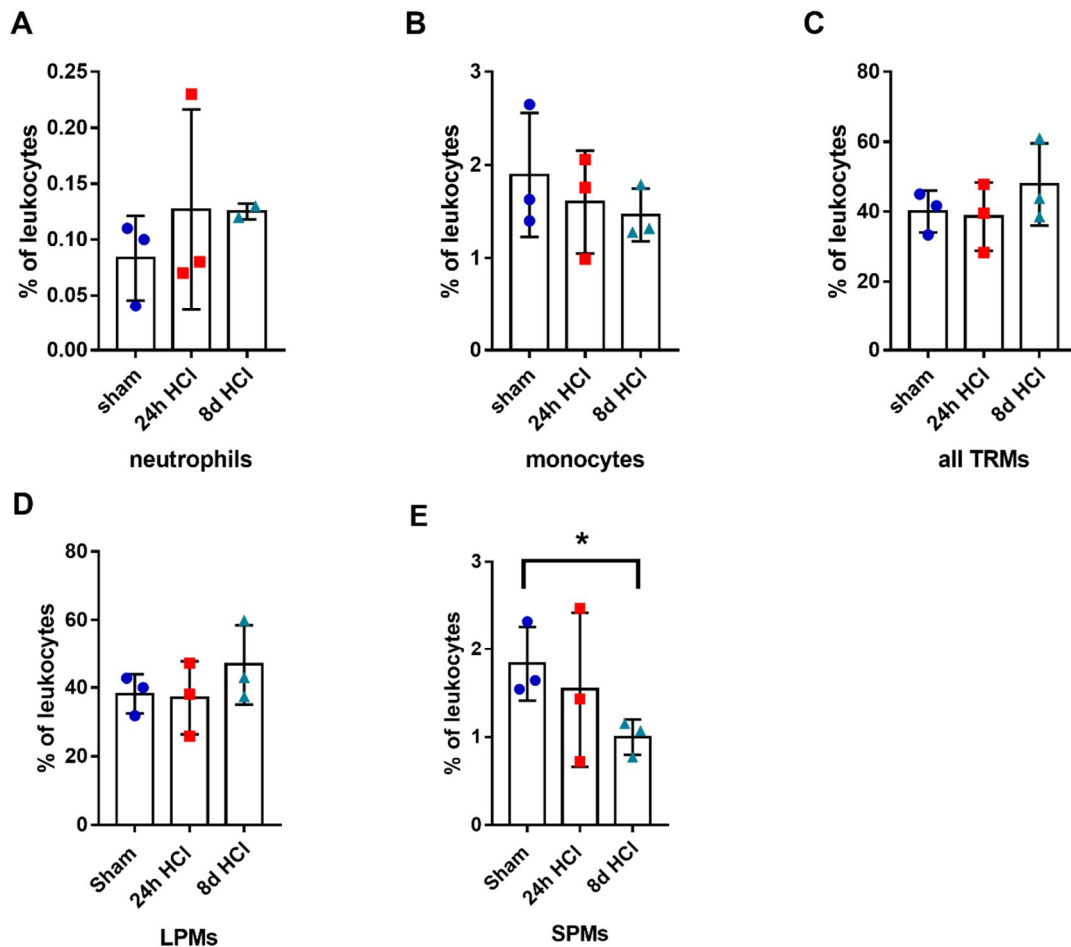
**Figure 3.25 Cellular composition of innate immune cells within the peritoneal cavity at indicated time points after acid or sham treatment**. Gating was done as follows: after the exclusion of debris, doublets, and dead cells (Sytox$^{pos}$), leukocytes were then gated as CD45$^{pos}$ cells. Neutrophils (**A**) were gated as CD11b$^{pos}$ and Ly6G$^{pos}$ leukocytes, monocytes (**B**) as Ly6C$^{pos}$ and F4/80$^{neg}$ leukocytes, and the "all TRMs" population (**C**) as F4/80$^{pos}$ and Ly6C$^{neg}$ leukocytes. LPMs (**D**) were gated as F4/80$^{high}$ and CD11b$^{high}$ leukocytes, and SPMs (**E**) were defined as F4/80$^{low}$ and CD11b$^{low}$ leukocytes

## 3.5 Spleen

### 3.5.1 Transcriptional profile of splenic macrophages

Spleens were harvested after sham or acid treatment and splenic TRMs were isolated. The expression of key metabolic enzymes, as well as cytokines, was subsequently analyzed by real-time PCR.

One day after acid aspiration splenic TRMs displayed a distinct decrease in the transcription of key metabolic enzymes, affecting both the TCA cycle and glycolysis enzymes (Fig. 3.26 A). The transcription of major pro-and anti-inflammatory cytokines

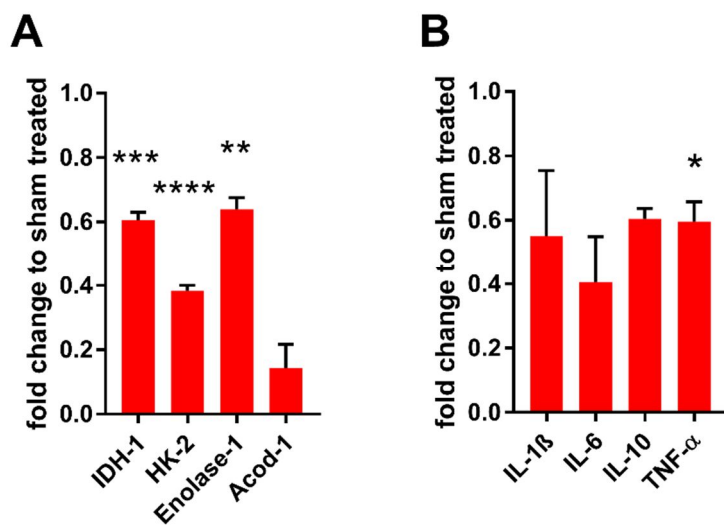was also diminished but only the downregulation of TNF-α met statistical significance (Fig. 3.26 B).



**Figure 3.26 Transcriptional profile of splenic TRMs 24h after acid aspiration**. Transcriptional changes of metabolic enzymes (**A**) and cytokines (**B**) were analyzed via RT-qPCR and are shown as fold changes to splenic TRMs from animals 24h after sham treatment normalized to the housekeeping-gene ß-actin.

Eight days after acid aspiration, the transcription of key enzymes was only slightly altered (Fig. 3.27 A). Only enolase-1 was significantly downregulated. Major cytokines displayed a decreased transcription, which was not statistically significant (Fig. 3.27 B).
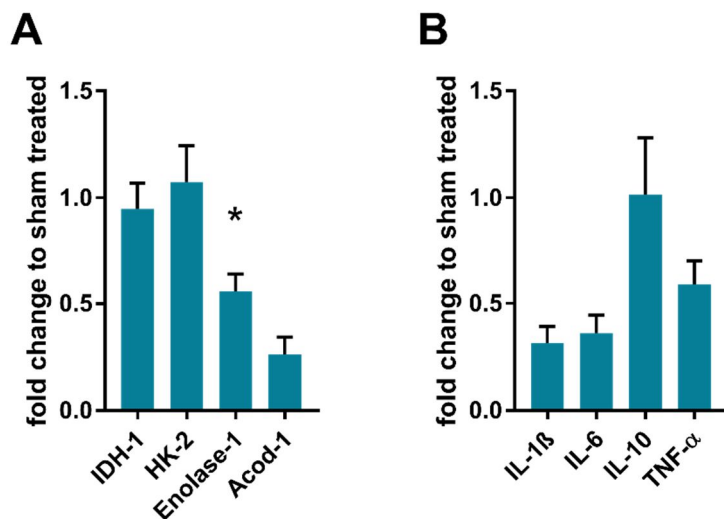


**Figure 3.27 Transcriptional profile of splenic TRMs 8d after acid aspiration**. Transcriptional changes of metabolic enzymes (**A**) and cytokines (**B**) were analyzed via RT-qPCR and are shown as fold changes to splenic TRMs from animals 8d after sham treatment normalized to the housekeeping-gene ß-actin.

### 3.5.2 Bactericidal properties of splenic macrophages

Transcriptional alterations (e.g. IDH-1) were paralleled by significant changes in effector functionsin the liver macrophages. Moreover, spleen and liver TRMs were shown to contribute to the clearance of bacteria in the bloodstream (Borges da Silva et al., 2015). Therefore, bactericidal properties were assessed after aspiration *ex vivo*. Here, splenic TRMs exhibited no difference in the phagocytosis of extracellular bacteria (Fig. 3.28 A).

Similarly, in terms of bacterial killing, we observed no difference between sham or acid treatment 24h after acid aspiration (Fig. 3.28 B).



**Figure 3.28 *Ex vivo* antibacterial properties of splenic TRMs 24h after sham or acid treatment with *P. aeruginosa*.** Splenic TRMs were harvested, and the assay was performed as described for liver TRMs. Part (**A**) shows the bacterial load in each well after the lysis of the macrophages. Part (**B**) shows the killing capacity, which was calculated as 100% minus the percentage of bacteria remaining at T1 compared to T0.
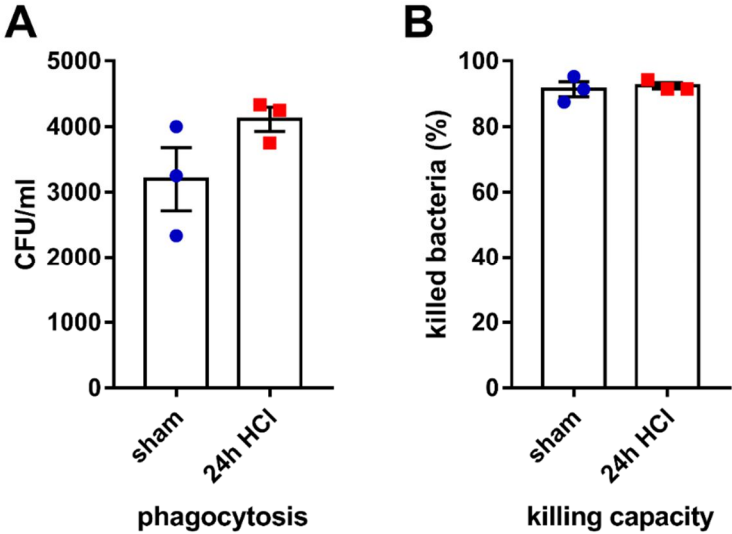
# 4 Discussion

Acid aspiration is a common cause of ALI and may lead to an ARDS which to this day is characterized by high morbidity and mortality (Marik, 2001; Sakai et al., 2006; Son et al., 2017). Acid-induced lung damage can affect other organs like the liver and kidneys (Hoag et al., 2008; Heuer et al., 2012), but the underlying mechanisms remain elusive. TRMs occupy a pivotal role in the homeostasis of their respective organ (Davies et al., 2013; Wynn and Vannella, 2016; Vannella and Wynn, 2017), yet their role in extrapulmonary organ damage after acid aspiration remains virtually unknown.

In this study, TRMs of the kidneys, liver, peritoneum, and spleen were analyzed after acid aspiration on a transcriptional level followed by functional readouts.

## 4.1 Methodical limitations

TRMs do not constitute one distinct population but are made up of various subpopulations which are unique for each organ (den Haan and Kraal, 2012; Kawakami et al., 2013; Tacke and Zimmermann, 2014; Cassado et al., 2015; Blériot and Ginhoux, 2019). To embrace a large proportion of all TRM subpopulations, a positive selection via F4/80 was chosen since this surface marker is abundantly expressed on most TRMs in the liver (Blériot and Ginhoux, 2019), the kidney (Kawakami et al., 2013), the spleen (Borges da Silva et al., 2015), and the peritoneum (Dos Anjos Cassado, 2017). Although the majority of TRMs is included in the following analysis by utilizing this surface antigen, some subpopulations, namely spleen white pulp macrophages (Dos Anjos Cassado, 2017), which do not express F4/80, are not included. Additionally, monocytes might be included in kidney transcriptional analysis since some authors describe them as F4/80[low] (Li et al., 2008).

Moreover, splenic, and peritoneal macrophages were harvested differently for PCR and *ex vivo* assays. The MicroBead-based isolation resulted in a very high purity but low cell numbers. Therefore, macrophages were harvested via their strong adherence for ex vivo assays. This might cause differences in the isolated cell populations and thus cumber the interpretation of the generated data.

However, it is not the aim of this study to characterize every single subpopulation after aspiration in the first place. The exact composition, differentiation, and function of these subpopulations is to this day subject of intense research. Nevertheless, the generalized

approach is a clear limitation, as it does not allow drawing any conclusion on subpopulations of TRMs.

Moreover, the analysis of previously selected genes constitutes a biased approach. Previous studies were able to demonstrate that TRMs alter the expression of hundreds of genes during distant organ injuries (Hoyer et al., 2019). In future work, it will be interesting to perform bulk sequencing of TRMs such as liver or kidney macrophages after acid pneumonitis to disentangle contributions of subpopulations and unravel yet unrecognized responses.

On the other hand, a clear strength of this study is the chosen straightforward approach and the use of functional *ex vivo* assays which allow sound statements about the macrophages´ effector functions.

.

## 4.2 Kidney

In contrast to the other TRMs tested, kidney TRMs exhibited a pro-inflammatory gene expression profile 24h after acid aspiration while key metabolic enzymes were not affected. Moreover, there was also a tendency toward an increased synthesis of IL-6 *in vivo*. Interestingly, when *in vitro* stimulated with plasma taken from animals 12h after aspiration, at the peak of pneumonitis (Matt et al., 2009), kidney TRMs mainly secreted TNF-α, which stands somewhat in contrast to the *in vivo* findings where IL-6 synthesis was increased. There are however multiple conceivable explanations for this inconsistency.

For once, as previously stated, the cell separation was done with an F4/80 positive selection. According to some authors, kidney blood-derived monocytes also express low levels of F4/80 (Li et al., 2008). The *in vitro* findings as well as the qPCR results may thus not exclusively be accredited to TRMs since monocytes may have been involved too. This fits the *in vivo* observation that monocytes displayed a distinct augmentation in TNF-α synthesis 24h after aspiration, although their numbers did not change after acid aspiration. However, after sham as well as acid treatment, the number of cytokine-containing cells was equally low.

Moreover, the *in vitro* as well as *in vivo* data demonstrate that there are certain signals after acid aspiration, most likely blood-derived, that induce a pro-inflammatory state in kidney TRMs. Previous research demonstrated the importance of the environment in which the macrophages reside (Amit et al., 2016; Wang et al., 2021). The same type of

macrophage may react to the same stimulus differently when in a different environment, for example, its native organ or a plastic dish (McNeill et al., 2014). Thus, the observed inconsistencies in cytokine synthesis might reflect the different experimental approaches applied.

Previous publications highlighted the crosstalk between kidneys and the lung during ALI and vice versa during AKI (Doi et al., 2011; Darmon et al., 2014; Husain-Syed et al., 2016; Domenech et al., 2017; Klein et al., 2018), yet the underlying mechanisms are not fully understood to this day. However, like ALI, AKI is not a single entity with one definitive pathophysiology but more of a blanket term summarizing various processes that eventually culminate in a rapid loss of kidney function (Ronco et al., 2019). Renal TRMs were shown to play a pivotal role in the pathophysiology of various entities of AKI (Jang and Rabb, 2015). During the initial phase of most forms of intrarenal AKI, macrophages assume a pro-inflammatory phenotype with distinct IL-1ß, IL-6, and TNF-α secretion peaking around one day after the triggering event. Later on, they turn more into M2-like macrophages and aid in tissue regeneration (Han et al., 2019). In terms of transcription, kidney TRMs behave similarly following acid aspiration with IL-1ß and IL-6 transcription being distinctly increased one day after aspiration. While the transcription of those cytokines is back to baseline after one week, here IL-10 gene expression is elevated, which represents a major anti-inflammatory cytokine (Rőszer, 2015).

Furthermore, on the eighth day after aspiration, we detected a rise in plasma levels of creatinine as well as urea. The time delay of roughly a week could be explained by the delayed kinetics of creatinine. Blood levels of retention parameters might take several days to rise after whatever elicitor of injury (Ronco et al., 2019).

However, not all data match the idea of acid-induced ALI triggering intrarenal AKI. For once, the initial phase of AKI is characterized by a marked influx of recruited immune cells, primarily neutrophils, and blood-derived monocytes (Zuk and Bonventre, 2016). Yet flow cytometric analysis of kidney immune cells 24h after aspiration did not show recruitment of leucocytes. This might be due to a cellular inflammatory response at earlier time points.

Moreover, an earlier study done by Hoag and colleagues analyzed the effects of acid aspiration on kidney function. Here, the creatinine levels remained also unchanged early after aspiration (Hoag et al., 2008). However, impairment of kidney function after aspiration might have been missed, since later time points were not analyzed.

Additionally, in a healthy individual, it requires a loss of roughly more than 50% of kidney function for creatinine levels to rise (Ronco et al., 2019). Hence smaller alterations in kidney function are not detected by using creatinine as the reference point.

Furthermore, histopathological analysis of the kidneys revealed no histologic damage neither one nor eight days after acid aspiration. This argues against the hypothesis of at least intrarenal AKI following aspiration in our model since almost all triggers of intrarenal AKI result in notable damage to the tubular system, the glomeruli, or the interstitium (Basile et al., 2012). However, some entities of AKI, like prerenal AKI due to renal hypoperfusion, were shown to elapse without notable tissue damage (Makris and Spanou, 2016), thus not completely ruling out the possibility of AKI in our model.

Most interestingly, a previous study performed on pigs by Heuer and colleagues unraveled tubular necrosis and infiltrating leukocytes following acid aspiration with, when allocated to the body weight, a similar amount of acid of the same pH as used in this study (Heuer et al., 2012). Yet they only conducted a histological analysis on kidneys, while kidney function was not assessed. Additionally, they focused on the early hours after aspiration and did not cover later time points. Moreover, the animals were intubated and mechanically ventilated during the entire time course of their experiment. Mechanical ventilation was shown to induce renal damage (Gurkan et al., 2003) and may thus have influenced their findings.

Interestingly, our laboratory found that up to 7 days after severe influenza infection, kidney retention parameters remained unaltered in infected mice despite significant morbidity (data not shown). Therefore, our findings suggest a specific lung-kidney cross-talk during aspiration pneumonitis.

## 4.3 Liver

### 4.3.1 Polarization and metabolism in liver TRMs

Regarding alterations in gene expression of key metabolic enzymes as well as major pro- and anti-inflammatory cytokines on the transcriptional level, all analyzed TRMs were affected. TRMs from the liver, spleen, and peritoneum displayed a similar pattern with downregulation of TCA-cycle and glycolysis enzymes 24h after aspiration. The most distinct alterations were found in liver macrophages. The key regulator enzyme of the TCA cycle IDH-1 (Ryan and O'Neill, 2017) was downregulated by around 90% one day after acid aspiration when compared to sham treatment. In line, liver TRMs displayed a

severely diminished capacity to perform OXPHOS *ex vivo*. Such a change in macrophage metabolism was previously described in BMDMs (Mills and O'Neill, 2016; Ryan and O'Neill, 2017) after LPS or IFN-γ treatment (Saha et al., 2017), referred to as the "broken TCA cycle" (O'Neill and Pearce, 2016).

Intriguingly, liver TRMs displayed impaired bactericidal properties *ex vivo* towards *P. aeruginosa* and *K. pneumoniae* 24h after acid aspiration while their phagocytic abilities remained unaltered.

*In vitro* studies using BMDMs (Viola et al., 2019) as well as liver macrophages (Dong et al., 2021) showed that treatment with LPS impairs OXPHOS, while the secretion of major proinflammatory cytokines was increased, hence, showing a typical M1-like phenotype. In our model, however, liver TRMs failed to increase their cytokine secretion upon *ex vivo* gram-negative stimulation after acid treatment. Moreover, a classical M1 macrophage is characterized by an enhanced antibacterial response (Russell et al., 2019). After aspiration though, liver TRMs displayed impaired bactericidal activity despite their M1-like OXPHOS. Thus, our data do not fit in the simplified model, where glycolysis equals inflammation and OXPHOS anti-inflammation and thereby support the increasing perception that those phenotypes are relevant *in vitro*, while macrophage polarization is much more complex *in vivo* (Sica and Mantovani, 2012; Tacke and Zimmermann, 2014; Guillot and Tacke, 2019). However, we only analyzed the "baseline" OXPHOS and not the level after stimulation with LPS or bacteria, Moreover, glycolysis was not assessed. Further investigations should address the clinically relevant question of metabolic regulations during secondary bacterial infections, which remains to be investigated.

Mitochondrial ROS were shown to be activators of the NLRP3 inflammasome (Sorbara and Girardin, 2011) as well as drivers of the secretion of pro-inflammatory cytokines (Bulua et al., 2011). Given that LPS is a potent inductor of a strong pro-inflammatory phenotype with distinct secretion of respective cytokines (West et al., 2011), the poor cytokine secretion of liver macrophages from acid-treated animals upon stimulation with the gram-negative *P. aeruginosa* can at least partially be due to their impaired mROS generation.

Hoyer and colleagues recently conducted a study in which they analyzed gene expression profiles of TRMs from the kidneys, the liver, the lung, the heart, and the brain using microarray after stroke, sepsis, and myocardial infarction. Interestingly, following all three triggers of systemic inflammation, genes coding for metabolic enzymes were barely affected in liver TRMs, while genes involved in the regulation of coagulation, wound

healing, antigen processing, and cell adhesion were affected in all three conditions. The most distinct effects were observed during sepsis using a model of cecal ligation and puncture. (Hoyer et al., 2019). Despite strong similarities in TRM responses to these three injuries, distinct changes in certain TRMs specific to one injury were shown. Strikingly, 4 days after myocardial infarction, AMs displayed enhanced abilities in the uptake of *Streptococcus pneumoniae* during an *in vivo* phagocytosis assay accompanied by better long-term survival of the mice upon intratracheal bacterial infection. This phenomenon appears to be mediated by IFN-γ. However, this was not observed 4d after stroke, sepsis, or sham treatment (Hoyer et al., 2019). Although a direct comparison of their results to ours is not feasible because of pronounced differences in the experimental setting (different injury models, time points, and readouts), their results confirm that TRMs and their effector functions can be altered by distant-organ injuries.

If and how coagulation, wound healing, antigen processing, and cell adhesion are altered in liver TRMs after acid aspiration remains to be established.

**4.3.2 Implications of an impaired bactericidal activity of liver TRMs**

Liver TRMs, which are largely comprised of Kupffer cells, constitute by far the largest population of macrophages in a mammal's body (Bilzer et al., 2006). Importantly, they are crucial for the clearance of bacteremia (Wong et al., 2013) due to their localization within the liver sinusoids and moreover, they also present a very early defense against invading pathogens from the gastrointestinal tract since most of its blood is drained into the liver via the portal vein (Kubes and Jenne, 2018).

Recently, our laboratory was able to demonstrate that the impairment in killing found *ex vivo* can also be observed *in vivo*. One day after acid or sham treatment, mice were subjected to the intravenous application of living *P. aeruginosa*. One and a half hours after infection, the bacterial load was twice as high in the livers of mice that underwent acid aspiration compared to sham-treated mice, while there was no significant difference in other organs tested, thus perfectly reflecting the *ex vivo* findings of this study (Langelage et al., 2021). Impaired bacterial killing by liver macrophages after aspiration might thus contribute to the increased susceptibility to nosocomial infections of intubated patients.

People that suffer from acid aspiration or ALI in general have a higher risk to develop secondary bacterial infections (Dreyfuss and Ricard, 2005), especially ventilator-associated pneumonia (Jean Chastre and Jean-Yves Fagon, 2011).

Interestingly, Dickson et al. observed in a mouse model as well as in humans that during ARDS, gut-derived bacteria translocate into the lung and alter the pulmonary microbiome (Dickson et al., 2016). While the mechanism remains unclear, the authors speculated that the transfer of gut bacteria into the lung might be a common feature in the pathophysiology of ARDS and sepsis. Kupffer cells are constantly exposed to gut-derived bacteria and prevent them from entering the systemic circulation (Kubes and Jenne, 2018). Previous studies unveiled that in conditions of critical illness like ARDS, gut permeability as well as alveolar-capillary permeability are increased (Mukherjee and Hanidziar, 2018). Diminished antibacterial properties within the liver's TRMs might thus result in more bacteria reaching the lung and thereby altering its microbiome.

However, the impairment in bacterial eradication was only demonstrated in the aftermath of acid aspiration. Therefore, it would be interesting to analyze liver TRMs and bacterial clearance following other common elicitors of ALI/ARDS such as bacterial or viral pneumonia (Matthay et al., 2019).

In line with our findings, Hanslin and colleagues induced systemic inflammation via intravenous LPS administration, where they observed impaired hepatic bacterial clearance 24 hours after the onset of the inflammation (Hanslin et al., 2019).

### 4.3.3 Mechanism of impaired bactericidal activity by liver TRMs

Mitochondrial and non-mitochondrial ROS are crucial for macrophages to combat pathogens (Weinberg et al., 2015), as well as important intracellular messengers (Sena and Chandel, 2012). West and colleagues described the diminished bactericidal activity of BMDMs through decreased mROS production (West et al., 2011). Similar results have been observed in AMs (Bewley et al., 2017). Given the impairment in mROS generation of liver TRMs found in this study, we conclude that this is the key contributor to the observed decrease in bactericidal activity *in vivo* (Langelage et al., 2021).

Acute liver injury was shown to impair bacterial killing in hepatic, splenic, and peritoneal macrophages via IL-10 produced by liver TRMs (Abe et al., 2004). Moreover, massive bacteremia was shown to induce severe liver injury which was accompanied by impaired hepatic bacterial clearance (Ashare et al., 2006). However, we did not detect liver injury or inflammation after acid aspiration. Histopathologic analysis of the livers showed no inflammation after acid aspiration. Moreover, cytokines were not elevated in liver homogenates after aspiration. In line, mRNA levels of cytokines were merely altered in liver TRMs of acid-treated animals. Accordingly, plasma levels of liver function

parameters were unchanged 24h after acid aspiration, which excludes considerable hepatocyte damage. Additionally, flow cytometric analysis of innate immune cells exhibited no increase in infiltrating blood monocytes or neutrophils, which increase during hepatic damage (Guillot and Tacke, 2019). Thus, acute liver injury is rather unlikely to cause the changes observed in liver macrophages one day after aspiration.

Of note, Heuer et al. observed distinct leukocyte infiltration and areas of necrosis within livers only 4 hours after the occurrence of acid aspiration in pigs (Heuer et al., 2012). In this study, animals were mechanically ventilated, which was shown to induce liver injury by itself (Kredel et al., 2007). If ventilation alone similarly impairs the bactericidal properties of liver TRMs is a clinically relevant question, which remains to be investigated.

Depending on the severity of the aspiration, the arterial partial pressure of oxygen shifts towards severely hypoxemic levels minutes after the aspiration took place (Richter et al., 2013), remains diminished for around one day (Setzer et al., 2018), and returns to the levels of healthy individuals around one to two weeks after the aspiration (Amigoni et al., 2008; Richter et al., 2015). There are contradicting data regarding the effects of hypoxia on macrophages´ bactericidal activity.

Hypoxia was shown to impair the bactericidal activity against gram-negative as well as gram-positive bacteria in BMDMs *in vitro* due to altered mitochondrial metabolism (Wiese et al., 2012). Under hypoxemic conditions, mitochondria dampen OXPHOS, yet can still generate a basal level of mROS, which is pivotal for signaling purposes through adaptations in the ETC. However, these adaptations preclude a rise in mROS in response to bacteria (Wiese et al., 2012; Fuhrmann and Brüne, 2017). Additionally, Koch and colleagues were able to demonstrate that systemic hypoxia distinctly impairs bacterial clearance from the bloodstream in the liver and the spleen (Koch et al., 1993). Therefore, it is tempting to speculate that the phenotype observed in liver TRMs is at least partially caused by systemic hypoxia due to pulmonary damage since they exhibited diminished OXPHOS as well as impaired mROS generation and bactericidal activity.

In contrast, other studies observed an increase in phagocytosis and bactericidal activity in PMs *in vivo* during systemic hypoxia (Anand et al., 2007). In addition, hypoxia was shown to induce HIFs in macrophages which are potent drivers of a pro-inflammatory phenotype and induce among others the expression of IL-1ß (McGettrick and O'Neill, 2020). Moreover, liver TRMs exhibited a strong pro-inflammatory phenotype with the consecutive release of pro-inflammatory cytokines and large amounts of ROS in a model

of ischemia and reperfusion (Teoh, 2011; Sena and Chandel, 2012). Given that IL-1ß mRNA levels were virtually unaltered in liver TRMs after aspiration, it seems unlikely that liver TRMs experience HIF-1α activations, and thus severe hypoxia.

Ultimately, the question of whether hypoxia contributes to the impairment in bacterial killing remains unanswered since, to the knowledge of this author, there is to this day no study that directly analyzed liver macrophages' bactericidal properties dependent on the ambient oxygen concentration.

Interestingly, Kinoshita and colleagues described two different populations within the pool of F4/80$^{pos}$ Kupffer cells. The first was classified as CD68$^{pos}$CD11b$^{neg}$ and constitutes the most abundant one under steady-state conditions with a marked capacity for phagocytosis and generation of ROS upon LPS stimulation (Kinoshita et al., 2010). The CD11b$^{pos}$CD68$^{neg}$ Kupffer cells possess a weaker capability to phagocytose and mount ROS but instead are capable to produce TNF-α in response to LPS. In the case of bacteremia, the latter rapidly expands and becomes the dominant population with augmented phagocytic capacities but still poor ROS production. Okamoto and colleagues found that CD11b$^{pos}$CD68$^{neg}$ Kupffer cells exhibit strong bactericidal activity *in vitro* and deletion of CD11b$^{pos}$CD68$^{neg}$ Kupffer cells impaired survival in a model with *Enterococcus faecalis* bacteremia (Okamoto et al., 2021). In contrast, the CD68$^{pos}$ CD11b$^{neg}$ population did not exhibit bactericidal properties.

Since the previously mentioned subpopulations were not analyzed in this study, we can only speculate about their role in our model. Our functional data, however, do not support the idea of an altered composition of Kupffer cell subpopulations. The reduced mROS generation favors the idea of an increase in the CD11b$^{pos}$CD68$^{neg}$ population since this one is less capable of ROS generation. Yet the impairment in the bacterial killing would be indicative of a decrease of the CD11b$^{pos}$ CD68$^{neg}$ population since only this one exhibits antibacterial properties. Moreover, Kinoshita et al. did not elucidate the source of ROS production, thus further hampering the comparison of their work to ours.

TNF-α is a pivotal mediator for the extra-pulmonary response to acid aspiration (Goldman et al., 1990). We observed increased levels of TNF-α in the blood after acid aspiration (no data shown). Therefore, it seems reasonable to assume that the phenotype observed in liver TRMs after aspiration is influenced by TNF-α as well. However, previous studies unveiled that *in vitro* stimulation of liver TRMs with TNF-α enhances their bactericidal activity (Salimi and Ghadirian, 1993). Additionally, blood-derived TNF-α does not impair bacterial clearance in the liver *in vivo* (Koch et al., 1993).

Our laboratory recently identified myeloperoxidase (MPO) from apoptotic pulmonary neutrophils as the mediator that precludes mROS production in response to bacteria in AMs (Better et al., 2023). Intriguingly, Liu and colleagues revealed that plasma levels of MPO rise soon after acid aspiration (Liu et al., 2009). Therefore, it is tempting to speculate that liver TRMs may be influenced by circulating MPO. This hypothesis is supported by the findings of Holub and colleagues, who observed that phagocytosed neutrophils convey marked anti-inflammatory effects on liver macrophages (Holub et al., 2009).

The hepatic APR constitutes another factor that influences the functional polarization of liver TRMs. Whenever tissue damage occurs, cellular debris and cytokines secreted from immune cells on the damaged site are released into the bloodstream, which induce the production of acute-phase proteins in hepatocytes to support a balanced immune response (Cray et al., 2009; Quinton et al., 2009). Previous studies highlighted the interactions between the liver and the lung herein and introduced the term "lung-liver axis". Hilliard et al. elegantly demonstrated that hepatic acute-phase proteins support a well-performing pulmonary immune response during bacterial pneumonia (Hilliard et al., 2015). More precisely, the APR augments cytokine secretion in AMs as well as the innate immune system of the lungs in general and thus its bactericidal abilities. Interestingly they also discovered that the absence of acute-phase proteins results in large-scale liver damage mainly mediated through TNF-α during bacterial pneumonia peaking 24h after infection (Hilliard et al., 2015). Sander and colleagues observed increased systemic inflammation and massive hepatic damage during bacterial sepsis in APR-deficient mice (Sander et al., 2010). Moreover, Renckens et al. found that the APR impaired the host response against *P. aeruginosa* (Renckens et al., 2008) as well as *Acinetobacter baumanii* (Renckens et al., 2006). These last two studies are of particular interest since they induced the APR in a sterile manner 24h before the administration of bacteria, and thereby exhibit important similarities to our model. Furthermore, Inatsu and colleagues observed that pretreatment with CRP, one of the main APR proteins, reduced the ability of liver TRMs to generate ROS upon LPS stimulation (Inatsu et al., 2009).

Overall, the hepatic APR has strong immunomodulatory capabilities. Acid aspiration elicits an APR (Ayala et al., 2016), which might thereby influence liver TRMs. However, more research is required to fully understand the role of liver TRMs in the induction of the APR and the impact of the APR on the function of liver TRMs.

Eventually, the underlying mechanism that impaired the bactericidal properties of liver TRMs remains unknown. Ultimately, a profound mechanistic understanding may pave the way to therapeutic approaches to potentially reduce nosocomial infections in patients suffering from acid aspiration or ALI in general.

## 4.4 Peritoneum

PMs are abundantly used for *in vitro* studies of macrophage physiology because they are easily available. However, considerably fewer studies focus on their role *in vivo*. PMs are made up of two subpopulations: LPMs and SPMs (Dos Anjos Cassado, 2017). In this study, we did not discriminate between these two populations for gene expression and *ex vivo* analysis due to F4/80 expression by both populations (Dos Anjos Cassado, 2017). However, as LPMs constitute roughly 90% of all PMs at steady state (Cassado et al., 2015) and at all analyzed time points after acid aspiration, we consider this population as the main contributor in our experiments.

The bactericidal activity of PMs was unaltered when tested *ex vivo* 24h after aspiration and there was no significant difference in peritoneal bacterial loads during systemic *in vivo* bacterial infection 24h after acid aspiration (Langelage et al., 2021). The ability of PMs to combat pathogens is influenced by a plethora of factors like variations in ambient fatty acids (Grando et al., 2009), multiple cytokines (Spight et al., 2008; Tran et al., 2014), or food composition (Wang et al., 2003). Therefore, the unaltered bactericidal capabilities of PMs one day after aspiration argue against a considerable affection of the peritoneum. In line with this, the flow cytometric analysis of peritoneal innate immune cells also didn´t reveal significant alterations at this time point.

The transcriptional data display a pro-inflammatory profile in PMs 8d after acid aspiration. However, the occurrence of peritonitis after acid aspiration seems very unlikely since flow cytometric analysis of peritoneal lavage cells did not show an increase in monocytes or neutrophils and inflammatory cytokines were below detection limit in the lavage fluid. Furthermore, diminished LPM numbers accompanied by a massive increase in SPMs are hallmark features of peritoneal inflammation (Ghosn et al., 2010), yet the ratio between LPMs and SPMs remained unaltered after acid aspiration. Thus, the significance of a transcriptionally increased expression of cytokines 8 days after acid aspiration remains unclear.

## 4.5 Spleen

Splenic TRMs were shown to be able to clear bacteria from the systemic circulation (den Haan and Kraal, 2012; Borges da Silva et al., 2015). Moreover, splenic TRMs contribute to iron metabolism by the removal of aged erythrocytes and constitute an important bridge between innate and adaptive immune systems (Borges da Silva et al., 2015). Our finding of unaltered bactericidal properties after acid aspiration *in vitro* as well as *in vivo* of splenic TRMs is interesting since the spleen and the liver are both well supplied with blood. Thus, they are exposed to the same mediators released from the damaged lung or more generalized the same alteration in oxygenation or blood ingredients like MPO.

Roquilly and colleagues observed that splenic TRMs and BMDMs did not show impaired phagocytic capabilities 7 days after *E. coli* pneumonia (Roquilly et al., 2020). This is in line with our findings since phagocytosis was not altered in splenic macrophages after acid aspiration pneumonitis. However, Roquilly et al. solely analyzed the bacterial uptake and not their eradication at one time point after pneumonia.

Recent studies unveiled that splenic macrophages and not AMs are the main source of sustained bacteremia during pneumococcal pneumonia (Carreno et al., 2021), with pneumococci even proliferating within these macrophages (Ercoli et al., 2018). Most interestingly, splenic macrophages are typically very efficient in the clearance of bacteria (Aichele et al., 2003; Perez et al., 2017). Hence, differences between pathogens or inflammatory stimuli during pneumococcal pneumonia might account for varying effects on splenic macrophages.

In a model of ALI induced by AKI splenic macrophages were, amongst other immune cells, shown to dampen the pulmonary inflammation by IL-10 production, which was triggered by increased serum levels of IL-6 (Andres-Hernando et al., 2017). A similarly beneficial effect was described for spleen-derived macrophages which aid in dampening pulmonary inflammation and enhance tissue regeneration during nitrogen mustard-induced lung inflammation (Venosa et al., 2015). Although Venosa and colleagues did not elucidate a specific mechanism, they observed that splenectomy results in a preponderance of pro-inflammatory macrophages in the damaged lungs, which leads to increased fibrosis. In contrast, during severe acute pancreatitis, the spleen was identified as a potent amplifier of systemic inflammation resulting in liver damage (Zhou et al., 2019).

To sum up, the role of the spleen and its macrophages during systemic inflammation and more specifically its role in ALI / ARDS is poorly understood and constitutes an interesting topic for further research.

# 5 Summary

Acid aspiration is a major cause of ALI and induces sterile pneumonitis. The immune response to acid aspiration is not limited to the lungs but also involves extrapulmonary organs. This study investigated the effects of acid-induced ALI on TRMs in the kidneys, the liver, the peritoneum, and the spleen at indicated time points after aspiration in a mouse model.

Kidney TRMs displayed a pro-inflammatory phenotype with upregulation of IL-1ß and IL-6 transcripts 24h after aspiration. Flow cytometric analysis revealed an increased IL-6 protein synthesis at this time. Creatinine levels were unaltered one day after aspiration but mounted eight days afterward. Subsequent histopathologic analysis did not show any tissue damage.

Further transcriptional analysis revealed key metabolic enzymes, especially the TCA cycle regulator enzyme IDH-1, to be distinctly downregulated 24h after acid aspiration in hepatic, splenic, and peritoneal TRMs with the most marked manifestation in liver TRMs. *Ex vivo* seahorse analysis of liver TRMs unveiled a distinct impairment to perform OXPHOS one day after aspiration. Bacterial killing assays performed *ex vivo* with *P. aeruginosa* and *K. pneumoniae* revealed a marked impairment in the bactericidal activity of liver TRMs 24h after aspiration, while splenic and peritoneal TRMs were not affected. The following investigation unraveled a compromised generation of mROS upon bacterial encounter as a mechanism for the impairment in bactericidal activity.

Subsequent analysis did not detect hepatic inflammation as an elicitor of the alterations in liver TRMs.

The liver harbors the majority of macrophages in a mammal's body and is crucial for clearing bacteria from systemic circulation. We found liver TRMs to be involved in the systemic response to acid aspiration. Their impaired bactericidal activity one day after aspiration may thus result in increased susceptibility to nosocomial infection after aspiration as commonly seen in intubated patients.

# 6 Zusammenfassung

Säureaspiration ist eine Hauptursache für akutes Lungenversagen, und initiiert eine zunächst sterile Entzündung der Lunge. Die Immunantwort auf Säureaspiration ist nicht auf die Lunge beschränkt, sondern schließt auch extrapulmonale Organe mit ein. Die vorliegende Studie untersuchte die Auswirkungen von Säureaspiration auf gewebsresidente Makrophagen in Nieren, Leber, Peritoneum und Milz zu mehreren Zeitpunkten nach Aspiration an einem Mausmodel.

In Nierenmakrophagen imponierte 24 Stunden nach Aspiration ein proinflammatorisches Genexpressionsprofil mit besonders ausgeprägter transkriptioneller Steigerung von IL-1ß und IL-6. Druchflusszytometrische Untersuchungen zeigten ebenfalls eine gesteigerte IL-6 Proteinsynthese. Der Kreatininspiegel war am ersten Tag nach Aspiration nicht erhöht, stieg jedoch 1 Woche später an. Histopathologische Untersuchungen lieferten keinen Anhalt für eine renale Gewebsschädigung.

Weiterführende transkriptionelle Analysen offenbarten, dass metabolische Schlüsselenzyme, insbesondere das Citratzyklusregulatorenzym IDH-1, in Leber-, Milz- und Peritonealmakrophagen einen Tag nach Aspiration deutlich vermindert transkribiert werden. *Ex vivo* Untersuchungen von Lebermakrophagen zeigten eine deutlich herabgesetzte Kapazität dieser Zellen oxidative Phosphorylierung durchzuführen. Weiterhin konnte eine verminderte Fähigkeit von Lebermakrophagen Bakterien zu eradizieren an *P. aeruginosa* sowie *K. pneumoniae* einen Tag nach Aspiration nachgewiesen werden. Als zugrundeliegender Mechanismus wurde eine Minderung der Generierung mitochondrialer reaktiver Sauerstoffspezies identifiziert.

Nachfolgende Untersuchungen konnten Gewebeschäden bzw. Entzündungsreaktionen in der Leber als Auslöser der beobachteten Veränderungen in Lebermakrophagen ausschließen.

Die Leber beherbergt den Großteil aller Makrophagen im Körper eines Säugetieres und ist essenziell für die Entfernung von Bakterien aus dem Blutstrom. In dieser Arbeit konnte eine Beteiligung von Lebermakrophagen an der systemischen Reaktion auf Säureaspiration nachgewiesen werden. Ihre verminderte Fähigkeit einen Tag nach Aspiration Bakterien zu eradizieren, kann eine Mitursache der erhöhten Anfälligkeit für nosokomiale Infektionen bei intubierten Patienten sein.

# 7 List of abbreviations

| | |
|---|---|
| °C | degree Celsius |
| µl | microliter |
| µm | micrometer |
| µM | micromolar |
| ACOD-1 | aconitate decarboxylase-1 |
| AKI | acute kidney injury |
| ALI | acute lung injury |
| ALT | alanine transaminase |
| AMs | alveolar macrophages |
| APC | allophycocyanin |
| APR | acute-phase response |
| ARDS | acute respiratory distress syndrome |
| AST | aspartate transaminase |
| ATP | adenosine triphosphate |
| BMDMs | bone marrow-derived macrophages |
| BSA | bovine serum albumin |
| BV | brilliant violet |
| CD | cluster of differentiation |
| cDNA | complementary desoxyribonucleic acid |
| CFU | colony forming units |
| CKD | chronic kidney disease |
| $CO_2$ | carbon dioxide |
| CRP | C-reactive protein |

| | |
|---|---|
| d | day(s) |
| DAMPs | danger-associated molecular patterns |
| DAPI | 4′,6-diamidino-2-phenylindole |
| DMEM | dulbeco´s modified eagles' medium |
| DMSO | dimethylsulfoxide |
| DNA | desoxyribonucleic acid |
| dNTP | deoxynucleotide triphosphate |
| DTT | dithiothreitol |
| EDTA | ethylenediaminetetraacetic acid |
| ETC | electron transport chain |
| FACS | fluorescence-activated cell sorting |
| FBS | fetal bovine serum |
| FCCP | carbonyl cyanide-p-trifluoromethoxyphenylhydrazone |
| Fig | figure |
| FITC | fluorescein isothiocyanate |
| G | Gauge |
| g | gram(s) |
| G-CSF | granulocyte colony-stimulating factor |
| GM-CSF | granulocyte-macrophage colony-stimulating factor |
| GOT | glutamic oxaloacetic transaminase |
| GPT | glutamate-pyruvate transaminase |
| h | hour(s) |
| HBSS | hanks buffered saline solution |
| HCl | hydrochloric acid |

| | |
|---|---|
| HE | hematoxyline & eosin |
| HEPES | 4-(2-hydroxyethyl)-1-piperazineethanesulfonic acid |
| HK-2 | hexokinase-2 |
| ICAM-1 | intercellular adhesion molecule-1 |
| IDH-1 | isocitrate dehydrogenase-1 |
| IFN | interferon |
| IL | interleukin |
| IRG-1 | immune responsive gene-1 |
| *K. pneumoniae* | *Klebsiella pneumoniae* |
| KC | keratinocyte-derived chemokine |
| LB medium | Luria Broth medium |
| LPMs | large peritoneal macrophages |
| LPS | lipopolysaccharide |
| Ly6C | lymphocyte antigen 6 C |
| Ly6G | lymphocyte antigen 6 G |
| MACS | magnetic cell separation |
| MCP-1 | monocyte chemoattractant protein-1 |
| MDMs | monocyte-derived macrophages |
| MHC | major histocompatibility complex |
| min | minute(s) |
| MIP-1α | macrophage inflammatory protein-1α |
| MIP-1ß | macrophage inflammatory protein-1ß |
| ml | milliliter |
| mM | millimolar |

| | |
|---|---|
| MOI | multiplicity of infection |
| MPO | myeloperoxidase |
| mROS | mitochondrial reactive oxygen species |
| NaCl | sodium chloride |
| NADPH | nicotinamide adenine dinucleotide phosphate |
| NOD-like | nucleotide-binding oligomerization domain-like |
| OCR | oxygen consumption rate |
| OD | optic density |
| OXPHOS | oxidative phosphorylation |
| *P. aeruginosa* | *Pseudomonas aeruginosa* |
| PAMPs | pathogen-associated molecular patterns |
| PaO$_2$ | arterial partial pressure of oxygen |
| PBS | phosphate-buffered saline |
| PCR | polymerase chain reaction |
| PE | phycoerythrin |
| PEEP | positive end-expiratory pressure |
| PFA | paraformaldehyde |
| Pfkfb3 | phosphofructokinase / fructose-2,6-bisphosphatase 3 |
| PLF | peritoneal lavage fluid |
| PMs | peritoneal macrophages |
| pmol | picomol |
| PRR | pattern-recognition receptor |
| qPCR | quantitative PCR |
| RBC | red blood cell |

| | |
|---|---|
| RNA | ribonucleic acid |
| ROS | reactive oxygen species |
| rpm | rounds per minute |
| RPMI medium | Roswell Park Memorial Institute medium |
| RT M-MLV | reverse transcriptase from moloney murine leukemia virus |
| RT-qPCR | reverse transcriptase quantitative polymerase chain reaction |
| SDH | succinate dehydrogenase |
| sec | second(s) |
| SEM | standard error of the mean |
| SPMs | small peritoneal macrophages |
| SUCNR-1 | succinate receptor-1 |
| TCA cycle | tricarboxylic acid cycle |
| Tim4 | T-cell immunoglobulin mucin 4 |
| TLR(s) | toll-like receptor(s) |
| TNF | tumor necrosis factor |
| TRMs | tissue-resident macrophages |
| XF | extracellular flux |

# 8 References

Abe, T., Arai, T., Ogawa, A., Hiromatsu, T., Masuda, A., Matsuguchi, T., Nimura, Y., and Yoshikai, Y. (2004). Kupffer cell-derived interleukin 10 is responsible for impaired bacterial clearance in bile duct-ligated mice. Hepatology (Baltimore, Md.) *40*, 414-423. https://doi.org/10.1002/hep.20301.

Adnet, F., and Baud, F. (1996). Relation between Glasgow Coma Scale and aspiration pneumonia. The Lancet *348*, 123-124. https://doi.org/10.1016/S0140-6736(05)64630-2.

Aichele, P., Zinke, J., Grode, L., Schwendener, R.A., Kaufmann, S.H.E., and Seiler, P. (2003). Macrophages of the splenic marginal zone are essential for trapping of blood-borne particulate antigen but dispensable for induction of specific T cell responses. Journal of immunology (Baltimore, Md. : 1950) *171*, 1148-1155. https://doi.org/10.4049/jimmunol.171.3.1148.

Aldrich, T., Morrison, J., and Cesario, T. (1980). Aspiration after overdosage of sedative or hypnotic drugs. Southern medical journal *73*, 456-458. https://doi.org/10.1097/00007611-198004000-00017.

Amigoni, Bellani G, Scanziani M, Masson S, Bertoli E, Radaelli E, Patroniti N, Di Lelio A, Pesenti A, and Latini R. (2008). Lung Injury and Recovery in a Murine Model of Unilateral Acid Aspiration - Functional, Biochemical, and Morphologic Characterization. Anesthseiology *108*, 1037-1046. https://doi.org/10.1097/ALN.0b013e318173f64f.

Amit, I., Winter, D.R., and Jung, S. (2016). The role of the local environment and epigenetics in shaping macrophage identity and their effect on tissue homeostasis. Nature immunology *17*, 18-25. https://doi.org/10.1038/ni.3325.

Anand, R.J., Gribar, S.C., Li, J., Kohler, J.W., Branca, M.F., Dubowski, T., Sodhi, C.P., and Hackam, D.J. (2007). Hypoxia causes an increase in phagocytosis by macrophages in a HIF-1alpha-dependent manner. Journal of leukocyte biology *82*, 1257-1265. https://doi.org/10.1189/jlb.0307195.

Andres-Hernando, A., Okamura, K., Bhargava, R., Kiekhaefer, C.M., Soranno, D., Kirkbride-Romeo, L.A., Gil, H.-W., Altmann, C., and Faubel, S. (2017). Circulating IL-6 upregulates IL-10 production in splenic CD4+ T cells and limits

acute kidney injury-induced lung inflammation. Kidney international *91*, 1057-1069. https://doi.org/10.1016/j.kint.2016.12.014.

Ashare, A., Monick, M.M., Powers, L.S., Yarovinsky, T., and Hunninghake, G.W. (2006). Severe bacteremia results in a loss of hepatic bacterial clearance. American journal of respiratory and critical care medicine *173*, 644-652. https://doi.org/10.1164/rccm.200509-1470OC.

Ayala, P., Meneses, M., Olmos, P., Montalva, R., Droguett, K., Ríos, M., and Borzone, G. (2016). Acute lung injury induced by whole gastric fluid: hepatic acute phase response contributes to increase lung antiprotease protection. Respir Res *17*, 71. https://doi.org/10.1186/s12931-016-0379-7.

Bain, C.C., Bravo-Blas, A., Scott, C.L., Perdiguero, E.G., Geissmann, F., Henri, S., Malissen, B., Osborne, L.C., Artis, D., and Mowat, A.M. (2014). Constant replenishment from circulating monocytes maintains the macrophage pool in the intestine of adult mice. Nature immunology *15*, 929-937. https://doi.org/10.1038/ni.2967.

Basile, D.P., Anderson, M.D., and Sutton, T.A. (2012). Pathophysiology of acute kidney injury. Comprehensive Physiology *2*, 1303-1353. https://doi.org/10.1002/cphy.c110041.

Bdeir, K., Higazi, A.A.-R., Kulikovskaya, I., Christofidou-Solomidou, M., Vinogradov, S.A., Allen, T.C., Idell, S., Linzmeier, R., Ganz, T., and Cines, D.B. (2010). Neutrophil alpha-defensins cause lung injury by disrupting the capillary-epithelial barrier. American journal of respiratory and critical care medicine *181*, 935-946. https://doi.org/10.1164/rccm.200907-1128OC.

Beck-Schimmer, B., Rosenberger, D.S., Neff, S.B., Jamnicki, M., Suter, D., Fuhrer, T., Schwendener, R., Booy, C., Reyes, L., and Pasch, T., et al. (2005). Pulmonary aspiration: new therapeutic approaches in the experimental model. Anesthesiology *103*, 556-566. https://doi.org/10.1097/00000542-200509000-00019.

Bernard Gordon R., Luce John M., Sprung Charles L., Rinaldo Jean E., Tate Robert M., Sibbald William J., Kariman Khalil, Higgins Stanley, Bradley Roberta, and Metz Craig A., et al. (1987). High-Dose Corticosteroids in Patients with the Adult

Respiratory Distress Syndrome. The New England journal of medicine *317*, 1565-1570. https://doi.org/10.1056/NEJM198712173172504.

Better, J., Wetstein, M., Estiri, M., Malainou, C., Ferrero, M., Langelage, M., Kuznetsova, I., Vazquez-Armendariz, I., Kimmig, L., and Mansouri, S., et al. (2023). Neutrophil efferocytosis reprograms mitochondrial metabolism to switch alveolar macrophages to a pro-resolution phenotype at the cost of bacterial control. bioRxiv, 2023.03.07.528464. https://doi.org/10.1101/2023.03.07.528464.

Bewley, M.A., Preston, J.A., Mohasin, M., Marriott, H.M., Budd, R.C., Swales, J., Collini, P., Greaves, D.R., Craig, R.W., and Brightling, C.E., et al. (2017). Impaired Mitochondrial Microbicidal Responses in Chronic Obstructive Pulmonary Disease Macrophages. American journal of respiratory and critical care medicine *196*, 845-855. https://doi.org/10.1164/rccm.201608-1714OC.

Bilzer, M., Roggel, F., and Gerbes, A.L. (2006). Role of Kupffer cells in host defense and liver disease. Liver international : official journal of the International Association for the Study of the Liver *26*, 1175-1186. https://doi.org/10.1111/j.1478-3231.2006.01342.x.

Blériot, C., and Ginhoux, F. (2019). Understanding the Heterogeneity of Resident Liver Macrophages. Frontiers in immunology *10*, 2694. https://doi.org/10.3389/fimmu.2019.02694.

Borges da Silva, H., Fonseca, R., Pereira, R.M., Cassado, A.D.A., Álvarez, J.M., and D'Império Lima, M.R. (2015). Splenic Macrophage Subsets and Their Function during Blood-Borne Infections. Frontiers in immunology *6*, 480. https://doi.org/10.3389/fimmu.2015.00480.

Brito, M.A., Silva, R., Tiribelli, C., and Brites, D. (2000). Assessment of bilirubin toxicity to erythrocytes. Implication in neonatal jaundice management. European journal of clinical investigation *30*, 239-247. https://doi.org/10.1046/j.1365-2362.2000.00612.x.

Bulua, A.C., Simon, A., Maddipati, R., Pelletier, M., Park, H., Kim, K.-Y., Sack, M.N., Kastner, D.L., and Siegel, R.M. (2011). Mitochondrial reactive oxygen species promote production of proinflammatory cytokines and are elevated in TNFR1-

associated periodic syndrome (TRAPS). The Journal of experimental medicine *208*, 519-533. https://doi.org/10.1084/jem.20102049.

Cao, Q., Harris, D.C.H., and Wang, Y. (2015). Macrophages in kidney injury, inflammation, and fibrosis. Physiology (Bethesda, Md.) *30*, 183-194. https://doi.org/10.1152/physiol.00046.2014.

Carreno, D., Wanford, J.J., Jasiunaite, Z., Hames, R.G., Chung, W.Y., Dennison, A.R., Straatman, K., Martinez-Pomares, L., Pareek, M., and Orihuela, C.J., et al. (2021). Splenic macrophages as the source of bacteraemia during pneumococcal pneumonia. EBioMedicine *72*, 103601. https://doi.org/10.1016/j.ebiom.2021.103601.

Cassado, A.D.A., D'Imperio Lima, M.R., and Bortoluci, K.R. (2015). Revisiting mouse peritoneal macrophages: heterogeneity, development, and function. Frontiers in immunology *6*, 225. https://doi.org/10.3389/fimmu.2015.00225.

Chao, J., Wood, J.G., and Gonzalez, N.C. (2009). Alveolar hypoxia, alveolar macrophages, and systemic inflammation. Respiratory research *10*, 54. https://doi.org/10.1186/1465-9921-10-54.

Chen, T., Yang, C., Li, M., and Tan, X. (2016). Alveolar Hypoxia-Induced Pulmonary Inflammation: From Local Initiation to Secondary Promotion by Activated Systemic Inflammation. Journal of vascular research *53*, 317-329. https://doi.org/10.1159/000452800.

Cray, C., Zaias, J., and Altman, N.H. (2009). Acute phase response in animals: a review. Comparative medicine *59*, 517-526.

Dalli, J., and Serhan, C.N. (2017). Pro-Resolving Mediators in Regulating and Conferring Macrophage Function. Frontiers in immunology *8*, 1400. https://doi.org/10.3389/fimmu.2017.01400.

Darmon, M., Clec'h, C., Adrie, C., Argaud, L., Allaouchiche, B., Azoulay, E., Bouadma, L., Garrouste-Orgeas, M., Haouache, H., and Schwebel, C., et al. (2014). Acute respiratory distress syndrome and risk of AKI among critically ill patients. Clinical journal of the American Society of Nephrology : CJASN *9*, 1347-1353. https://doi.org/10.2215/CJN.08300813.

Davidson, B.A., Knight, P.R., Helinski, J.D., Nader, N.D., Shanley, T.P., and Johnson, K.J. (1999). The role of tumor necrosis factor-alpha in the pathogenesis of aspiration pneumonitis in rats. Anesthesiology *91*, 486-499.

Davidson, B.A., Knight, P.R., Wang, Z., Chess, P.R., Holm, B.A., Russo, T.A., Hutson, A., and Notter, R.H. (2005). Surfactant alterations in acute inflammatory lung injury from aspiration of acid and gastric particulates. American journal of physiology. Lung cellular and molecular physiology *288*, L699-708. https://doi.org/10.1152/ajplung.00229.2004.

Davidson, B.A., Vethanayagam, R.R., Grimm, M.J., Mullan, B.A., Raghavendran, K., Blackwell, T.S., Freeman, M.L., Ayyasamy, V., Singh, K.K., and Sporn, M.B., et al. (2013). NADPH oxidase and Nrf2 regulate gastric aspiration-induced inflammation and acute lung injury. Journal of immunology (Baltimore, Md. : 1950) *190*, 1714-1724. https://doi.org/10.4049/jimmunol.1202410.

Davies, L.C., Jenkins, S.J., Allen, J.E., and Taylor, P.R. (2013). Tissue-resident macrophages. Nature immunology *14*, 986-995. https://doi.org/10.1038/ni.2705.

Davies, L.C., Rice, C.M., Palmieri, E.M., Taylor, P.R., Kuhns, D.B., and McVicar, D.W. (2017). Peritoneal tissue-resident macrophages are metabolically poised to engage microbes using tissue-niche fuels. Nature communications *8*, 2074. https://doi.org/10.1038/s41467-017-02092-0.

den Haan, J.M.M., and Kraal, G. (2012). Innate immune functions of macrophage subpopulations in the spleen. Journal of innate immunity *4*, 437-445. https://doi.org/10.1159/000335216.

Dickson, R.P., Singer, B.H., Newstead, M.W., Falkowski, N.R., Erb-Downward, J.R., Standiford, T.J., and Huffnagle, G.B. (2016). Enrichment of the lung microbiome with gut bacteria in sepsis and the acute respiratory distress syndrome. Nat Microbiol *1*, 1-9. https://doi.org/10.1038/nmicrobiol.2016.113.

Doi, K., Ishizu, T., Fujita, T., and Noiri, E. (2011). Lung injury following acute kidney injury: kidney-lung crosstalk. Clinical and experimental nephrology *15*, 464-470. https://doi.org/10.1007/s10157-011-0459-4.

Domenech, P., Perez, T., Saldarini, A., Uad, P., and Musso, C.G. (2017). Kidney-lung pathophysiological crosstalk: its characteristics and importance. International

urology and nephrology *49*, 1211-1215. https://doi.org/10.1007/s11255-017-1585-z.

Dong, H., Feng, Y., Yang, Y., Hu, Y., Jia, Y., Yang, S., Zhao, N., and Zhao, R. (2021). A Novel Function of Mitochondrial Phosphoenolpyruvate Carboxykinase as a Regulator of Inflammatory Response in Kupffer Cells. Front. Cell Dev. Biol. *9*, 726931. https://doi.org/10.3389/fcell.2021.726931.

Dos Anjos Cassado, A. (2017). F4/80 as a Major Macrophage Marker: The Case of the Peritoneum and Spleen. Results and problems in cell differentiation *62*, 161-179. https://doi.org/10.1007/978-3-319-54090-0_7.

Dragan, V., Wei, Y., Elligsen, M., Kiss, A., Walker, S.A.N., and Leis, J.A. (2018). Prophylactic Antimicrobial Therapy for Acute Aspiration Pneumonitis. Clinical infectious diseases : an official publication of the Infectious Diseases Society of America *67*, 513-518. https://doi.org/10.1093/cid/ciy120.

Dreyfuss, D., and Ricard, J.-D. (2005). Acute lung injury and bacterial infection. Clinics in chest medicine *26*, 105-112. https://doi.org/10.1016/j.ccm.2004.10.014.

El-Solh, A.A., Vora, H., Knight, P.R., and Porhomayon, J. (2011). Diagnostic use of serum procalcitonin levels in pulmonary aspiration syndromes. Critical care medicine *39*, 1251-1256. https://doi.org/10.1097/CCM.0b013e31820a942c.

Ercoli, G., Fernandes, V.E., Chung, W.Y., Wanford, J.J., Thomson, S., Bayliss, C.D., Straatman, K., Crocker, P.R., Dennison, A., and Martinez-Pomares, L., et al. (2018). Intracellular replication of Streptococcus pneumoniae inside splenic macrophages serves as a reservoir for septicaemia. Nature microbiology *3*, 600-610. https://doi.org/10.1038/s41564-018-0147-1.

Eworuke, E., Major, J.M., and Gilbert McClain, L.I. (2018). National incidence rates for Acute Respiratory Distress Syndrome (ARDS) and ARDS cause-specific factors in the United States (2006-2014). Journal of critical care *47*, 192-197. https://doi.org/10.1016/j.jcrc.2018.07.002.

Exarhos, Logan, Abbott, and Hatcher (1965). THE IMPORTANCE OF PH AND VOLUME IN TRACHEOBRONCHIAL ASPIRATION. Diseases of the chest *47*, 167-169. https://doi.org/10.1378/chest.47.2.167.

Fernandes, A., Falcão, A.S., Silva, R.F.M., Gordo, A.C., Gama, M.J., Brito, M.A., and Brites, D. (2006). Inflammatory signalling pathways involved in astroglial activation by unconjugated bilirubin. Journal of neurochemistry *96*, 1667-1679. https://doi.org/10.1111/j.1471-4159.2006.03680.x.

Flannagan, R.S., Cosío, G., and Grinstein, S. (2009). Antimicrobial mechanisms of phagocytes and bacterial evasion strategies. Nature reviews. Microbiology *7*, 355-366. https://doi.org/10.1038/nrmicro2128.

Flannagan, R.S., Heit, B., and Heinrichs, D.E. (2015). Antimicrobial Mechanisms of Macrophages and the Immune Evasion Strategies of Staphylococcus aureus. Pathogens (Basel, Switzerland) *4*, 826-868. https://doi.org/10.3390/pathogens4040826.

Franken, L., Klein, M., Spasova, M., Elsukova, A., Wiedwald, U., Welz, M., Knolle, P., Farle, M., Limmer, A., and Kurts, C. (2015). Splenic red pulp macrophages are intrinsically superparamagnetic and contaminate magnetic cell isolates. Scientific reports *5*, 12940. https://doi.org/10.1038/srep12940.

Fuhrmann, D.C., and Brüne, B. (2017). Mitochondrial composition and function under the control of hypoxia. Redox biology *12*, 208-215. https://doi.org/10.1016/j.redox.2017.02.012.

Gacouin, A., Locufier, M., Uhel, F., Letheulle, J., Bouju, P., Fillatre, P., Le Tulzo, Y., and Tadié, J.M. (2016). Liver Cirrhosis is Independently Associated With 90-Day Mortality in ARDS Patients. Shock (Augusta, Ga.) *45*, 16-21. https://doi.org/10.1097/SHK.0000000000000487.

Gates, S., Huang, T., and Cheney, F.W. (1983). Effects of methylprednisolone on resolution of acid-aspiration pneumonitis. Archives of surgery (Chicago, Ill. : 1960) *118*, 1262-1265. https://doi.org/10.1001/archsurg.1983.01390110020005.

Ghoneim, H.E., Thomas, P.G., and McCullers, J.A. (2013). Depletion of alveolar macrophages during influenza infection facilitates bacterial superinfections. Journal of immunology (Baltimore, Md. : 1950) *191*, 1250-1259. https://doi.org/10.4049/jimmunol.1300014.

Ghosn, E.E.B., Cassado, A.A., Govoni, G.R., Fukuhara, T., Yang, Y., Monack, D.M., Bortoluci, K.R., Almeida, S.R., Herzenberg, L.A., and Herzenberg, L.A. (2010).

Two physically, functionally, and developmentally distinct peritoneal macrophage subsets. Proceedings of the National Academy of Sciences of the United States of America *107*, 2568-2573. https://doi.org/10.1073/pnas.0915000107.

Ginhoux, F., and Guilliams, M. (2016). Tissue-Resident Macrophage Ontogeny and Homeostasis. Immunity *44*, 439-449. https://doi.org/10.1016/j.immuni.2016.02.024.

Goldman, R Welbourn, L Kobzik, C R Valeri, and D Shepro, and H B Hechtman (1990). Goldman, Ann Surg, 1990, Tumor necrosis factor-alpha mediates acid aspiration-induced systemic organ injury. Annals of Surgery, 513-520.

Goldman, Welbourn R, Kobzik L, and Valeri CR, Shepro D, Hechtman HB. (1995). Neutrophil adhesion receptor CD18 mediates remote but not localized acid aspiration injury. Surgery *117*, 83-89.

Goldman, G., Welbourn, R., Klausner, J.M., Kobzik, L., Valeri, C.R., Shepro, D., and Hechtman, H.B. (1993). Leukocytes mediate acid aspiration-induced multiorgan edema. Surgery *114*, 13-20.

Goldman., Welbourn, R., Kobzik, L., Valeri, C.R., Shepro, D., and Hechtman, H.B. (1992). Reactive oxygen species and elastase mediate lung permeability after acid aspiration. Journal of applied physiology (Bethesda, Md. : 1985) *73*, 271-575.

Gordon, S., Hamann, J., Lin, H.-H., and Stacey, M. (2011). F4/80 and the related adhesion-GPCRs. European journal of immunology *41*, 2472-2476. https://doi.org/10.1002/eji.201141715.

Gordon, S., and Pluddemann, A. (2017). Tissue macrophages: heterogeneity and functions. BMC biology *15*, 53. https://doi.org/10.1186/s12915-017-0392-4.

Grando, F.C.C., Felício, C.A., Twardowschy, A., Paula, F.M., Batista, V.G., Fernandes, L.C., Curi, R., and Nishiyama, A. (2009). Modulation of peritoneal macrophage activity by the saturation state of the fatty acid moiety of phosphatidylcholine. Braz J Med Biol Res *42*, 599-605. https://doi.org/10.1590/S0100-879X2009005000003.

Guillot, A., and Tacke, F. (2019). Liver Macrophages: Old Dogmas and New Insights. Hepatol Commun *3*, 730-743. https://doi.org/10.1002/hep4.1356.

Gurkan, O.U., O'Donnell, C., Brower, R., Ruckdeschel, E., and Becker, P.M. (2003). Differential effects of mechanical ventilatory strategy on lung injury and systemic organ inflammation in mice. American journal of physiology. Lung cellular and molecular physiology *285*, L710-8. https://doi.org/10.1152/ajplung.00044.2003.

Haase, J., Buchloh, D.C., Hammermuller, S., Salz, P., Mrongowius, J., Carvalho, N.C., Beda, A., Rau, A., Starke, H., and Spieth, P.M., et al. (2019). Mechanical Ventilation Strategies Targeting Different Magnitudes of Collapse and Tidal Recruitment in Porcine Acid Aspiration-Induced Lung Injury. Journal of clinical medicine *8*. https://doi.org/10.3390/jcm8081250.

Han, H.I., Skvarca, L.B., Espiritu, E.B., Davidson, A.J., and Hukriede, N.A. (2019). The role of macrophages during acute kidney injury: destruction and repair. Pediatric nephrology (Berlin, Germany) *34*, 561-569. https://doi.org/10.1007/s00467-017-3883-1.

Hanslin, K., Sjölin, J., Skorup, P., Wilske, F., Frithiof, R., Larsson, A., Castegren, M., Tano, E., and Lipcsey, M. (2019). The impact of the systemic inflammatory response on hepatic bacterial elimination in experimental abdominal sepsis. ICMx *7*, 52. https://doi.org/10.1186/s40635-019-0266-x.

Herb, M., and Schramm, M. (2021). Functions of ROS in Macrophages and Antimicrobial Immunity. Antioxidants (Basel, Switzerland) *10*. https://doi.org/10.3390/antiox10020313.

Herrero, R., Sánchez, G., Asensio, I., López, E., Ferruelo, A., Vaquero, J., Moreno, L., Lorenzo, A. de, Bañares, R., and Lorente, J.A. (2020). Liver–lung interactions in acute respiratory distress syndrome. ICMx *8*, 1-13. https://doi.org/10.1186/s40635-020-00337-9.

Heuer, J.F., Sauter, P., Pelosi, P., Herrmann, P., Bruck, W., Perske, C., Schondube, F., Crozier, T.A., Bleckmann, A., and Beissbarth, T., et al. (2012). Effects of pulmonary acid aspiration on the lungs and extra-pulmonary organs: a randomized study in pigs. Critical care (London, England) *16*, R35. https://doi.org/10.1186/cc11214.

Hilliard, K.L., Allen, E., Traber, K.E., Yamamoto, K., Stauffer, N.M., Wasserman, G.A., Jones, M.R., Mizgerd, J.P., and Quinton, L.J. (2015). The Lung-Liver Axis: A Requirement for Maximal Innate Immunity and Hepatoprotection during

Pneumonia. American journal of respiratory cell and molecular biology *53*, 378-390. https://doi.org/10.1165/rcmb.2014-0195OC.

Hoag, J.B., Liu, M., Easley, R.B., Britos-Bray, M.F., Kesari, P., Hassoun, H., Haas, M., Tuder, R.M., Rabb, H., and Simon, B.A. (2008). Effects of acid aspiration-induced acute lung injury on kidney function. American journal of physiology. Renal physiology *294*, F900-8. https://doi.org/10.1152/ajprenal.00357.2007.

Holub, M., Cheng, C.-W., Mott, S., Wintermeyer, P., van Rooijen, N., and Gregory, S.H. (2009). Neutrophils sequestered in the liver suppress the proinflammatory response of Kupffer cells to systemic bacterial infection. Journal of immunology (Baltimore, Md. : 1950) *183*, 3309-3316. https://doi.org/10.4049/jimmunol.0803041.

Hough, R.F., Islam, M.N., Gusarova, G.A., Jin, G., Das, S., and Bhattacharya, J. (2019). Endothelial mitochondria determine rapid barrier failure in chemical lung injury. JCI insight *4*. https://doi.org/10.1172/jci.insight.124329.

Hoyer, F.F., Naxerova, K., Schloss, M.J., Hulsmans, M., Nair, A.V., Dutta, P., Calcagno, D.M., Herisson, F., Anzai, A., and Sun, Y., et al. (2019). Tissue-Specific Macrophage Responses to Remote Injury Impact the Outcome of Subsequent Local Immune Challenge. Immunity *51*, 899-914.e7. https://doi.org/10.1016/j.immuni.2019.10.010.

Hu, X., Lee, J.S., Pianosi, P.T., and Ryu, J.H. (2015). Aspiration-related pulmonary syndromes. Chest *147*, 815-823. https://doi.org/10.1378/chest.14-1049.

Husain-Syed, F., Slutsky, A.S., and Ronco, C. (2016). Lung-Kidney Cross-Talk in the Critically Ill Patient. American journal of respiratory and critical care medicine *194*, 402-414. https://doi.org/10.1164/rccm.201602-0420CP.

Huxley, E.J., Viroslav, J., Gray, W.R., and Pierce, A.K. (1978). Pharyngeal aspiration in normal adults and patients with depressed consciousness. The American journal of medicine *64*, 564-568. https://doi.org/10.1016/0002-9343(78)90574-0.

Imai, Y., Kuba, K., Neely, G.G., Yaghubian-Malhami, R., Perkmann, T., van Loo, G., Ermolaeva, M., Veldhuizen, R., Leung, Y.H.C., and Wang, H., et al. (2008). Identification of oxidative stress and Toll-like receptor 4 signaling as a key

pathway of acute lung injury. Cell *133*, 235-249. https://doi.org/10.1016/j.cell.2008.02.043.

Imai, Y., Parodo, J., Kajikawa, O., Perrot, M. de, Fischer, S., Edwards, V., Cutz, E., Liu, M., Keshavjee, S., and Martin, T.R., et al. (2003). Injurious mechanical ventilation and end-organ epithelial cell apoptosis and organ dysfunction in an experimental model of acute respiratory distress syndrome. JAMA *289*, 2104-2112. https://doi.org/10.1001/jama.289.16.2104.

Inatsu, A., Kinoshita, M., Nakashima, H., Shimizu, J., Saitoh, D., Tamai, S., and Seki, S. (2009). Novel mechanism of C-reactive protein for enhancing mouse liver innate immunity. Hepatology (Baltimore, Md.) *49*, 2044-2054. https://doi.org/10.1002/hep.22888.

James, C.F., Modell, J.H., Gibbs, C.P., Kuck, E.J., and Ruiz, B.C. (1984). Pulmonary aspiration--effects of volume and pH in the rat. Anesthesia and analgesia *63*, 665-668.

Jang, H.R., and Rabb, H. (2015). Immune cells in experimental acute kidney injury. Nature reviews. Nephrology *11*, 88-101. https://doi.org/10.1038/nrneph.2014.180.

Jean Chastre and Jean-Yves Fagon (2011). Ventilator-Associated Pneumonia. In SpringerReference (Berlin/Heidelberg: Springer-Verlag).

Johnson, J.L., and Hirsch, C.S. (2003). Aspiration pneumonia. Recognizing and managing a potentially growing disorder. Postgraduate medicine *113*, 99-102, 105-6, 111-2. https://doi.org/10.3810/pgm.2003.03.1390.

Kawakami, T., Lichtnekert, J., Thompson, L.J., Karna, P., Bouabe, H., Hohl, T.M., Heinecke, J.W., Ziegler, S.F., Nelson, P.J., and Duffield, J.S. (2013). Resident renal mononuclear phagocytes comprise five discrete populations with distinct phenotypes and functions. Journal of immunology (Baltimore, Md. : 1950) *191*, 3358-3372. https://doi.org/10.4049/jimmunol.1300342.

Kazankov, K., Jørgensen, S.M.D., Thomsen, K.L., Møller, H.J., Vilstrup, H., George, J., Schuppan, D., and Grønbæk, H. (2019). The role of macrophages in nonalcoholic fatty liver disease and nonalcoholic steatohepatitis. Nature reviews.

Gastroenterology & hepatology *16*, 145-159. https://doi.org/10.1038/s41575-018-0082-x.

Kennedy Thomas P. MU, Johnson, K.J.M., Kunkel, Robin G. BS, MA, Ward, P.A.M., Knight, Paul R. MD, PhD, and Finch, J.S.M. (1989). Acute acid aspiration lung injury in the rat: biphasic pathogenesis. Anesthesia & Analgesia *1989*, 87-92.

Kierdorf, K., Prinz, M., Geissmann, F., and Gomez Perdiguero, E. (2015). Development and function of tissue resident macrophages in mice. Seminars in immunology *27*, 369-378. https://doi.org/10.1016/j.smim.2016.03.017.

Kinoshita, M., Uchida, T., Sato, A., Nakashima, M., Nakashima, H., Shono, S., Habu, Y., Miyazaki, H., Hiroi, S., and Seki, S. (2010). Characterization of two F4/80-positive Kupffer cell subsets by their function and phenotype in mice. Journal of hepatology *53*, 903-910. https://doi.org/10.1016/j.jhep.2010.04.037.

Klein, S.J., Husain-Syed, F., Karagiannidis, C., Lehner, G.F., Singbartl, K., and Joannidis, M. (2018). Lunge-Nieren-Interaktionen bei kritisch Kranken. Medizinische Klinik, Intensivmedizin und Notfallmedizin *113*, 448-455. https://doi.org/10.1007/s00063-018-0472-4.

Knauer-Fischer, S., and Ratjen, F. (1999). Lipid-laden macrophages in bronchoalveolar lavage fluid as a marker for pulmonary aspiration. Pediatr. Pulmonol. *27*, 419-422. https://doi.org/10.1002/(SICI)1099-0496(199906)27:6<419::AID-PPUL9>3.0.CO;2-U.

Knight, P.R., Kurek, C., Davidson, B.A., Nader, N.D., Patel, A., Sokolowski, J., Notter, R.H., and Holm, B.A. (2000). Acid aspiration increases sensitivity to increased ambient oxygen concentrations. American journal of physiology. Lung cellular and molecular physiology *278*, L1240-7. https://doi.org/10.1152/ajplung.2000.278.6.L1240.

Koch, T., Duncker, H.P., Axt, R., Schiefer, H.G., van Ackern, K., and Neuhof, H. (1993). Effects of hemorrhage, hypoxia, and intravascular coagulation on bacterial clearance and translocation. Critical care medicine *21*, 1758-1764. https://doi.org/10.1097/00003246-199311000-00027.

Koyama, Y., and Brenner, D.A. (2017). Liver inflammation and fibrosis. The Journal of clinical investigation *127*, 55-64. https://doi.org/10.1172/JCI88881.

Kredel, M., Muellenbach, R.M., Brock, R.W., Wilckens, H.-H., Brederlau, J., Roewer, N., and Wunder, C. (2007). Liver dysfunction after lung recruitment manoeuvres during pressure-controlled ventilation in experimental acute respiratory distress. Critical care (London, England) *11*, R13. https://doi.org/10.1186/cc5674.

Kubes, P., and Jenne, C. (2018). Immune Responses in the Liver. Annual review of immunology *36*, 247-277. https://doi.org/10.1146/annurev-immunol-051116-052415.

Lampropoulou, V., Sergushichev, A., Bambouskova, M., Nair, S., Vincent, E.E., Loginicheva, E., Cervantes-Barragan, L., Ma, X., Huang, S.C.-C., and Griss, T., et al. (2016). Itaconate Links Inhibition of Succinate Dehydrogenase with Macrophage Metabolic Remodeling and Regulation of Inflammation. Cell metabolism *24*, 158-166. https://doi.org/10.1016/j.cmet.2016.06.004.

Langelage, M., Better, J., Wetstein, M., Selvakumar, B., Malainou, C., Kimmig, L., Arneth, B., Köhler, K., Herden, C., and Herold, S., et al. (2021). Acid Aspiration Impairs Antibacterial Properties of Liver Macrophages. American journal of respiratory cell and molecular biology *64*, 641-643. https://doi.org/10.1165/rcmb.2020-0575LE.

Lavin, Y., Winter, D., Blecher-Gonen, R., David, E., Keren-Shaul, H., Merad, M., Jung, S., and Amit, I. (2014). Tissue-resident macrophage enhancer landscapes are shaped by the local microenvironment. Cell *159*, 1312-1326. https://doi.org/10.1016/j.cell.2014.11.018.

Li, D., and Wu, M. (2021). Pattern recognition receptors in health and diseases. Sig Transduct Target Ther *6*, 291. https://doi.org/10.1038/s41392-021-00687-0.

Li, H., Zhou, X., Tan, H., Hu, Y., Zhang, L., Liu, S., Dai, M., Li, Y., Li, Q., and Mao, Z., et al. (2018). Neutrophil extracellular traps contribute to the pathogenesis of acid-aspiration-induced ALI/ARDS. Oncotarget *9*, 1772-1784. https://doi.org/10.18632/oncotarget.22744.

Li, L., Huang, L., Sung, S.J., Vergis, A.L., Rosin, D.L., Rose, C.E., Lobo, P.I., and Okusa, M.D. (2008). The chemokine receptors CCR2 and CX3CR1 mediate monocyte/macrophage trafficking in kidney ischemia-reperfusion injury. Kidney international *74*, 1526-1537. https://doi.org/10.1038/ki.2008.500.

Li, P., Li, J., Li, M., Gong, J., and He, K. (2014). An efficient method to isolate and culture mouse Kupffer cells. Immunology letters *158*, 52-56. https://doi.org/10.1016/j.imlet.2013.12.002.

Liu, D.D., Lin, H.I., Hsieh, N.-K., and Chen, H.I. (2009). Enhancement effects of hypercapnia on the acute lung injury caused by acid aspiration. The Chinese journal of physiology *52*, 115-127. https://doi.org/10.4077/cjp.2009.amh025.

Livak, K.J., and Schmittgen, T.D. (2001). Analysis of Relative Gene Expression Data Using Real-Time Quantitative PCR and the $2^{-\Delta\Delta CT}$ Method. Methods *25*, 402-408. https://doi.org/10.1006/meth.2001.1262.

Maarten Hulsmans, Sebastian Clauss, Ling Xiao, Aaron D. Aguirre, Kevin R. King, Alan Hanley, William J. Hucker, Eike M. Wülfers, Gunnar Seemann, and Gabriel Courties, et al. Macrophages Facilitate Electrical Conduction in the Heart.

Makris, K., and Spanou, L. (2016). Acute Kidney Injury: Definition, Pathophysiology and Clinical Phenotypes. The Clinical biochemist. Reviews *37*, 85-98. https://doi.org/Review.

Mandell, L.A., and Niederman, M.S. (2019). Aspiration Pneumonia. The New England journal of medicine *380*, 651-663. https://doi.org/10.1056/NEJMra1714562.

Manny, J., Manny, N., Lelcuk, S., Alexander, F., Feingold, H., Kobzik, L., Valeri, C.R., Shepro, D., and Hechtman, H.B. (1986). Pulmonary and systemic consequences of localized acid aspiration. Surgery, gynecology & obstetrics *162*, 259-267. https://doi.org/10.1016/s0883-9441(86)80024-7.

Marik, P.E. (2001). Aspiration Pneumonitis and Aspiration Pneumonia. The New England journal of medicine *344*, 665-671. https://doi.org/10.1056/NEJM200103013440908.

Marik, P.E. (2011). Pulmonary aspiration syndromes. Current opinion in pulmonary medicine *17*, 148-154. https://doi.org/10.1097/MCP.0b013e32834397d6.

Matt, U., Warszawska, J.M., Bauer, M., Dietl, W., Mesteri, I., Doninger, B., Haslinger, I., Schabbauer, G., Perkmann, T., and Binder, C.J., et al. (2009). Bbeta(15-42) protects against acid-induced acute lung injury and secondary pseudomonas pneumonia in vivo. American journal of respiratory and critical care medicine *180*, 1208-1217. https://doi.org/10.1164/rccm.200904-0626OC.

Matthay, M.A., Zemans, R.L., Zimmerman, G.A., Arabi, Y.M., Beitler, J.R., Mercat, A., Herridge, M., Randolph, A.G., and Calfee, C.S. (2019). Acute respiratory distress syndrome. Nature reviews. Disease primers *5*, 18. https://doi.org/10.1038/s41572-019-0069-0.

McDonald, B., Zucoloto, A.Z., Yu, I.-L., Burkhard, R., Brown, K., Geuking, M.B., and McCoy, K.D. (2020). Programing of an Intravascular Immune Firewall by the Gut Microbiota Protects against Pathogen Dissemination during Infection. Cell Host & Microbe *28*, 660-668.e4. https://doi.org/10.1016/j.chom.2020.07.014.

McFadden, B.A., and Purohit, S. (1977). Itaconate, an isocitrate lyase-directed inhibitor in Pseudomonas indigofera. Journal of Bacteriology *131*, 136-144. https://doi.org/10.1128/jb.131.1.136-144.1977.

McGettrick, A.F., and O'Neill, L.A.J. (2020). The Role of HIF in Immunity and Inflammation. Cell metabolism *32*, 524-536. https://doi.org/10.1016/j.cmet.2020.08.002.

McNeill, E., Iqbal, A.J., Patel, J., White, G.E., Regan-Komito, D., Greaves, D.R., and Channon, K.M. (2014). Contrasting in vitro vs. in vivo effects of a cell membrane-specific CC-chemokine binding protein on macrophage chemotaxis. Journal of Molecular Medicine (Berlin, Germany) *92*, 1169-1178. https://doi.org/10.1007/s00109-014-1194-6.

Mendelson, C.L. (1946). The Aspiration of Stomach Contents into the Lungs During Obstetric Anesthesia. American journal of obstetrics and gynecology *52*, 191-205. https://doi.org/10.1016/S0002-9378(16)39829-5.

Metheny, N.A., Clouse, R.E., Chang, Y.-H., Stewart, B.J., Oliver, D.A., and Kollef, M.H. (2006). Tracheobronchial aspiration of gastric contents in critically ill tube-fed patients: frequency, outcomes, and risk factors. Critical care medicine *34*, 1007-1015. https://doi.org/10.1097/01.CCM.0000206106.65220.59.

Mills, E.L., and O'Neill, L.A. (2016). Reprogramming mitochondrial metabolism in macrophages as an anti-inflammatory signal. European journal of immunology *46*, 13-21. https://doi.org/10.1002/eji.201445427.

Mitsushima, H., Oishi, K., Nagao, T., Ichinose, A., Senba, M., Iwasaki, T., and Nagatake, T. (2002). Acid aspiration induces bacterial pneumonia by enhanced bacterial

adherence in mice. Microbial pathogenesis *33*, 203-210. https://doi.org/10.1006/mpat.2002.0529.

Mukherjee, S., and Hanidziar, D. (2018). More of the Gut in the Lung: How Two Microbiomes Meet in ARDS. The Yale journal of biology and medicine *91*, 143-149.

Nader-Djalal, N., Knight, P.R., Thusu, K., Davidson, B.A., Holm, B.A., Johnson, K.J., and Dandona, P. (1998). Reactive oxygen species contribute to oxygen-related lung injury after acid aspiration. Anesthesia and analgesia *87*, 127-133. https://doi.org/10.1097/00000539-199807000-00028.

Nagase, T., Ohga, E., Sudo, E., Katayama, H., Uejima, Y., Matsuse, T., and Fukuchi, Y. (1996). Intercellular adhesion molecule-1 mediates acid aspiration-induced lung injury. American journal of respiratory and critical care medicine *154*, 504-510. https://doi.org/10.1164/ajrccm.154.2.8756829.

Nobs, S.P., and Kopf, M. (2021). Tissue-resident macrophages: guardians of organ homeostasis. Trends in immunology *42*, 495-507. https://doi.org/10.1016/j.it.2021.04.007.

Okamoto, N., Ohama, H., Matsui, M., Fukunishi, S., Higuchi, K., and Asai, A. (2021). Hepatic F4/80(+) CD11b(+) CD68(-) cells influence the antibacterial response in irradiated mice with sepsis by Enterococcus faecalis. Journal of leukocyte biology *109*, 943-952. https://doi.org/10.1002/JLB.4A0820-550RR.

O'Neill, L.A.J., and Pearce, E.J. (2016). Immunometabolism governs dendritic cell and macrophage function. The Journal of experimental medicine *213*, 15-23. https://doi.org/10.1084/jem.20151570.

Orecchioni, M., Ghosheh, Y., Pramod, A.B., and Ley, K. (2019). Macrophage Polarization: Different Gene Signatures in M1(LPS+) vs. Classically and M2(LPS-) vs. Alternatively Activated Macrophages. Frontiers in immunology *10*, 1084. https://doi.org/10.3389/fimmu.2019.01084.

Ostrow, J.D., Pascolo, L., Brites, D., and Tiribelli, C. (2004). Molecular basis of bilirubin-induced neurotoxicity. Trends in molecular medicine *10*, 65-70. https://doi.org/10.1016/j.molmed.2003.12.003.

Patel, B.V., Wilson, M.R., and Takata, M. (2012). Resolution of acute lung injury and inflammation: a translational mouse model. The European respiratory journal *39*, 1162-1170. https://doi.org/10.1183/09031936.00093911.

Pawlik, M.T., Lubnow, M., Gruber, M., Taeger, K., Riegger, G., Pfeifer, M., and Ittner, K.P. (2009). Hydrochloric acid aspiration increases right ventricular systolic pressure in rats. European journal of anaesthesiology *26*, 285-292. https://doi.org/10.1097/EJA.0b013e32831ac614.

Perez, O.A., Yeung, S.T., Vera-Licona, P., Romagnoli, P.A., Samji, T., Ural, B.B., Maher, L., Tanaka, M., and Khanna, K.M. (2017). CD169+ macrophages orchestrate innate immune responses by regulating bacterial localization in the spleen. Science immunology *2*. https://doi.org/10.1126/sciimmunol.aah5520.

Prather, A.D., Smith, T.R., Poletto, D.M., Tavora, F., Chung, J.H., Nallamshetty, L., Hazelton, T.R., and Rojas, C.A. (2014). Aspiration-related lung diseases. Journal of thoracic imaging *29*, 304-309. https://doi.org/10.1097/RTI.0000000000000092.

Prinz, M., Masuda, T., Wheeler, M.A., and Quintana, F.J. (2021). Microglia and Central Nervous System-Associated Macrophages-From Origin to Disease Modulation. Annual review of immunology *39*, 251-277. https://doi.org/10.1146/annurev-immunol-093019-110159.

Quinton, L.J., Jones, M.R., Robson, B.E., and Mizgerd, J.P. (2009). Mechanisms of the hepatic acute-phase response during bacterial pneumonia. Infection and immunity *77*, 2417-2426. https://doi.org/10.1128/IAI.01300-08.

Raghavendran, K., Nemzek, J., Napolitano, L.M., and Knight, P.R. (2011). Aspiration-induced lung injury. Critical care medicine *39*, 818-826. https://doi.org/10.1097/CCM.0b013e31820a856b.

Ramakers, J.D., Verstege, M.I., Thuijls, G., Te Velde, A.A., Mensink, R.P., and Plat, J. (2007). The PPARgamma agonist rosiglitazone impairs colonic inflammation in mice with experimental colitis. Journal of clinical immunology *27*, 275-283. https://doi.org/10.1007/s10875-007-9074-2.

Renckens, R., Roelofs, Joris J T H, Knapp, S., Vos, A.F. de, and Florquin, S. (2006). The acute-phase response and serum amyloid A inhibit the inflammatory response to

Acinetobacter baumannii Pneumonia. The Journal of infectious diseases *193*, 187-195. https://doi.org/10.1086/498876.

Renckens, R., van Westerloo, D.J., Roelofs, J.J.T.H., Pater, J.M., Schultz, M.J., Florquin, S., and van der Poll, T. (2008). Acute phase response impairs host defense against Pseudomonas aeruginosa pneumonia in mice. Critical care medicine *36*, 580-587. https://doi.org/10.1097/01.CCM.0B013E3181620652.

Richter, T., Bergmann, R., Knels, L., Hofheinz, F., Kasper, M., Deile, M., Pietzsch, J., Ragaller, M., and Koch, T. (2013). Pulmonary blood flow increases in damaged regions directly after acid aspiration in rats. Anesthesiology *119*, 890-900. https://doi.org/10.1097/ALN.0b013e3182a17e5b.

Richter, T., Bergmann, R., Musch, G., Pietzsch, J., and Koch, T. (2015). Reduced pulmonary blood flow in regions of injury 2 hours after acid aspiration in rats. BMC anesthesiology *15*, 36. https://doi.org/10.1186/s12871-015-0013-0.

Roberts, A.W., Lee, B.L., Deguine, J., John, S., Shlomchik, M.J., and Barton, G.M. (2017). Tissue-Resident Macrophages Are Locally Programmed for Silent Clearance of Apoptotic Cells. Immunity *47*, 913-927.e6. https://doi.org/10.1016/j.immuni.2017.10.006.

Ronco, C., Bellomo, R., and Kellum, J.A. (2019). Acute kidney injury. The Lancet *394*, 1949-1964. https://doi.org/10.1016/S0140-6736(19)32563-2.

Roquilly, A., Jacqueline, C., Davieau, M., Mollé, A., Sadek, A., Fourgeux, C., Rooze, P., Broquet, A., Misme-Aucouturier, B., and Chaumette, T., et al. (2020). Alveolar macrophages are epigenetically altered after inflammation, leading to long-term lung immunoparalysis. Nature immunology *21*, 636-648. https://doi.org/10.1038/s41590-020-0673-x.

Roshan, R., Dhanapal, S.G., Joshua, V., Madhiyazhagan, M., Amirtharaj, J., Priya, G., and Abhilash, K.P. (2021). Aspiration during Rapid Sequence Induction: Prevalence and Risk Factors. Indian Journal of Critical Care Medicine : Peer-reviewed, Official Publication of Indian Society of Critical Care Medicine *25*, 140-145. https://doi.org/10.5005/jp-journals-10071-23714.

Rőszer, T. (2015). Understanding the Mysterious M2 Macrophage through Activation Markers and Effector Mechanisms. Mediators of inflammation *2015*, 816460. https://doi.org/10.1155/2015/816460.

Rotta, A.T., Shiley, K.T., Davidson, B.A., Helinski, J.D., Russo, T.A., and Knight, P.R. (2004). Gastric acid and particulate aspiration injury inhibits pulmonary bacterial clearance. Critical care medicine *32*, 747-754. https://doi.org/10.1097/01.ccm.0000114577.10352.46.

Russell, D.G., Huang, L., and VanderVen, B.C. (2019). Immunometabolism at the interface between macrophages and pathogens. Nature reviews. Immunology *19*, 291-304. https://doi.org/10.1038/s41577-019-0124-9.

Ryan, D.G., and O'Neill, L.A.J. (2017). Krebs cycle rewired for macrophage and dendritic cell effector functions. FEBS letters *591*, 2992-3006. https://doi.org/10.1002/1873-3468.12744.

Saha, S., Shalova, I.N., and Biswas, S.K. (2017). Metabolic regulation of macrophage phenotype and function. Immunological reviews *280*, 102-111. https://doi.org/10.1111/imr.12603.

Sakai, T., Planinsic, R.M., Quinlan, J.J., Handley, L.J., Kim, T.-Y., and Hilmi, I.A. (2006). The incidence and outcome of perioperative pulmonary aspiration in a university hospital: a 4-year retrospective analysis. Anesthesia and analgesia *103*, 941-947. https://doi.org/10.1213/01.ane.0000237296.57941.e7.

Salimi, A., and Ghadirian, E. (1993). Effect of recombinant tumor necrosis factor alpha on in vitro amoebicidal activity of murine Kupffer cellsactivity of murine Kupffer cells. Microbial pathogenesis *14*, 261-274. https://doi.org/10.1006/mpat.1993.1026.

Sander, L.E., Sackett, S.D., Dierssen, U., Beraza, N., Linke, R.P., Müller, M., Blander, J.M., Tacke, F., and Trautwein, C. (2010). Hepatic acute-phase proteins control innate immune responses during infection by promoting myeloid-derived suppressor cell function. The Journal of experimental medicine *207*, 1453-1464. https://doi.org/10.1084/jem.20091474.

Schertel, E.R., Pratt, J.W., Schaefer, S.L., Valentine, A.K., and McCreary, M.R. (1996). Effects of Acid Aspiration-Induced Lung Injury on Left Ventricular Function. Surgery *119*, 81-88. https://doi.org/10.1016/s0039-6060(96)80218-2.

Schulte-Schrepping, J., Reusch, N., Paclik, D., Baßler, K., Schlickeiser, S., Zhang, B., Krämer, B., Krammer, T., Brumhard, S., and Bonaguro, L., et al. (2020). Severe COVID-19 Is Marked by a Dysregulated Myeloid Cell Compartment. Cell *182*, 1419-1440.e23. https://doi.org/10.1016/j.cell.2020.08.001.

Sellers, S.A., Hagan, R.S., Hayden, F.G., and Fischer, W.A.2. (2017). The hidden burden of influenza: A review of the extra-pulmonary complications of influenza infection. Influenza and other respiratory viruses *11*, 372-393. https://doi.org/10.1111/irv.12470.

Sena, L.A., and Chandel, N.S. (2012). Physiological roles of mitochondrial reactive oxygen species. Molecular cell *48*, 158-167. https://doi.org/10.1016/j.molcel.2012.09.025.

Setzer, F., Schmidt, B., Hueter, L., Schwarzkopf, K., Sänger, J., and Schreiber, T. (2018). Characterization of the seven-day course of pulmonary response following unilateral lung acid injury in rats. PloS one *13*, e0198440. https://doi.org/10.1371/journal.pone.0198440.

Sharif, O., Matt, U., Saluzzo, S., Lakovits, K., Haslinger, I., Furtner, T., Doninger, B., and Knapp, S. (2013). The scavenger receptor CD36 downmodulates the early inflammatory response while enhancing bacterial phagocytosis during pneumococcal pneumonia. Journal of immunology (Baltimore, Md. : 1950) *190*, 5640-5648. https://doi.org/10.4049/jimmunol.1202270.

Sica, A., and Mantovani, A. (2012). Macrophage plasticity and polarization: in vivo veritas. The Journal of clinical investigation *122*, 787-795. https://doi.org/10.1172/JCI59643.

Siore, A.M., Parker, R.E., Stecenko, A.A., Cuppels, C., McKean, M., Christman, B.W., Cruz-Gervis, R., and Brigham, K.L. (2005). Endotoxin-induced acute lung injury requires interaction with the liver. American journal of physiology. Lung cellular and molecular physiology *289*, L769-76. https://doi.org/10.1152/ajplung.00137.2005.

Smeeth Liam, Thomas Sara L., Hall Andrew J., Hubbard Richard, Farrington Paddy, and Vallance Patrick (2004). Risk of Myocardial Infarction and Stroke after Acute Infection or Vaccination. The New England journal of medicine *351*, 2611-2618. https://doi.org/10.1056/NEJMoa041747.

Son, Y.G., Shin, J., and Ryu, H.G. (2017). Pneumonitis and pneumonia after aspiration. Journal of dental anesthesia and pain medicine *17*, 1-12. https://doi.org/10.17245/jdapm.2017.17.1.1.

Sorbara, M.T., and Girardin, S.E. (2011). Mitochondrial ROS fuel the inflammasome. Cell research *21*, 558-560. https://doi.org/10.1038/cr.2011.20.

Spight, D., Trapnell, B., Zhao, B., Berclaz, P., and Shanley, T.P. (2008). Granulocyte-macrophage-colony-stimulating factor-dependent peritoneal macrophage responses determine survival in experimentally induced peritonitis and sepsis in mice. Shock (Augusta, Ga.) *30*, 434-442. https://doi.org/10.1097/SHK.0b013e3181673543.

Stamatiades, E.G., Tremblay, M.-E., Bohm, M., Crozet, L., Bisht, K., Kao, D., Coelho, C., Fan, X., Yewdell, W.T., and Davidson, A., et al. (2016). Immune Monitoring of Trans-endothelial Transport by Kidney-Resident Macrophages. Cell *166*, 991-1003. https://doi.org/10.1016/j.cell.2016.06.058.

Tacke, F., and Zimmermann, H.W. (2014). Macrophage heterogeneity in liver injury and fibrosis. Journal of hepatology *60*, 1090-1096. https://doi.org/10.1016/j.jhep.2013.12.025.

Teoh, N.C. (2011). Hepatic ischemia reperfusion injury: Contemporary perspectives on pathogenic mechanisms and basis for hepatoprotection-the good, bad and deadly. Journal of gastroenterology and hepatology *26 Suppl 1*, 180-187. https://doi.org/10.1111/j.1440-1746.2010.06584.x.

Tran, V.G., Cho, H.R., and Kwon, B. (2014). IL-33 Priming Enhances Peritoneal Macrophage Activity in Response to Candida albicans. Immune Network *14*, 201-206. https://doi.org/10.4110/in.2014.14.4.201.

Tsutsui, H., and Nishiguchi, S. (2014). Importance of Kupffer cells in the development of acute liver injuries in mice. International journal of molecular sciences *15*, 7711-7730. https://doi.org/10.3390/ijms15057711.

van der Laan, L.J., Döpp, E.A., Haworth, R., Pikkarainen, T., Kangas, M., Elomaa, O., Dijkstra, C.D., Gordon, S., Tryggvason, K., and Kraal, G. (1999). Regulation and functional involvement of macrophage scavenger receptor MARCO in clearance of bacteria in vivo. J Immunol *162*, 939-947.

van Furth, R., and Cohn, Z.A. (1968). The origin and kinetics of mononuclear phagocytes. The Journal of experimental medicine *128*, 415-435. https://doi.org/10.1084/jem.128.3.415.

Vannella, K.M., and Wynn, T.A. (2017). Mechanisms of Organ Injury and Repair by Macrophages. Annual review of physiology *79*, 593-617. https://doi.org/10.1146/annurev-physiol-022516-034356.

Venosa, A., Malaviya, R., Gow, A.J., Hall, L., Laskin, J.D., and Laskin, D.L. (2015). Protective role of spleen-derived macrophages in lung inflammation, injury, and fibrosis induced by nitrogen mustard. American journal of physiology. Lung cellular and molecular physiology *309*, L1487-98. https://doi.org/10.1152/ajplung.00276.2015.

Viola, A., Munari, F., Sánchez-Rodríguez, R., Scolaro, T., and Castegna, A. (2019). The Metabolic Signature of Macrophage Responses. Frontiers in immunology *10*, 1462. https://doi.org/10.3389/fimmu.2019.01462.

Wang, H., Yung, M.M.H., Ngan, H.Y.S., Chan, K.K.L., and Chan, D.W. (2021). The Impact of the Tumor Microenvironment on Macrophage Polarization in Cancer Metastatic Progression. International journal of molecular sciences *22*, 6560. https://doi.org/10.3390/ijms22126560.

Wang, Y.-Y., Shang, H.-F., Lai, Y.-N., and Yeh, S.-L. (2003). Arginine supplementation enhances peritoneal macrophage phagocytic activity in rats with gut-derived sepsis. JPEN. Journal of parenteral and enteral nutrition *27*, 235-240. https://doi.org/10.1177/0148607103027004235.

Warner, M.A., Warner, M.E., and Weber, J.G. (1993). Clinical significance of pulmonary aspiration during the perioperative period. Anesthesiology *78*, 56-62. https://doi.org/10.1097/00000542-199301000-00010.

Weinberg, S.E., Sena, L.A., and Chandel, N.S. (2015). Mitochondria in the regulation of innate and adaptive immunity. Immunity *42*, 406-417. https://doi.org/10.1016/j.immuni.2015.02.002.

West, A.P., Brodsky, I.E., Rahner, C., Woo, D.K., Erdjument-Bromage, H., Tempst, P., Walsh, M.C., Choi, Y., Shadel, G.S., and Ghosh, S. (2011). TLR signalling augments macrophage bactericidal activity through mitochondrial ROS. Nature *472*, 476-480. https://doi.org/10.1038/nature09973.

Wiese, M., Gerlach, R.G., Popp, I., Matuszak, J., Mahapatro, M., Castiglione, K., Chakravortty, D., Willam, C., Hensel, M., and Bogdan, C., et al. (2012). Hypoxia-mediated impairment of the mitochondrial respiratory chain inhibits the bactericidal activity of macrophages. Infection and immunity *80*, 1455-1466. https://doi.org/10.1128/IAI.05972-11.

Wolfe, J.E., Bone, R.C., and Ruth, W.E. (1977). Effects of corticosteroids in the treatment of patients with gastric aspiration. The American journal of medicine *63*, 719-722. https://doi.org/10.1016/0002-9343(77)90157-7.

Wong, C.H.Y., Jenne, C.N., Petri, B., Chrobok, N.L., and Kubes, P. (2013). Nucleation of platelets with blood-borne pathogens on Kupffer cells precedes other innate immunity and contributes to bacterial clearance. Nature immunology *14*, 785-792. https://doi.org/10.1038/ni.2631.

Woods, P.S., Kimmig, L.M., Meliton, A.Y., Sun, K.A., Tian, Y., O'Leary, E.M., Gökalp, G.A., Hamanaka, R.B., and Mutlu, G.M. (2019). Tissue Resident Alveolar Macrophages Do Not Rely on Glycolysis for LPS-induced Inflammation. American journal of respiratory cell and molecular biology. https://doi.org/10.1165/rcmb.2019-0244OC.

Wynn, T.A., Chawla, A., and Pollard, J.W. (2013). Macrophage biology in development, homeostasis and disease. Nature *496*, 445-455. https://doi.org/10.1038/nature12034.

Wynn, T.A., and Vannella, K.M. (2016). Macrophages in Tissue Repair, Regeneration, and Fibrosis. Immunity *44*, 450-462. https://doi.org/10.1016/j.immuni.2016.02.015.

Yang, P., Formanek, P., Scaglione, S., and Afshar, M. (2019). Risk factors and outcomes of acute respiratory distress syndrome in critically ill patients with cirrhosis. Hepatology research : the official journal of the Japan Society of Hepatology *49*, 335-343. https://doi.org/10.1111/hepr.13240.

Zhai, R., Sheu, C.C., Su, L., Gong, M.N., Tejera, P., Chen, F., Wang, Z., Convery, M.P., Thompson, B.T., and Christiani, D.C. (2009). Serum bilirubin levels on ICU admission are associated with ARDS development and mortality in sepsis. Thorax *64*, 784-790. https://doi.org/10.1136/thx.2009.113464.

Zhou, R., Zhang, J., Bu, W., Zhang, W., Duan, B., Wang, X., Yao, L., Li, Z., and Li, J. (2019). A New Role for the Spleen: Aggravation of the Systemic Inflammatory Response in Rats with Severe Acute Pancreatitis. The American journal of pathology *189*, 2233-2245. https://doi.org/10.1016/j.ajpath.2019.07.008.

Zigmond, E., Samia-Grinberg, S., Pasmanik-Chor, M., Brazowski, E., Shibolet, O., Halpern, Z., and Varol, C. (2014). Infiltrating monocyte-derived macrophages and resident kupffer cells display different ontogeny and functions in acute liver injury. Journal of immunology (Baltimore, Md. : 1950) *193*, 344-353. https://doi.org/10.4049/jimmunol.1400574.

Zuk, A., and Bonventre, J.V. (2016). Acute Kidney Injury. Annual review of medicine *67*, 293-307. https://doi.org/10.1146/annurev-med-050214-013407.

# 9 Publication directory

**Posters:**

Martin Langelage, Julian Better, Ulrich Matt, Susanne Herold:

The role of tissue-resident macrophages in the extrapulmonary inflammatory response to acid aspiration

3rd Science Day of the Justus Liebig University Gießen, Friday, November 1st, 2019


**Publications:**

Martin Langelage & Julian Better, Michael Wetstein, Balachandar Selvakumar, Christina Malainou, Lucas Kimmig, Borros Arneth, Kernt Köhler, Christiane Herden, Susanne Herold, Ulrich Matt:

Acid Aspiration Impairs Antibacterial Properties of Liver Macrophages

American Journal of Respiratory Cell and Molecular Biology (AJRCMB), 2021, Volume 64, Issue number 5, Page range 641-643, DOI: 10.1165/rcmb.2020-0575LE, PMID: 33929292

# 10 Affirmation – Ehrenwörtliche Erklärung

**Erklärung zur Dissertation**

„Hiermit erkläre ich, dass ich die vorliegende Arbeit selbständig und ohne unzulässige Hilfe oder Benutzung anderer als der angegebenen Hilfsmittel angefertigt habe. Alle Textstellen, die wörtlich oder sinngemäß aus veröffentlichten oder nichtveröffentlichten Schriften entnommen sind, und alle Angaben, die auf mündlichen Auskünften beruhen, sind als solche kenntlich gemacht. Bei den von mir durchgeführten und in der Dissertation erwähnten Untersuchungen habe ich die Grundsätze guter wissenschaftlicher Praxis, wie sie in der „Satzung der Justus-Liebig-Universität Gießen zur Sicherung guter wissenschaftlicher Praxis" niedergelegt sind, eingehalten sowie ethische, datenschutzrechtliche und tierschutzrechtliche Grundsätze befolgt. Ich versichere, dass Dritte von mir weder unmittelbar noch mittelbar geldwerte Leistungen für Arbeiten erhalten haben, die im Zusammenhang mit dem Inhalt der vorgelegten Dissertation stehen, oder habe diese nachstehend spezifiziert. Die vorgelegte Arbeit wurde weder im Inland noch im Ausland in gleicher oder ähnlicher Form einer anderen Prüfungsbehörde zum Zweck einer Promotion oder eines anderen Prüfungsverfahrens vorgelegt. Alles aus anderen Quellen und von anderen Personen übernommene Material, das in der Arbeit verwendet wurde oder auf das direkt Bezug genommen wird, wurde als solches kenntlich gemacht. Insbesondere wurden alle Personen genannt, die direkt und indirekt an der Entstehung der vorliegenden Arbeit beteiligt waren. Mit der Überprüfung meiner Arbeit durch eine Plagiatserkennungssoftware bzw. ein internetbasiertes Softwareprogramm erkläre ich mich einverstanden."

_____          _____

Ort, Datum                       Unterschrift

# 11 Danksagung

Zuallererst möchte ich meine tiefe Dankbarkeit gegenüber meiner gesamten Familie aussprechen. Ohne eure fortwährende Unterstützung wäre die Dissertation von vorne hinein zum Scheitern verurteilt gewesen. Besonders hervorheben möchte ich hier meine Eltern, meinen Patenonkel sowie meine Großmutter. Ihr habt mir immer den Rücken freigehalten, sodass ich mich voll und ganz auf Studium und Promotion konzentrieren konnte.

Weiterhin möchte ich auch meine Freundin Theresa hier erwähnen, da sie immer mit Tipps und Ratschlägen aufwarten konnte, wenn ich vor Problemen stand.

Mein Dank gilt auch Frau Professor Herold, dass sie mir diese Dissertation in ihrem Labor überhaupt erst ermöglicht hat.

Besonders möchte ich auch den technischen Assistenten der Gruppe, Larissa, Florian und Steffi, danken. Es war eure Anleitung die es mir erst ermöglicht hat sinnvolle Laborarbeit zu verrichten.

Weiterhin möchte ich auch die Hilfe von Herrn Dr. Arneth bei der Messung der Plasmaproben der Mäuse und Herrn Dr. Köhler bei der Analyse der Leber- und Nierenproben hervorheben.

Natürlich möchte ich mich auch bei Julian Better bedanken. Vom ersten Tag an hast du mich freundlich empfangen und mir bei allen erdenklichen Sachen geholfen. Es fällt mir recht schwer in so wenigen Worten hinreichend auszudrücken, wie dankbar ich dir bin für all die Male, wo du mir geholfen hast und wie viel Zeit du immer für mich und meine Probleme gefunden hast.

Abschließend möchte ich auch meinen Dank gegenüber Ulrich Matt aussprechen: Es war deine Planung, ohne die dieses Projekt zweifellos gescheitert wäre. Besonders möchte ich mich bedanken, dass du immer Zeit gefunden hast, wenn Probleme aufgekommen sind und so geduldig mit mir warst.